

California State University, San Bernardino

**CSUSB ScholarWorks**

---

Theses Digitization Project

John M. Pfau Library

---

1998

## State sum invariants of three manifolds

Sharon Angela Newman-Gomez

Follow this and additional works at: <https://scholarworks.lib.csusb.edu/etd-project>



Part of the [Mathematics Commons](#)

---

### Recommended Citation

Newman-Gomez, Sharon Angela, "State sum invariants of three manifolds" (1998). *Theses Digitization Project*. 1510.

<https://scholarworks.lib.csusb.edu/etd-project/1510>

This Project is brought to you for free and open access by the John M. Pfau Library at CSUSB ScholarWorks. It has been accepted for inclusion in Theses Digitization Project by an authorized administrator of CSUSB ScholarWorks. For more information, please contact [scholarworks@csusb.edu](mailto:scholarworks@csusb.edu).

# STATE SUM INVARIANTS OF THREE MANIFOLDS

---

A Project  
Presented to the  
Faculty of  
California State University,  
San Bernardino

---

In Partial Fulfillment  
of the Requirements for the Degree  
Master of Arts  
in  
Mathematics

---

by  
Sharon Angela Newman-Gomez

June 1998

STATE SUM INVARIANTS OF THREE MANIFOLDS

---

A Project

Presented to the

Faculty of

California State University,

San Bernardino


---

by


Sharon Angela Newman-Gomez


June 1998

Approved by:

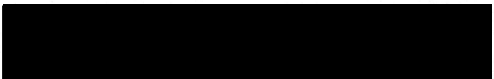
  
Chetan Prakash, Committee Chair

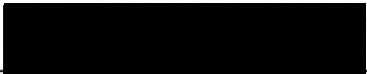
6/10/98  
Date

  
Paul Renteln, Committee Member

  
Davida Fischman, Committee Member

  
Rolland Trapp, Committee Member

  
Peter Williams, Chair  
Department of Mathematics

  
Terry Hallett,  
Graduate Coordinator  
Department of Mathematics

# Abstract

We investigate state sum invariants of two and three dimensional closed orientable manifolds. Specifically, we consider the Fukuma/Hosono/Kawai two dimensional topological lattice field theory; the Chung/Fukuma/Shapere three dimensional topological lattice field theory; and the Kauffman/Lins tangle theoretic presentation of the Turaev/Viro state sum invariant of 3-manifolds. We also explain how each of these theories fit Atiyah's basic category theoretic description of a topological quantum field theory.



# Acknowledgments

I extend my sincere appreciation to my academic advisor, Paul Renteln, for the many years of hard work he has invested in my education, and for taking me to all those scary mathematical places that nobody else dared to. I thank John Baez for gently guiding me through the foundations of category theory, James Dolan for his carefully explanation of the material of chapter five and Louis Kauffman for his comments on chapter four. I thank the entire California State University San Bernardino mathematics department, specifically Zahid Hasan, Wenxiang Wang, Davida Fischman and Rolland Trapp for teaching me algebra, geometry, Hopf algebra and knot theory, all of which are very important components of this paper. For their patient assistance concerning numerous LaTeX issues I thank Charles Stanton and Peter Williams. Finally, for assisting me with the sketches and for preparing my meals when I was too busy to take proper care of them, I thank my dear sons Isaac, Joshua and Elijah Newman-Gomez.

# Table of Contents

<b>Abstract</b> .....	<b>iii</b>
<b>Acknowledgements</b> .....	<b>iv</b>
<b>List of Figures</b> .....	<b>vii</b>
<b>List of Tables</b> .....	<b>xiii</b>
<b>1 Introduction</b> .....	<b>1</b>
<b>2 Two Dimensional Fukuma-Hosono-Kawai State Sum Invariant</b> .....	<b>4</b>
2.1 Formal Definitions .....	9
2.2 Topological Invariance .....	12
2.2.1 Extending to Non-Triangular Lattices .....	18
2.3 Algebraic Correspondence .....	20
2.4 Dual Formation .....	34
<b>3 Three Dimensional Chung-Fukuma-Shapere State Sum Invariant</b> ...	<b>38</b>
3.1 3-D Definitions, Weighting Rules and Partition Function .....	39
3.1.1 Weighting Rules for Triangles .....	40
3.1.2 Weighting Rules for 3-Hinges .....	41
3.1.3 Gluing Triangles to Triangles .....	42
3.1.4 Gluing 3-hinges to 3-hinges .....	44
3.1.5 Gluing Triangles to 3-hinges .....	47
3.2 Algebraic and Coalgebraic Structure .....	52
3.2.1 Graphical representation of $u_x$ .....	53
3.2.2 Graphical representation of $\epsilon_x$ .....	55
3.3 Topological Invariance and Correspondence to Hopf Algebra .....	57
<b>4 Turaev-Viro (Kauffman-Lins) State Sum Invariant</b> .....	<b>104</b>

4.1 Knot Theory and Bracket Polynomial Basics .....	107
4.2 Tangles and Braids .....	113
4.3 The Braid Group .....	115
4.4 The Temperley-Lieb Algebra .....	118
4.5 The Jones-Wenzl Projectors .....	125
4.6 The $q$ -symmetrizer .....	131
4.7 Partition Function Weights .....	140
4.8 Topological Invariance .....	147
4.9 3 Vertex as Sum of Tangles .....	152
4.10 Topological Invariance Proof Tools .....	156
4.11 Invariance Proofs .....	162
<b>5 Category Theory and Topological Quantum Field Theory .....</b>	<b>177</b>
5.1 Category Theory Foundation .....	178
5.2 TQFT Defined .....	182
5.3 Reinterpreting Two and Three Dimensional TLFT's .....	190
5.3.1 2d Generalization .....	191
5.3.2 3d Generalization .....	192
5.4 Conclusion .....	194

# List of Figures

Figure 2.1 (a) $M^1$ , (b) $M^2$ , and (c) $M^3$ consist of “pieces” of $\mathbb{R}^1$ , $\mathbb{R}^2$ , and $\mathbb{R}^3$ , respectively .....	4
Figure 2.4 Continuous function $f : X \rightarrow Y$ .....	5
Figure 2.7 A chart on topological space $X$ .....	6
Figure 2.9 Manifold $M$ .....	6
Figure 2.11 (2-sphere) (tetrahedron) .....	7
Figure 2.12 Decomposition of triangulation of manifold .....	7
Figure 2.13 Reassembly of triangulation .....	8
Figure 2.16 Coloring of a triangular face in the lattice .....	10
Figure 2.19 Gluing faces .....	10
Figure 2.22 The partition function $Z$ for two distinct triangulations of the same closed 2-manifold produces an identical complex value .....	11
Figure 2.23 Two-two move .....	12
Figure 2.24 Bubble move .....	12
Figure 2.25 Construction of left-hand side triangle for 2-2 move .....	13
Figure 2.26 Construction of right-hand side triangle for 2-2 move .....	13
Figure 2.27 2-2 move algebraic condition .....	14
Figure 2.29 Construction of the bubble .....	15
Figure 2.30 Algebraic description of the bubble .....	15
Figure 2.31 Algebraic condition for the bubble move .....	16
Figure 2.33 Classifying homeomorphic manifolds .....	17
Figure 2.34 Coding the cone .....	17
Figure 2.35 Developing the cone invariance move .....	18

Figure 2.37 Decomposition of n-gon into triangles .....	19
Figure 2.64 Trivalent graph corresponding to face weights .....	34
Figure 2.65 Gluing operation in both formations .....	35
Figure 2.67 2-2 invariance .....	36
Figure 2.70 Bubble invariance .....	36
Figure 3.3 Decomposition into polygonal faces and 4-valent hinge .....	39
Figure 3.4 Triangular decomposition .....	40
Figure 3.5 Triangle weight .....	41
Figure 3.6 Hinge weights indicating that $\Delta^{xyz} = \Delta^{xyz}$ , when the second sketch is read counterclockwise and the third clockwise .....	41
Figure 3.7 Graphical representation of the gluing operator .....	42
Figure 3.8 Graphical representation of the inverse gluing operator .....	42
Figure 3.9 Gluing restrictions .....	43
Figure 3.10 Summation convention on glued edges .....	43
Figure 3.11 Algebraic code for 3d face gluing .....	43
Figure 3.12 Gluing an arbitrary polygonal face .....	44
Figure 3.15 Graphical representation of hinge gluing operators (a) $h_{xy} = h_{yx}$ (b) $h^{xy} = h^{yx}$ .....	45
Figure 3.16 Four hinge weight $\Delta^{xyzw}$ .....	45
Figure 3.17 Decomposition of $\Delta^{x_1 x_2 \dots x_n}$ into $\Delta_{a_1}^{x_1 a_2} \Delta_{a_2}^{x_2 a_3} \dots \Delta_{a_n}^{x_n a_1}$ .....	46
Figure 3.19 Dual 2-2 move .....	46
Figure 3.21 Dual bubble move .....	47
Figure 3.22 Triangles glued to 3-hinge, $C_{abx} C_{cdy} C_{efz} \Delta^{xyz}$ .....	47
Figure 3.23 The action of the arrow changing operator .....	48
Figure 3.24 A configuration requiring the arrow changing operator .....	48
Figure 3.25 Identical hinge weights .....	49

Figure 3.27 Constraints on $S_y^x$ and $\Delta^{xyz}$ .....	49
Figure 3.28 Weighting rules for 3d LFT .....	50
Figure 3.33 Graphical representation of $u_x$ .....	53
Figure 3.43 Count $\epsilon_x$ in graphical representation	55
Figure 3.53 Graphical proof of Equation (3.50) $u_x \Delta_x^{yz} = u^y u^z$ .....	62
Figure 3.56 Hinge Move .....	63
Figure 3.61 The count $\epsilon_x$ .....	66
Figure 3.62 The unit $u_x$ .....	67
Figure 3.63 The action of arrow-changing operator .....	67
Figure 3.64 The 3D cone move .....	68
Figure 3.69 Cone move: Variation 2 .....	69
Figure 3.70 Cone move: Variation 3 .....	69
Figure 3.71 Cone move: Variation 4 .....	69
Figure 3.103 Polyhedron P, where we have shown m faces and suppressed (F-m) faces, for a total of F faces .....	78
Figure 3.104 Polyhedron P with vertex 0 raised .....	78
Figure 3.105 Forming a tetrahedron from two adjacent faces P at vertex 0 .....	79
Figure 3.106 Forming (m-2) tetrahedra from polyhedron P .....	80
Figure 3.107 Modified polyhedron P, where we have shown (m-2) faces and suppress (F-m) faces, for a total of (F-2) faces in P .....	80
Figure 3.108 Removing (m-2) tetrahedra from polyhedron P .....	81
Figure 3.109 The three dimensional 2-3 move .....	82
Figure 3.110 Exploded view of the three dimensional 2-3 move .....	83
Figure 3.111 Three dimensional bubble move .....	83
Figure 3.112 Topological detail of the 3-D bubble move .....	85
Figure 3.120 Detail of inflation move .....	102

Figure 3.121 Two tetrahedra sharing a common face ABC .....	103
Figure 4.1 Labeling of crossing .....	107
Figure 4.2 Smoothings of a crossing .....	107
Figure 4.5 Recursion relations for the bracket .....	108
Figure 4.6 The normalization of the bracket .....	108
Figure 4.11 The A-smoothing state for trefoil .....	109
Figure 4.14 The three Reidemeister moves .....	110
Figure 4.16 The unknot with a twist .....	111
Figure 4.17 The bracket of a twist .....	111
Figure 4.18 The sign of a crossing .....	112
Figure 4.20 A tangle (a), and a braid (b) .....	113
Figure 4.21 The closure of the tangles in Figure 4.20 .....	113
Figure 4.23 The product of two braids in $B_3$ .....	115
Figure 4.24 The identity element of $B_n$ .....	115
Figure 4.25 The generators of $B_n$ and their inverses .....	116
Figure 4.27 A braid word in $B_3$ .....	116
Figure 4.30 Demonstration of (4.28) in $B_3$ , $\sigma_1\sigma_3 = \sigma_3\sigma_1$ .....	117
Figure 4.31 Demonstration of (4.29) in $B_3$ , $\sigma_1\sigma_2\sigma_1 = \sigma_2\sigma_1\sigma_2$ .....	117
Figure 4.32 The identity tangle together with elementary tangles on 4 strands ..	118
Figure 4.33 Example of multiplication of 4 strand tangles .....	118
Figure 4.74 The canonical inductive construction of the braid set $\{\hat{\sigma} \sigma \in S_3\}$ ...	136
Figure 4.77 A four 3-cell arrangement of space .....	141
Figure 4.78 Skeletal remains of four 3-cells .....	141
Figure 4.79 Dual to tetrahedron .....	142
Figure 4.80 Special spine .....	142
Figure 4.82 Vertex weight .....	144



Figure 4.83 Edge weight .....	144
Figure 4.84 An edge relative to a face of our tetrahedron .....	145
Figure 4.85 Face weight .....	145
Figure 4.87 The lune move involves the creation/removal of two vertices .....	147
Figure 4.88 The Y-move interpolates between a two and three vertex spine .....	147
Figure 4.89 The bubble move creates/removes a 3-cell .....	148
Figure 4.90 The edge dilation move creates/removes a 3-cell on an edge .....	148
Figure 4.91 Shadow world lune move .....	149
Figure 4.92 Shadow world Y-move .....	149
Figure 4.93 Shadow world bubble move .....	150
Figure 4.94 Shadow world edge dilation .....	150
Figure 4.95 Horizontal 2-vertex trivalent graph .....	151
Figure 4.96 Vertical 2-vertex trivalent graph .....	151
Figure 5.2 Geometric representation of a catagory .....	179
Figure 5.5 Geometric representation of functor $F$ from category $C$ to category $D$ .....	180
Figure 5.11 Composition of morphisms in $n\text{Cob}$ .....	182
Figure 5.14 Functorial tensor product in a monoidal category: shifted depiction (a), and original depiction (b) where all dots are identified .....	185
Figure 5.15 Tensor product of morphisms in $2\text{Cob}$ , $f : y \rightarrow z, g : x \rightarrow y, f \otimes g : y \otimes x \rightarrow z \otimes y$ .....	185
Figure 5.16 Symmetry in $2\text{Cob}$ .....	186
Figure 5.17 Duality (star) structure on objects in $2\text{Cob}$ .....	186
Figure 5.18 Unit, counit, and triangular identities .....	187
Figure 5.20 Duality structure on morphisms in $2\text{Cob}$ .....	188
Figure 5.22 Duties of (a) 2d and (b) 3d TLFTs .....	190
Figure 5.23 Partition function $Z$ mapping 2-manifold $M$ to numerical constant $Z(M)$ .....	

arising from “partition functor” $Z$ .....	192
Figure 5.24 Example of 3-manifold $M$ (shaded) whose boundary is the disjoint union of $S^2$ and $T^2$ (nested) .....	193
Figure 5.25 Dual of tetrahedron .....	195

# List of Tables

Table 5.13 The Three Levels of a Monoidal Category .....	184
Table 5.26 Translation Key for Dual of Tetrahedron .....	195

# Chapter 1

## Introduction

A long standing problem in the history of mathematics is that of giving a complete topological classification of manifolds. Although the problem has essentially been resolved in one and two dimensions, a complete invariant of three and four manifolds has yet to be established.

A variety of methods have been employed in researching the area of 3-manifold invariants. In 1988 Witten [Wt88] discovered an invariant of closed, orientable 3-manifolds via surgery on a framed link. He invented a tool called topological quantum field theory (TQFT) to construct his invariant. Atiyah [At88] formalized the concept of TQFT at roughly the same time when he defined a topological quantum field theory as a particular type of category representation from  $n\text{Cob}$  (the category of compact oriented  $(n - 1)$ -manifolds as objects, and oriented cobordisms as morphisms) to  $\text{Vect}$ , the category of vector spaces. Since then the study of TQFTs has become a rapidly developing area of study.

Another type of 3-manifold invariant that has appeared in many mathematics and physics publications recently is the state sum invariant, often referred to as a partition function. It is a number, usually defined in terms of a triangulation, that depends only on the topology of the underlying manifold. In 1991 Reshetikhin and Turaev [RT91] made Witten's theory mathematically

rigorous by constructing a TQFT using quantum groups. Turaev and Viro [TV92] established a state sum invariant of 3-manifolds using quantum 6j symbols.

Kuperberg [Ku91] constructed a state sum invariant using surgery methods, while Chung, Fukuma and Shapere (CFS) [CFS94] developed their invariant via topological lattice field theory (TLFT).

A number of mathematicians have generalized the study of topological quantum field theory in order to understand the “big picture”. Crane [Cr95], and Baez and Dolan [BD95] for instance, have suggested the application of category theory to clarify the question of why topology has a different personality in each different dimension. Crane argues that three dimensional TQFTs are just a categorification of two dimensional theories. Baez and Dolan suggest that  $n$ -category theory, for arbitrary  $n$ , explains topology in dimension  $n$ .

My research has focused on three areas: Fukuma-Hosono-Kawai’s [FHK94] and Chung-Fukuma-Shapere’s TLFT method of constructing a state sum invariant of two and three dimensional closed orientable manifolds; Kauffman-Lins’ [Kau94] interpretation of the Turaev-Viro [TV92] state sum invariant of three dimensional closed orientable manifolds; and Baez-Dolan’s [BD95] description of Atiyah’s TQFT in terms of category theory, the foundational idea that synthesizes the other approaches.

Although the classification of 2-manifolds has been resolved, the search for 3 dimensional topological invariants is still an expanding field of study. The 3-manifold invariants mentioned above do not provide a complete classification. The study of 2 and 3-manifolds is especially intriguing because it is essential to the understanding of the theory of 4-manifolds, which is, in some sense, more complex than that of lower or even higher dimensions. We can learn much about the universe by understanding the four dimensional case because the universe itself is

believed to be four dimensional, the fourth dimension being time.

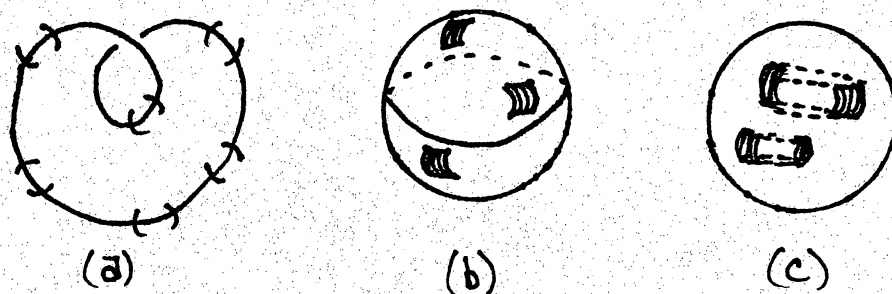
State sum invariants in two and three dimensions are associated to well understood families of algebras. Such an association provides us with a correspondence between the somewhat elusive topology of manifolds and the well developed theory of algebra. Extending the correspondence to four dimensions provides hope that the topology of spacetime may one day be defined in purely algebraic terms, allowing us to develop coordinate and metric free theories of physics, such as quantum gravity. Indeed, the study of state sum invariants of low dimensional manifolds has important mathematical implications in developing a more thorough understanding of topology. But perhaps the most promising feature of the continuing research on the topological classification of manifolds is that it may one day open doors to a better understanding of the universe.

After the brief introduction in chapter one the paper is arranged in a manner that guides the uninitiated reader through an example in chapter two of a topological lattice field theory in two dimensions, Fukuma/Hosono/Kawai (FHK) triangulation theory. Chapter three involves the extension of FHK theory to three dimensions, Chung/Fukuma/Shapere theory. In chapter four we consider a different approach of constructing a three dimensional state sum invariant via a dual triangulation, Kauffman/Lin's presentation of the Turaev-Viro invariant. Finally in chapter five we conclude by investigating Atiyah's basic description of a TQFT as presented by Baez/Dolan. We explain how the examples of chapters two, three and four fit into such a description, and consider how this method provides a basic structure that lends itself to general expansion into higher dimensions.

## Chapter 2

# Two Dimensional Fukuma-Hosono-Kawai State Sum Invariant

We begin by defining a manifold, but to do so requires that we build a mathematical foundation. An  $n$ -manifold ( $n$  dimensional manifold  $M^n$ ) is roughly described to be similar to a patchwork quilt made up of pieces of  $\mathbb{R}^n$ . In other words, a local picture of  $M^n$  looks very much like  $\mathbb{R}^n$ . (See Fig. 2.1)



**Figure 2.1** (a)  $M^1$ , (b)  $M^2$ , and (c)  $M^3$  consist of “pieces” of  $\mathbb{R}^1$ ,  $\mathbb{R}^2$ , and  $\mathbb{R}^3$ , respectively

For a formal definition of a manifold we need some definitions. [BM94]

**Definition 2.2** A *topological space* is a set  $X$  together with a family of subsets of  $X$ , called the *open sets*, satisfying the following conditions:

1. The empty set and  $X$  are open.

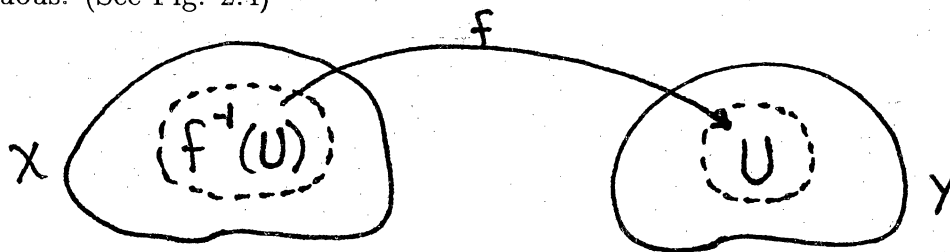


2. If  $U, V \subseteq X$  are open, then  $U \cap V$  is open.
3. If sets  $U_\alpha \subseteq X$  are open, then the union  $\bigcup U_\alpha$  is open.

The set  $\mathbb{R}^n$  with the usual family of open subsets  $U$  (for example, the Cartesian product  $\underbrace{\mathbb{R} \times \cdots \times \mathbb{R}}_{n \text{ times}}$ , where the open sets are the open balls  $B_r(x) = \{y | d(x, y) < r\}$ ) is a simple example of a topological space.

**Definition 2.3** Let  $X, Y$  be topological spaces. A function  $f : X \rightarrow Y$  is called *continuous* if, given any open set  $U \subseteq Y$ , its inverse image  $f^{-1}U \subseteq X$  is open.

So basically, if a function sends nearby points to nearby points it is continuous. (See Fig. 2.4)

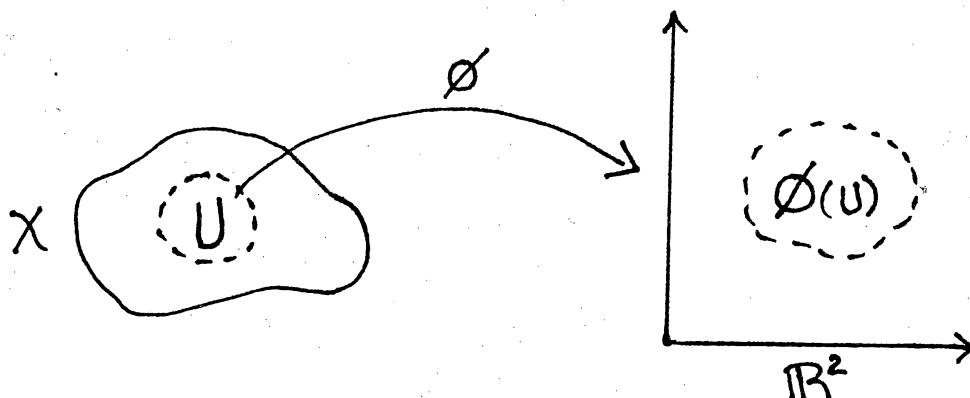


**Figure 2.4** Continuous function  $f : X \rightarrow Y$

**Definition 2.5** A collection of open sets *covers* a topological space  $X$  if the union of the collection is exactly  $X$ .

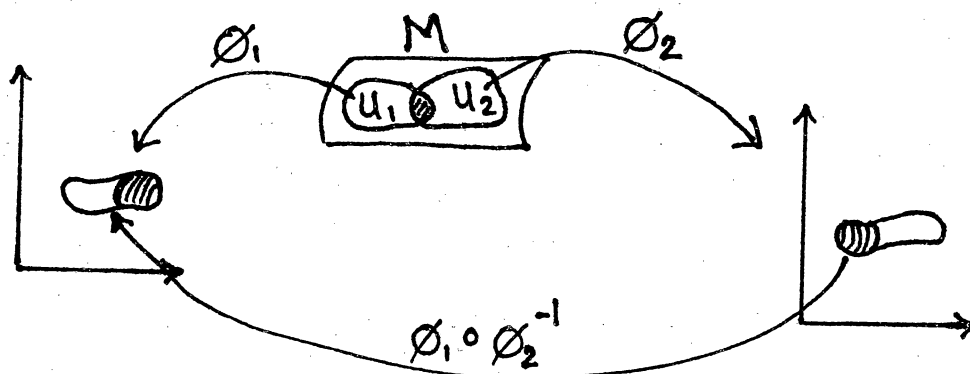
Now we define a special continuous function.

**Definition 2.6** Let  $X$  be a topological space and  $U \subseteq X$  be an open set. A *chart* is a continuous function  $\phi : U \rightarrow \mathbb{R}^n$  that has a continuous inverse  $\phi^{-1} : \phi(U) \rightarrow U$ .



**Figure 2.7** A chart on topological space  $X$

**Definition 2.8** An  $n$ -manifold is a topological space  $M$  equipped with charts  $\phi_\alpha : U_\alpha \rightarrow \mathbb{R}^n$ , where  $U_\alpha$  are open sets covering  $M$ , such that the transition functions  $\phi_\alpha \circ \phi_\beta^{-1}$  are continuous. We refer to the set of charts as an *atlas*. (See Fig. 2.9)



**Figure 2.9** Manifold  $M$

**Definition 2.10** An invariant  $\chi(M)$  of a manifold  $M$  is a map from the set of all manifolds to the complex numbers such that homeomorphic manifolds have the same invariant. (Recall that a homeomorphism between two topological spaces is a continuous bijection with continuous inverse.)

Our intention in this chapter is to describe Fukuma/Hosono/Kawai's (FHK) [FHK94] construction method for building a topological invariant (state sum invariant) of a closed orientable 2-manifold. Investigating the two dimensional case

will provide us with a better understanding of Chung/Fukuma/Shapere's (CFS) state sum invariant of 3-manifolds [CFS94]. Before turning to the FHK invariant in detail we provide a brief overview of the theory below.

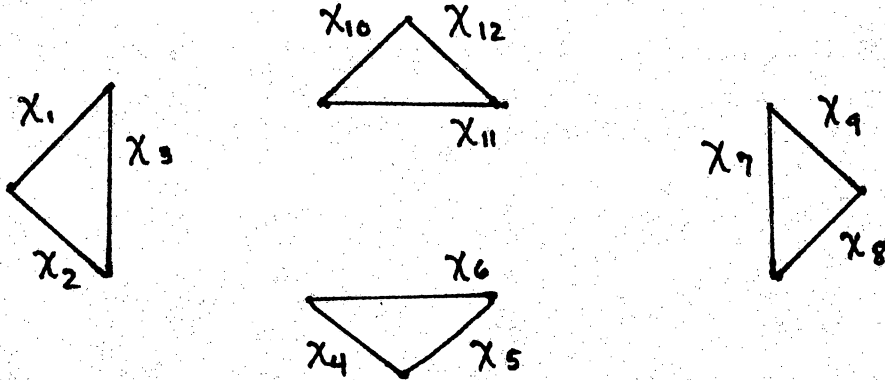
FHK begin with a triangulation of a 2-manifold. (See Fig. 2.11)



**Figure 2.11** (*2-sphere*)

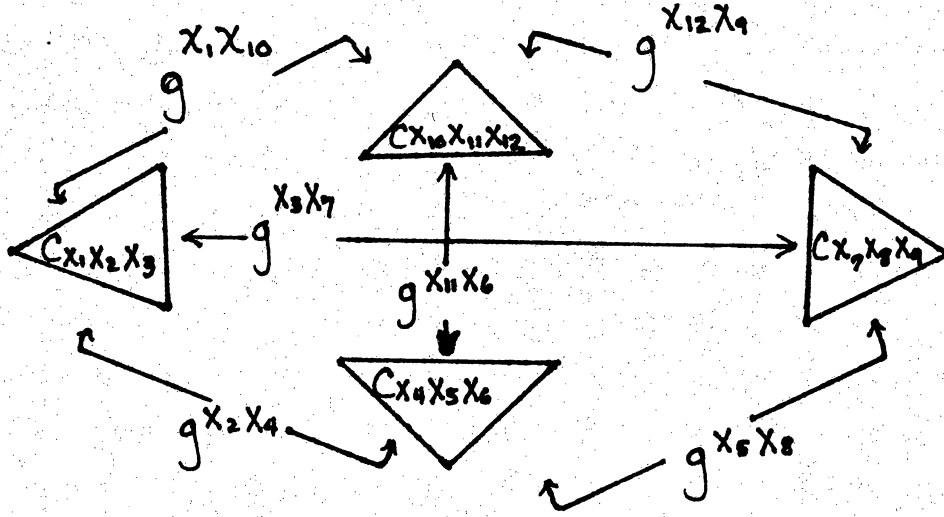
(*tetrahedron*)

They decompose the triangulated manifold and label all the edges with some choice of elements from an index set  $\{x_i\}$ .



**Figure 2.12** *Decomposition of triangulation of manifold*

Each triangle of the decomposition is identified by a complex value  $C_{x_i x_j x_k}$ , where  $x_i$  are the labels on the face edges. These values are referred to in FHK theory as the *face weights*. In preparation to reassemble the triangulation adjacent edges are identified using a complex quantity  $g^{x_i x_j}$ , referred to as a *gluing operator*, which is indexed by the labelling of corresponding edges in the decomposition.



**Figure 2.13** *Reassembly of triangulation*

For a given labelling of edges with elements from the index set the product of all face weights and gluing operators is taken. Edges in the triangulation are then assigned a different labelling from the same index set and the entire procedure is repeated. This process continues until all the possible labellings from the index set have been exhausted. The Fukuma/Hosono/Kawai state sum invariant is acquired by taking the sum of all the products for every labelling of the decomposed triangulation.

$$Z = \sum_{\text{labellings}} \prod_{\Delta \in D} \prod_{\langle uv \rangle} C_{xyz}(\Delta) g^{uv} \quad (2.14)$$

where  $\Delta \in D$  indicates product over all triangles in the decomposition  $D$ , and  $\langle uv \rangle$  indicates product over all glued edges.

If the weights  $g_{xy}$  and  $C_{xyz}$  are chosen judiciously we can be certain that the complex valued function  $Z$  (our state sum invariant) is topologically invariant and effectively partitions the space of underlying manifolds by their topological types.

## 2.1 Formal Definitions

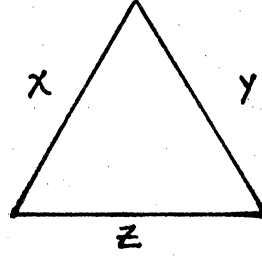
Having presented the basic idea behind the construction of the FHK state sum invariant, we now embark upon a formal presentation of their theory.

What we referred to informally as a *decomposition* of the triangulation of the closed orientable manifold is referred to by FHK as a *two dimensional lattice*. The word lattice is not standard mathematical terminology in this context, but is rather used in the sense that physicists use the term: A collection of polygons with edges identified pairwise. What we referred to earlier as *labellings* of the lattice with elements of an index set is formally described as *colorings of the lattice  $L$*  with elements of a *color set*.

**Definition 2.15** A *lattice field theory* (LFT) is a specification of a rule for assigning a weight (complex value in this case) to each possible coloring of the lattice.

In order to make FHK's theory *topological* it is necessary that we demonstrate that the resulting weight will remain unchanged under arbitrary local deformations of the underlying lattice. These deformations must be topologically legal moves (ie. basically no ripping or tearing). It is only after such a requirement is satisfied that we may refer to the theory as a *topological lattice field theory*, TLFT. We will investigate these arbitrary deformations in section 2.2.

After labelling a triangular face in the lattice with three elements of an index set, say  $x, y, z \in X$ , we determine a value associated to that face. The coloring of the triangle is read in a counter clockwise fashion and the complex value that is assigned to that triangular face in the process is referred to formally as a *face weight*  $C_{xyz}(\Delta) \in \mathbb{C}$ . It is natural to impose cyclic symmetry in the coloring of triangular faces such that the following weights are identical:



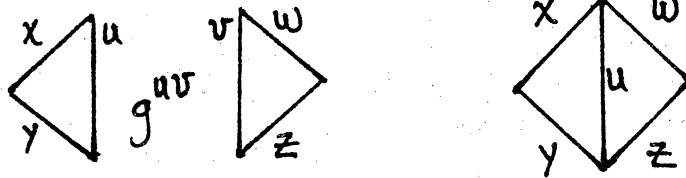
$$C_{xyz} = C_{yzx} = C_{zxy}$$

**Figure 2.16** *Coloring of a triangular face in the lattice*

In the reassembling process of FHK's theory a mysterious complex valued gluing operator  $g^{xy}$  was introduced. At this point all we know is that it is used to identify edges of adjacent triangles.

**Example 2.17** In gluing two faces of the lattice the following diagrams and products of complex numbers are equivalent:

$$\sum_{u,v} C_{xyu} \cdot g^{uv} \cdot C_{vzw} \equiv \sum_u C_{xy}^u \cdot C_{uzw} \quad (2.18)$$



**Figure 2.19** *Gluing faces*

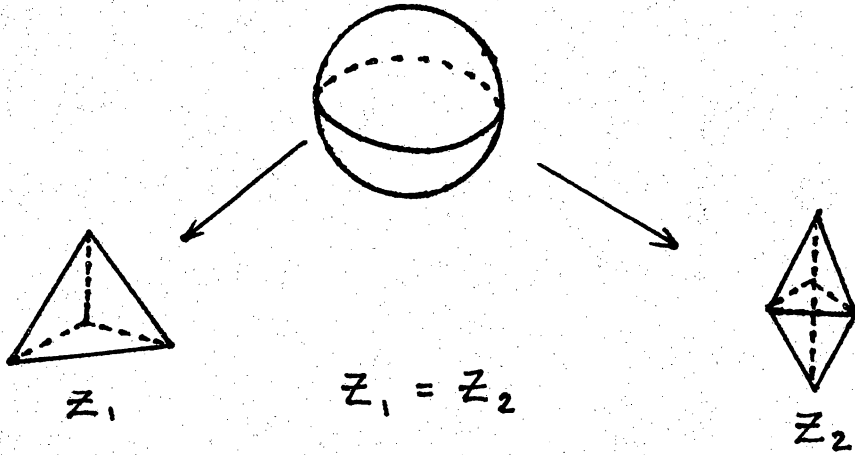
**Remark:** Indices of  $C_{xyz}$  are raised by contracting with gluing operator. In this case the  $v$  coloring becomes a  $u$  coloring when contracted. (Hereafter summation notation will be suppressed.)

**Definition 2.20** The *partition function* of a LFT is a weighted sum over all possible colorings of the lattice. It is given schematically by:

$$Z(L) = \sum_{\text{colorings}} \prod_{\Delta \in L} \prod_{\langle uv \rangle} C_{xyz}(\Delta) g^{uv} \quad (2.21)$$

where  $\prod_{\Delta \in L}$  indicates product over all triangles in the lattice  $L$ , and  $\prod_{\langle uv \rangle}$  indicates product over all glued edges.

The FHK partition function is a number that is associated to a particular triangulation (lattice)  $L$  of a closed orientable 2-manifold. It will be a *topological invariant* because it will be carefully constructed in such a manner that will not depend upon the triangulation, but only upon the topological type of the underlying manifold. (See Fig. 2.20)



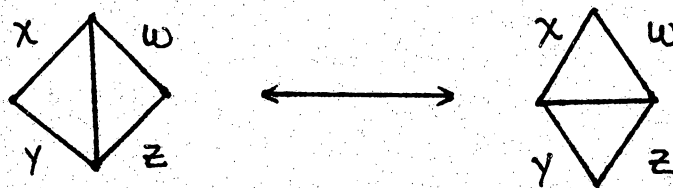
**Figure 2.22** The partition function  $Z$  for two distinct triangulations of the same closed 2-manifold produces an identical complex value



## 2.2 Topological Invariance

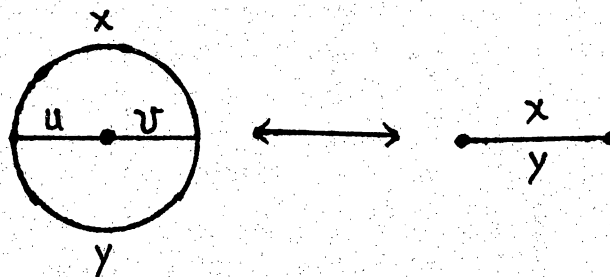
Our research leads us now to the issue of topological invariance of the FHK theory. Alexander demonstrated [A30] that all triangulations of a topological manifold are related by a set of topology-preserving moves. Later [GV92] [TV92] [B92] it was shown that two basic moves generate all topologically equivalent two dimensional triangular lattices.

The *two-two move* flips an edge between two adjacent triangles, thus transforming two triangles into two new triangles.



**Figure 2.23** *Two-two move*

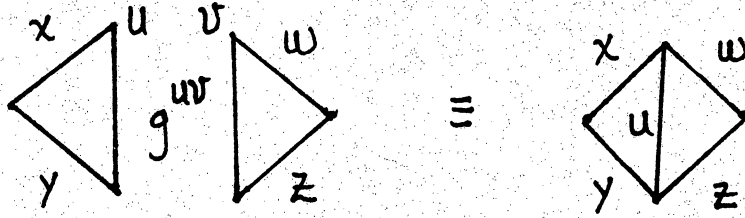
The *bubble move* collapses a pair of triangles with two edges in common to a single edge.



**Figure 2.24** *Bubble move*

By Alexander's theorem (as in [GV92]) a LFT whose partition function is invariant under the 2-2 move and the bubble move is invariant under *any* local changes of triangulation. Therefore, the lattice field theory is independent of the triangulation chosen and depends only upon the topology of the underlying manifold. This is indeed the defining property of a topological lattice field theory.

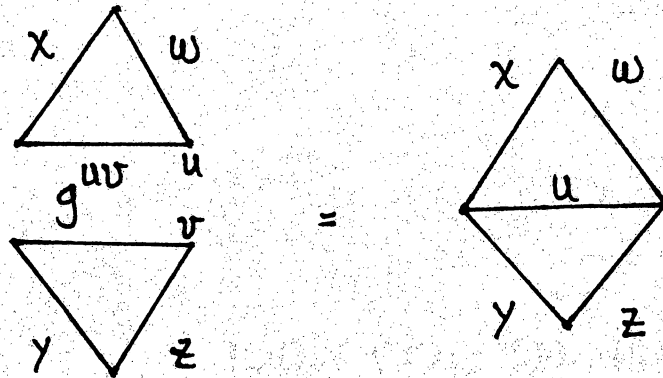
We intend to determine the algebraic expression representing the 2-2 and bubble moves. Such expressions will represent the algebraic conditions on the fundamental weights  $C_{xyz}$  that will ensure invariance of the theory under the Alexander moves. We first consider figure 2.22. The triangle on the left-hand side may be constructed via face weights and gluing operators as follows:



$$C_{xyu}C_{vzw}g^{uv} \equiv C_{xy}^u C_{uzw}$$

**Figure 2.25** Construction of left-hand side triangle for 2-2 move

The right-hand side triangle may be constructed via:



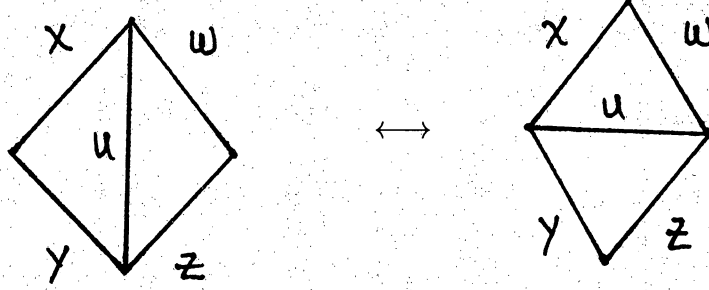
$$C_{wxu}C_{vyz}g^{uv} = C_{yz}^u C_{uwx}$$

**Figure 2.26** Construction of right-hand side triangle for 2-2 move

By application of the cyclic symmetry of our face weights and the commutativity of  $\mathbb{C}$  we may express the right-hand side triangle in a modified form:

$$\begin{aligned}
C_{wxu}C_{vyz}g^{uv} &\equiv C_{yz}{}^u C_{uwx} \\
&= C_{uwx}C_{yz}{}^u \\
&= C_{xuw}C_{yz}{}^u
\end{aligned}$$

Therefore, to ensure the topological invariance of the partition function  $Z(L)$  under the 2-2 move we must have the following equivalence:



$$C_{xy}{}^u C_{uzw} = C_{xuw} C_{yz}{}^u$$

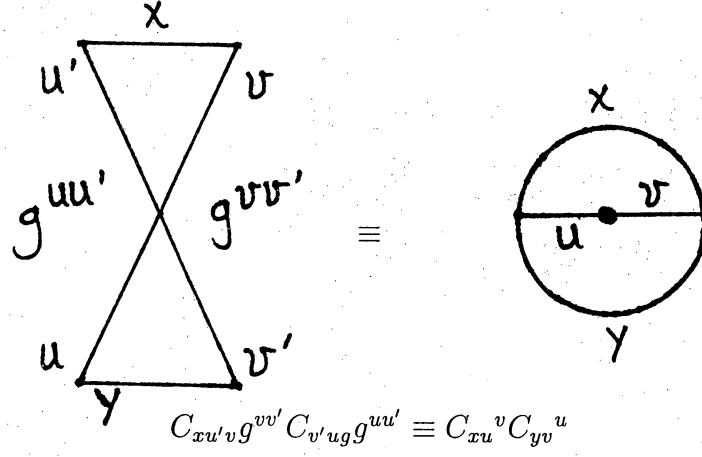
**Figure 2.27** 2-2 move algebraic condition

Our algebraic condition for 2-2 invariance may be expressed as

$$C_{xy}{}^u C_{uz}{}^w = C_{xu}{}^w C_{yz}{}^u \quad (2.28)$$

where we have raised  $w$  on both sides for later convenience.

To develop the bubble invariance equation we first observe that the “bubble” may be constructed as follows:

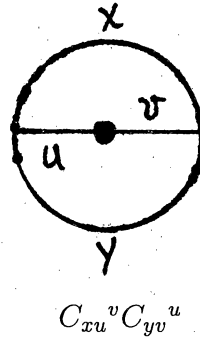


**Figure 2.29** *Construction of the bubble*

Algebraically, this is represented by:

$$\begin{aligned}
 C_{xu'} g^{vv'} C_{v'u} g^{uu'} &= C_{xu'}^v C_{v'u} g^{uu'} && \text{\{by action of } g^{vv'}\text{\}} \\
 &= C_{xu}^v C_{yv}^u && \text{\{by action of } g^{uu'}\text{\}} \\
 &= C_{xu}^v C_{yv}^u && \text{\{by cyclic symmetry\}}
 \end{aligned}$$

Therefore, the two triangles with two common edges is represented by the product  $C_{xu}^v C_{yv}^u$ . (See figure 2.29)

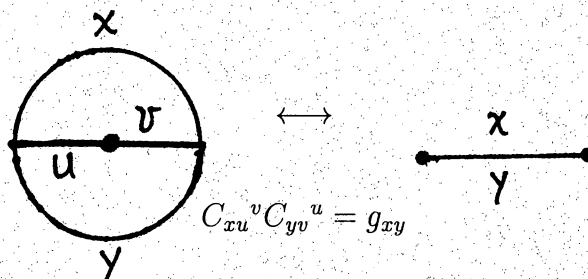


**Figure 2.30** *Algebraic description of the bubble*

We now identify the diagram  $\frac{x}{y}$  with  $g_{xy}$ , the matrix inverse of the gluing operator  $g^{xy}$ . (The matrix inverse  $g_{ij}$  satisfies  $g^{ik} g_{kj} = \delta_i^j$ , where  $\delta_i^j$  is the

Kronecker Delta.) With lowered indices  $g_{xy}$  is referred to as the *metric*. Then the inverse metric is just the gluing operator  $g^{xy}$ .

It follows that invariance under the bubble move implies:



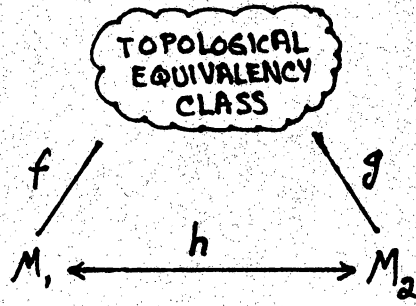
**Figure 2.31** Algebraic condition for the bubble move

Invariance under the bubble move is represented in the following algebraic condition which we refer to as the bubble invariance equation. It actually defines our metric in terms of face weights.

$$C_{xu}^v C_{yv}^u = g_{xy} \quad (2.32)$$

In conclusion, given a lattice field theory defined by data  $(C_{xyz}, g^{xy})$  the necessary and sufficient conditions for it to be topological (ie. for the partition function to be invariant under changes of triangulation of the underlying manifold) are equations (2.27) 2-2 invariance and equation (2.31) bubble invariance.

The general idea is that when we have two homeomorphic 2-manifolds their triangulations are in the same topological equivalency class, where all triangulations are related by the two invariance moves described above. The partition function for each of the classes is unique. Therefore a partition function classifies homeomorphic manifolds, making it a genuine topological invariant of the manifold. (See Fig. 2.28)

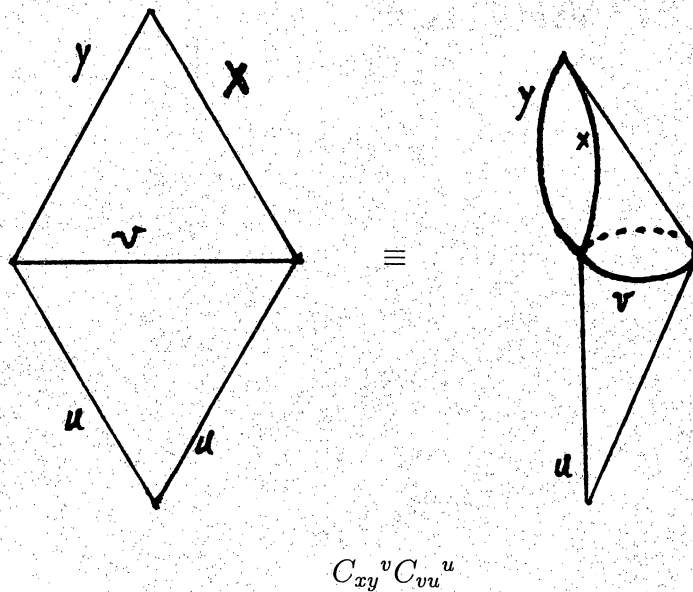


Let  $f, g, h$  be homeomorphisms and  $M_1, M_2$  be 2-manifolds.

**Figure 2.33** *Classifying homeomorphic manifolds*

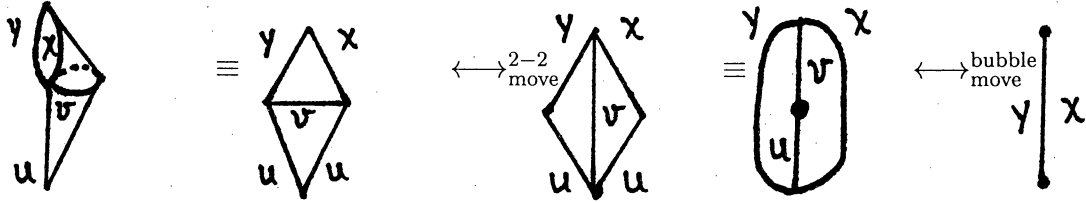
Before leaving this subsection, we demonstrate how our two invariance equations (2.27) and (2.31) lead to a third, the *cone move*. The purpose of studying invariance under the cone move is that it will aid in our development of the three dimensional TLFT in chapter three.

The two triangles on the left of figure 2.27 can be manipulated into a three dimensional cone by identifying the two edges labelled by  $u$ . Assigning the same algebraic code for the cone picture as we did for the two triangles on the left, we identify the cone by  $C_{xy}^v C_{vu}^u$ .



**Figure 2.34** *Coding the cone*

If we apply the 2-2 and bubble moves to the cone we may develop a new invariance move.



$$C_{xy}^v C_{vu}^u = C_{xv}^u C_{yu}^v = g_{xy}$$

**Figure 2.35** *Developing the cone invariance move*

So we may express the cone move by the equation:

$$C_{xy}^v C_{vu}^u = g_{xy} \quad (2.36)$$

Figure 2.30 effectively demonstrates that the cone and bubble move are equivalent; therefore, we may use either the pair (2.27) and (2.31), or the pair (2.27) and (2.34) to generate all topology preserving deformations of our lattice.

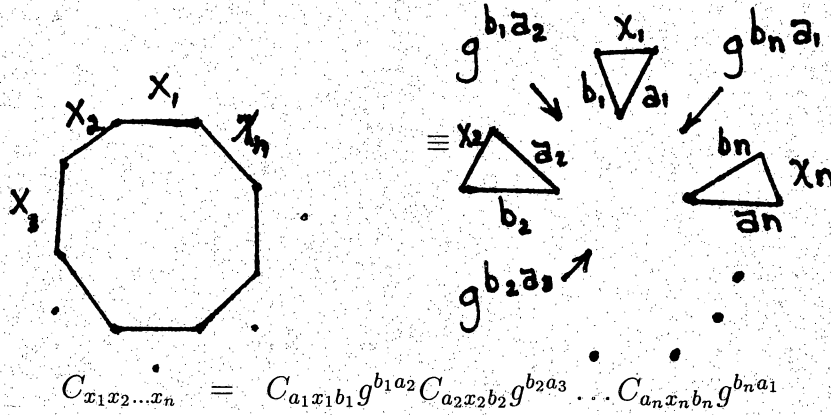
### 2.2.1 Extending to Non-Triangular Lattices

What if we triangulated our manifold into a non-triangular lattice, or more generally, into a lattice with both triangular and non-triangular faces? Can we still use our current approach to define a topological lattice field theory on the lattice?

Yes. For the triangular faces we simply use the topology preserving 2-2 and bubble moves to relate all topologically equivalent triangular lattice sections.



For the polygonal lattices containing no triangles we will simply impose subdivision invariance on the generalized weights for arbitrary n-gons  $C_{x_1 x_2 \dots x_n}$ . Since n-gons can be decomposed into triangles, we note that they are completely determined by our old triangular weights. So we lose no generality by considering any type of triangulated manifold.



**Figure 2.37** *Decomposition of n-gon into triangles*

The topological invariance established in equations (2.27) and (2.31) for triangular lattices is applicable to our general lattice. The 2-2 and bubble invariance equations guarantee that the weights for n-gonal faces (*generalized weights*) are well defined. In the context of our lattice this means that the partition function is independent of the triangular decomposition selected.

Since all higher weights are completely determined by the original triangular weights, we gain nothing new (ie. no new TQFT) by considering a generalized arbitrary polygonal lattice. Therefore, our lattice field theory is valid for any type of triangulation.

## 2.3 Algebraic Correspondence

We have shown that a two dimensional TLFT is comprised of a set of colors  $X$ , face weights  $C_{xyz}$ , gluing operators  $g^{xy}$  whose action on face weights is defined by  $C_{xyz'}g^{zz'} := C_{xy}^z$ ; all subject to the constraints imposed by the 2-2 invariance (2.27) and bubble invariance (2.31) equations. In this section we will show that these conditions are precisely the defining conditions of a semisimple associative algebra. The main theorem is

**Theorem 2.38** *Two dimensional topological lattice field theories are in one-to-one correspondence with semisimple associative algebras with unit.*

*Proof:* The outline of the proof is as follows. First we will show that, given a TLFT we may construct a semisimple associative algebra with the weights  $C_{xy}^z$  as structure constants. Semisimplicity will be shown to follow from the invertibility of the metric defined by the bubble invariance Equation (2.31). The reverse implication follows essentially from Wedderburn's Theorem, but it will be easy enough to prove directly using the facts at our disposal after the first half of the proof.

( $\Rightarrow$ ) We will prove the right implication in the following detail:

- Define a set  $A$  indexed by our given set of colors  $X$ .
- Define a vector space structure on set  $A$ .
- Define multiplication on our vector space  $A$ , which transforms it into an algebra.
- Define the unit of our algebra  $A$ .
- Show that  $A$  is associative.
- Show that  $A$  is semisimple.

To begin, we construct an associative algebra  $A$ . To each  $x \in X$  define a set  $A$  consisting of formal symbols  $\phi_x$ . The vector space structure on  $A$  is given by

taking the formal direct sum of these symbols, which then become basis elements of  $A$ :

$$A := \bigoplus_{x \in X} \mathbb{C} \phi_x \quad (2.39)$$

Note that the dimension of the vector space  $A$  is equal to the order of the index set  $X$ .

Next we define multiplication on  $A$  by

$$\phi_x \cdot \phi_y := C_{xy}{}^z \phi_z \quad (2.40)$$

and extend by linearity. That is, we define the weights  $C_{xy}{}^z := C_{xyz'} g^{zz'}$  to be the structure constants of the algebra.

To define the unit of the algebra  $A$  we first demonstrate

$$u^x C_{xy}{}^z = \delta_y{}^z = u^x C_{yx}{}^z \quad (2.41)$$

where we set

$$u^x := g^{xy} C_{yu}{}^u \quad (2.42)$$

We then use this result to get the defining property of a unit element. We will be using the following variation of the cone equation (2.34)

$$C_x{}^{yv} C_{vu}{}^u = g_x{}^y \quad (2.43)$$

noting that  $g_x{}^y = \delta_x{}^y$ .

*Proof:* (of Equation (2.40))

$$\begin{aligned} \phi_i &= \\ \delta_z^i \phi_z &= \\ {}^z\phi_z \circ_x n &= \\ \phi_x \cdot \phi_x n &= \\ \phi_x n \cdot \phi_x &= I_A \cdot \phi_i \end{aligned}$$

and

$$\begin{aligned} \phi_i &= \\ \delta_z^i \phi_z &= \\ {}^z\phi_z \circ_x n &= \\ n \phi_x \cdot \phi_x &= I_A \cdot \phi_i \end{aligned}$$

because (2.40) implies

$$I_A := n \phi_x \quad (2.44)$$

The unit of the algebra  $A$  is given by the element

□

$$\begin{aligned} &= \\ \delta_z^{\hat{h}} &= \\ \delta_z^{\hat{h}} g_{xz} &= \\ g_{xz} g_{xz} &= \\ g_z^{\hat{h}} &= \\ C_z^{\hat{h}} \circ_w n &= \\ C_n^{\hat{h}} \circ_w n &= \\ C_n^{\hat{h}} \circ_w n &= \\ g_{xz} C_n^{\hat{h}} \circ_w n &= \\ g_{xz} C_n^{\hat{h}} \circ_w n &= \end{aligned}$$

And

$$\begin{aligned} &= \\ \delta_z^{\hat{h}} &= \\ g_{xz} g_{xz} &= \\ g_z^{\hat{h}} &= \\ C_z^{\hat{h}} \circ_w n &= \\ C_n^{\hat{h}} \circ_w n &= \\ C_n^{\hat{h}} \circ_w n &= \\ g_{xz} C_n^{\hat{h}} \circ_w n &= \\ g_{xz} C_n^{\hat{h}} \circ_w n &= \end{aligned}$$

{by assumption  
{action of  $g$   
{ $\mathbb{C}$  commutes  
{cyclic symmetry  
{Equation (2.42)  
{by action of  $g_{xz}$

Associativity of  $A$  follows from Equation (2.27) (invariance under the 2-2 move) and linearity:

$$\begin{aligned}
& C_{xy}^u C_{uz}^w \phi_w = C_{xu}^w C_{yz}^u \phi_w \quad \{\text{eq. (2.27)} \\
\Leftrightarrow & C_{xy}^u C_{uz}^w \phi_w = C_{yz}^u C_{xu}^w \phi_w \quad \{\mathbb{C} \text{ commutes} \\
\Leftrightarrow & C_{xy}^u \phi_u \cdot \phi_z = C_{yz}^u \phi_x \cdot \phi_u \quad \{\text{Def mult} \\
\Leftrightarrow & C_{xy}^u \phi_u \cdot \phi_z = \phi_x C_{yz}^u \phi_u \quad \{\text{commutivity} \\
\Leftrightarrow & (\phi_x \cdot \phi_y) \cdot \phi_z = \phi_x \cdot (\phi_y \cdot \phi_z)
\end{aligned}$$

It remains to show that the algebra  $A$  is semisimple (see, e.g., [DMG93]).

We are beginning with a TLFT, so it is assumed that the gluing operator  $g^{xy}$  exists. The gluing operator is the inverse metric, so we are specifically showing that the metric being invertible implies that our algebra is semisimple. We outline the proof of this claim as follows:

1. Define an algebra as semisimple if it may be written as the direct sum of simple algebras.
2. Show the metric  $g_{xy} := C_{xv}^u C_{yu}^v$  and the trace form on the algebra  $A$  given by  $g_{xy} := (\phi_x, \phi_y)$  are identical.
3. Show that left and right multiplication are adjoints relative to the trace form.
4. Define the radical of our algebra.
5. Show that the radical is a two sided ideal of the algebra.
6. Demonstrate that the radical is the largest two sided ideal of  $A$  consisting entirely of nilpotent elements.
7. Demonstrate that the invertibility of the metric is equivalent to the radical of our algebra being zero.

With the above items firmly established we may validate the claim that our algebra is semisimple. Applying items 1 and 7, we may restate our hypothesis as follows:

Show that if the radical of the algebra  $A$  vanishes, then  $A$  is the direct sum of simple algebras.

We will prove this conjecture with the following format:

- a) Let  $I$  be a minimal nonzero two sided ideal of  $A$ , and  $I^\perp$  be the orthogonal complement of  $I$  relative to the trace form.
- b) Prove that  $I^\perp$  is also a two sided ideal of  $A$ .
- c) Show that  $A$  is the algebra direct sum of  $I$  and  $I^\perp$ .
- d) Use the minimality of  $I$  and the fact that both  $I$  and  $I^\perp$  are both two sided ideals to show that  $I$  is a simple algebra.
- e) Observe that by induction on the dimension of the algebra  $A$ ,  $I^\perp$  is a direct sum of simple algebras.
- f) Conclude that  $A$  is semisimple.

First we recall some basic definitions.

**Definition 2.45** An algebra  $A$  is *simple* if it contains no nontrivial ideals (*i.e.* no ideals other than the trivial ones  $0$  and  $A$ ).

**Definition 2.46** An algebra  $A$  is the (algebra) *direct sum* of two algebras  $A_1$  and  $A_2$ , written  $A = A_1 \oplus A_2$  if every element  $a \in A$  may be written uniquely as  $a = a_1 + a_2$  where  $a_1 \in A_1$ ,  $a_2 \in A_2$ , and  $A_1 \cap A_2 = A_1 A_2 = A_2 A_1 = 0$ .

**Definition 2.47** An algebra  $A$  is *semisimple* if it may be expressed as the algebra direct sum of simple algebras.

Recall that bubble invariance (2.31) of our TLFT implies that the metric, defined by

$$g_{xy} := C_{xv}{}^u C_{yu}{}^v$$

is invertible. We may reformulate this condition as follows. For  $a \in A$  let the map  $a_L : A \rightarrow A$  be left multiplication by  $a$ , *i.e.*  $x \mapsto ax$ . Observe that

$(ab)_L = \iota(ab) = \iota(a)\iota(b) = a_L b_L$ . As  $A$  has a unit, the map  $\iota$  defined by  $a \mapsto a_L$  embeds  $A$  into  $End(A)$  as an algebra homomorphism, where  $End(A)$  is the endomorphism algebra of  $A$ .

Given an endomorphism  $S \in End(A)$  we may define  $tr(S)$ , the *trace* of  $S$ , to be the trace of the matrix representation of  $S$  in a given basis. By cyclic invariance of the trace we now argue that the map  $tr: End(A) \rightarrow \mathbb{C}$  is indeed a well defined function.

First we recognize that every element of  $End(A)$  has a matrix representation, hence the trace acts on all element of  $End(A)$ . Next we recall that, under a change of basis, the matrix representation of a linear endomorphism gets transformed via a similarity transformation. For instance, suppose that  $S$  is some endomorphism, and let  $S'$  and  $S''$  denote its matrix representation in two different bases. Then there exists some matrix element  $T$  such that  $S'' = TS'T^{-1}$ . So if we define  $tr(S)$  to be equal to  $tr(S')$  (*i.e.* we pick a particular basis, because we know what the trace of a matrix is) then we will find that  $tr(S) = tr(S'')$  as well. Hence  $tr$  maps all similar matrix representations of each element in  $End(A)$  to a unique complex number in its codomain.

Using the trace we may define a symmetric bilinear form  $( , ) : A \times A \rightarrow A$  by

$$(a, b) := tr(a_L b_L) \tag{2.48}$$

called the *trace form* on  $A$ . Then the metric components are simply given by

$$(\phi_x, \phi_y) = g_{xy} \quad (2.49)$$

*Proof:* By definition,

$$(\phi_x, \phi_y) = \text{tr}(\phi_{xL}\phi_{yL})$$

But we have

$$\begin{aligned} \phi_{xL}\phi_{yL} \cdot \phi_z &= \phi_{xL} \cdot \phi_y\phi_z && \{ \text{by left mult} \\ &= \phi_{xL} \cdot C_{yz}^w \phi_w && \{ \text{by mult of } \phi_i \\ &= C_{yz}^w \phi_{xL} \cdot \phi_w && \{ \text{by linearity} \\ &= C_{yz}^w \phi_x \phi_w && \{ \text{by left mult} \\ &= C_{yz}^w C_{xw}^u \phi_u \end{aligned}$$

which implies

$$\text{tr}(\phi_{xL}\phi_{yL}) = C_{yz}^w C_{xw}^z = g_{yx} = g_{xy}$$

as claimed.  $\square$

**Lemma 2.50** *Left and right multiplication are adjoints relative to the trace form*

$$(ax, b) = (a, xb), \forall a, b, x \in A \quad (2.51)$$

*Proof:*

$$\begin{aligned} (ax, b) &= \text{tr}((ax)_L b_L) \\ &= \text{tr}(a_L x_L b_L) \\ &= \text{tr}(a_L (xb)_L) \\ &= (a, xb) \quad \square \end{aligned}$$

**Definition 2.52** The *radical* of an algebra  $A$  is the subset

$$J(A) = \{x \in A \mid (x, y) = 0, \forall y \in A\} \quad (2.53)$$

**Lemma 2.54** *The radical is a two-sided ideal of  $A$ .*



*Proof:*

$$\begin{aligned}
a \in J(A) \text{ and } x, b \in A &\Rightarrow (a, xb) = 0 \\
&\Rightarrow (ax, b) = 0 \quad \{\text{by lemma 2.49}\} \\
&\Rightarrow (ax) \in J(A) \quad \{\text{by definition}\} \\
&\Rightarrow J(A) \text{ is a } \textit{right ideal}.
\end{aligned}$$

Similarly,

$$\begin{aligned}
&(a, bx) = 0 \\
&\Rightarrow (bx, a) = 0 \quad \{\text{by symmetry of trace}\} \\
&\Rightarrow (b, xa) = 0 \quad \{\text{by lemma 2.49}\} \\
&\Rightarrow (xa, b) = 0 \\
&\Rightarrow (xa) \in J(A) \\
&\Rightarrow J(A) \text{ is a } \textit{left ideal}.
\end{aligned}$$

Hence,  $J(A)$  is a two-sided ideal.

□

Recalling that a *nilpotent element*  $a$  of an algebra is one for which there exists a positive integer  $n$  such that  $a^n = 0$ , we observe a property of the radical with respect to nilpotent elements.

**Lemma 2.55**  *$J(A)$  is the largest right ideal of  $A$  consisting entirely of nilpotent elements.*

*Proof:* We first set out to prove that every element of the radical, which we already established to be a right ideal of  $A$  by Lemma 2.53, is nilpotent. Let  $x \in J(A)$ . We wish to argue that  $x^{n-1}$  is an element of  $A$ . Since  $x$  is in the radical it must be an element of the algebra  $A$ . By closure of  $A$  under multiplication  $x^n$  is in  $A$  for all positive integers  $n$  and since our algebra has a unit  $x^0$  is also in  $A$ . Therefore,  $x^{n-1}$  is in  $A$  for all positive integers  $n$ .

Since  $x \in J(A)$  means that  $(x, y) = 0$  for all  $y \in A$ , it is clear that  $(x, x^{n-1}) = 0$  for all positive integers  $n$ . Hence, by the definition of the trace,

$\text{tr}(x_L^n) = 0$  for all  $n$ . By a standard result in linear algebra (see, *e.g.* Herstein (1975) p. 315)  $x_L$ , and hence  $x$  itself, is nilpotent.

To show that  $J(A)$  is indeed the largest such ideal, we demonstrate that any other ideal consisting entirely of nilpotent elements must be contained in the radical. Suppose  $K$  is a right ideal consisting entirely of nilpotent elements. For any  $x \in K$  and all  $y \in A$ ,  $xy \in K$  because  $K$  is a right ideal. But  $xy$  is nilpotent since it lives in  $K$ , so  $(xy)_L$  is nilpotent, and therefore  $\text{tr}((xy)_L) = 0$  because all the characteristic values of a nilpotent transformation are zero. Hence, by the comment following Definition 2.46, we may show that  $(x, y) = 0$  for all  $y \in A$ :

$$\begin{aligned} 0 &= \text{tr}((xy)_L) \\ &= \text{tr}(x_L y_L) \\ &= (x, y) \end{aligned}$$

which implies that  $x \in J(A)$ . □

**Definition 2.56** We say that the trace form is *nondegenerate* if the radical vanishes (*i.e.*  $J(A) = \{0\}$ ), and *degenerate* otherwise.

We have yet to demonstrate that if the metric is invertible, then  $A$  is semisimple. But we claim that:

**Lemma 2.57** *The nondegeneracy of the trace form is equivalent to the invertibility of the metric.*

To prove our conjecture we will take one half of the implication, specifically

*the metric  $\mathbf{g}$  being invertible implies that the trace form is nondegenerate*

and prove the contrapositive:

*The trace form being degenerate implies that the metric  $\mathbf{g}$  is invertible.*

The reverse implication follows similarly.

*Proof:* Assume the trace form to be degenerate. Then for all  $b$  in  $A$  there exists an element  $a$  in  $A$  such that  $(a, b) = (b, a) = 0$ . Let  $a = a^x \phi_x$  and  $b = b^y \phi_y$  (summation convention). Then

$$\begin{aligned}
& (b, a) = 0 \\
\Rightarrow & (b^y \phi_y, a^x \phi_x) = 0 \\
\Rightarrow & b^y a^x (\phi_y, \phi_x) = 0 \\
\Rightarrow & b^y a^x g_{yx} = 0 && \text{(by definition } g_{xy}) \\
\Rightarrow & \vec{b}^T \cdot \mathbf{g} \cdot \vec{a} = 0 && \text{(} g_{xy} \text{ components of } \mathbf{g} \text{)} \\
\Rightarrow & \mathbf{g} \cdot \vec{a} = 0 && \text{(nondegeneracy of usual dot product)} \\
\Rightarrow & \mathbf{g} \cdot \vec{a} = 0 \cdot \vec{a} \\
\Rightarrow & \text{matrix } \mathbf{g} \text{ has a 0 eigenvalue} \\
\Rightarrow & \text{product of all eigenvalues equals zero} \\
\Rightarrow & \det \mathbf{g} = 0 \\
\Rightarrow & \mathbf{g} \text{ is not invertible}
\end{aligned}$$

As our proof is reversible, we have proved the entire conjecture.  $\square$

It remains to show that if the metric is invertible, *i.e.* the radical of  $A$  vanishes, then  $A$  is semisimple. Specifically, we will demonstrate that if  $J(A) = \{0\}$ , the algebra  $A$  is the direct sum of simple algebras. We begin by recalling that definition of a minimal ideal.

**Definition 2.58** An ideal  $I$  of a ring  $R$  is a *minimal ideal* if and only if for any other ideal  $I'$  in  $R$  with  $\{0\} \subseteq I' \subseteq I$ , either  $I' = \{0\}$  or  $I' = I$ .

If  $I \neq \{0\}$  is a minimal ideal then for every other ideal  $I'$  of the ring either  $I \subseteq I'$  or  $I \cap I' = \{0\}$ . The argument is that we assume that  $I$  is minimal according to our definition and we let  $I'' = I \cap I'$ , for  $I'$  some other arbitrary ideal of  $R$ . We note that  $I''$  is an ideal because the intersection of two ideals is again an ideal. It is obvious that  $\{0\} \subseteq I'' \subseteq I$  and since  $I$  is minimal either  $I'' = \{0\}$  or  $I'' = I$ . If the first case is true then  $I \cap I' = \{0\}$ . And if the second case is true then  $I \cap I' = I$ , which is equivalent to saying  $I \subseteq I'$ . Hence, if  $I \neq \{0\}$  is a minimal ideal we may conclude that  $I \subseteq I'$  or  $I \cap I' = \{0\}$  for any other ideal  $I'$ .

Let  $I$  be a minimal nonzero 2-sided ideal of  $A$  and let

$$I^\perp = \{x \in A \mid (x, y) = 0, \forall y \in I\}$$

be its orthogonal complement relative to the trace form. Then an argument similar to the proof of Lemma 2.53 implies  $I^\perp$  is also a two sided ideal of  $A$ .

By minimality of  $I$ , either  $I \subseteq I^\perp$  or  $I \cap I^\perp = \{0\}$ . Let us consider the first case. If  $I \subseteq I^\perp$  we would have  $\text{tr}(x_L^n) = 0$  for all  $x \in I$  and all positive integers  $n$ . (For example, if  $x \in I$  then  $\text{tr}(x_L^3) = 0$  by the following argument. If  $x \in I$ , then  $x^2 \in I$  since  $I$  is an ideal. However, due to the fact that  $I \subseteq I^\perp$ ,  $x^2$  must also live in  $I^\perp$ . Then, by the definition of  $I^\perp$ ,  $(x^2, x) = 0$ .) But Lemma 2.54 would imply that  $I \in J(A) = 0$ , contradicting our assumption that  $I$  is nonzero. Hence  $I \not\subseteq I^\perp$ .

So it must be the case that  $I \cap I^\perp = \{0\}$ , from which it follows from linear algebra that  $A = I \oplus I^\perp$  as vector spaces. But  $I$  and  $I^\perp$  are both two sided ideals, so we must also have

$$II^\perp = I^\perp I = 0 \tag{2.59}$$

whereupon we may conclude that  $A = I \oplus I^\perp$  as an algebra direct sum.

By minimality,  $I$  is a simple algebra. For, suppose it were not. Let  $H \subset I$  be a nontrivial two-sided ideal in  $I$ . Let  $h \in H$  and  $x \in A$ . For any  $x \in A$  we may write  $x = x_1 + x_2$  where  $x_1 \in I$  and  $x_2 \in I^\perp$ . Also, since  $h \in H \subset I$ , we know that  $hx_2 = 0$  by Equation (2.58). So it is clear that  $hx = h(x_1 + x_2) = hx_1 + 0 = hx \in H$ . Hence  $H$  is a right ideal of  $A$ . Similar reasoning shows that  $H$  is also a left ideal of  $A$ , contradicting the minimality of  $I$ . Therefore  $I$  is a simple algebra.

At this point in our argument we only know that our algebra  $A$  can be decomposed into the direct sum of a simple algebra  $I$  and its orthogonal complement. It is our desire to demonstrate that in the final analysis all the direct

summands of  $A$  are simple algebras. To that end we next argue that  $J(I^\perp) = \{0\}$ ; therefore, by induction we may argue that  $I^\perp$  is the direct sum of simple pieces.

**Lemma 2.60** *Let  $A = A_1 \oplus A_2$  be an algebra direct sum. Then*

$$J(A) = J(A_1) \oplus J(A_2).$$

*Proof:* Let  $x \in J(A_1) \oplus J(A_2)$ . Then  $x = x_1 + x_2$  where  $x_1 \in J(A_1)$  and  $x_2 \in J(A_2)$ .

By the definition of  $J(A_j)$  we also note that  $(x_j, y_j) = 0$  for all  $y_j \in A_j$ . (i.e.

$$(x_1, y_1) = 0 \text{ for all } y_1 \in A_1 \text{ and } (x_2, y_2) = 0 \text{ for all } y_2 \in A_2)$$

By the supposition of our lemma,  $A = A_1 \oplus A_2$ , we know that for any  $x, y \in A$  we have  $x = x_1 + x_2$  and  $y = y_1 + y_2$  for some  $x_1, y_1 \in A_1$  and  $x_2, y_2 \in A_2$ , so

$$\begin{aligned} (x, y) &= (xy, 1) \\ &= ((x_1 + x_2)(y_1 + y_2), 1) \\ &= (x_1y_1 + x_2y_2, 1) \\ &= (x_1y_1, 1) + (x_2y_2, 1) \\ &= (x_1, y_1) + (x_2, y_2) \end{aligned}$$

from which we conclude that

$$(x, y) = (x_1, y_1) + (x_2, y_2) \tag{2.61}$$

Hence, by our opening argument, in the case where  $x \in J(A_1) \oplus J(A_2)$  Equation (2.60) implies that  $(x, y) = 0$  for all  $y \in A$ , so  $x \in J(A)$ . The converse follows similarly.  $\square$

Since we have assumed that the radical of  $A$  vanishes, and that  $A = I \oplus I^\perp$  we conclude by Lemma 2.59 that the radical of its direct summands,  $J(I)$  and  $J(I^\perp)$ , each vanish. Hence we have established that  $J(I^\perp) = \{0\}$ .

By induction on dimension,  $I^\perp$  is an algebra direct sum of its minimal two-sided ideals, each of which is a simple algebra, so  $A$  is indeed semisimple.

( $\Leftarrow$ ) We must show that, given a semisimple associative algebra  $A$  with structure constants  $C_{xy}{}^z$  and unit  $1_A = u^x \phi_x$  we may construct a two dimensional TLFT. We begin by defining the metric on our algebra as

$$g_{xy} = C_{xw}{}^z C_{yz}{}^w \quad (2.62)$$

This is the bubble invariance equation, but we must also show that  $g_{xy}$ , so defined, is nondegenerate.

In our attempt to demonstrate the existence of the inverse metric  $g^{xy}$  we next observe that since we assumed  $A$  was semisimple we may write  $A = A_1 \oplus \cdots \oplus A_m$  where each  $A_i$  is a simple algebra. By the definition of a simple algebra the radicals of  $A_i$  must vanish, because  $J(A_i) = A_i$  would imply by Lemma 2.54 the absurd conclusion that every element in  $A_i$ , including the unit, is nilpotent. Hence all the radicals  $J(A_i) = \{0\}$  and we may conclude via Lemma 2.59 that their direct sum,  $J(A)$ , also vanishes. By Definition 2.55 such a conclusion implies that the metric  $g_{xy}$  defined by Equation (2.48) is nondegenerate. Therefore, by Lemma 2.56, the inverse metric (*i.e.* the gluing operator of our TLFT) does indeed exist.

The 2-2 invariance equation follows because the associativity argument given in the first half of the proof is reversible. Specifically, associativity implies the 2-2 invariance equation:

$$C_{xy}{}^u C_{uz}{}^w = C_{yz}{}^u C_{xu}{}^w \quad (2.63)$$

Finally, applying the nondegenerate metric to the structure constants we may define triangular weights

$$C_{xyz} := C_{xy}{}^{z'} g_{z'z}$$

satisfying cyclic symmetry  $C_{xyz} = C_{yzx} = C_{zxy}$  by:

$$\begin{aligned}
C_{xyz} &= C_{xy}{}^{z'} g_{zz'} && \{\text{by definition}\} \\
&= C_{xy}{}^{z'} C_{z'u}{}^v C_{zu}{}^u && \{\text{by def. } g_{zz'}\} \\
&= C_{xz'}{}^v C_{yu}{}^{z'} C_{zv}{}^u && \{\text{by eq. (2.27)}\} \\
&= C_{xz'}{}^v C_{yz}{}^u C_{uv}{}^{z'} && \{\text{by eq. (2.27)}\} \\
&= C_{yz}{}^u C_{uv}{}^z C_{xz'}{}^v \\
&= C_{yz}{}^u g_{ux} \\
&\equiv C_{yzx} && \{\text{by definition}\}
\end{aligned}$$

Similarly:

$$\begin{aligned}
C_{yzx} &= C_{yz}{}^{x'} g_{x'x} && \{\text{by definition}\} \\
&= C_{yzx'} C_{x'u}{}^v C_{xv}{}^u && \{\text{by def. } g_{x'x}\} \\
&= C_{yx'}{}^v C_{zu}{}^{x'} C_{xv}{}^u && \{\text{by eq. (2.27)}\} \\
&= C_{yx'}{}^v C_{zx}{}^u C_{uv}{}^{x'} && \{\text{by eq. (2.27)}\} \\
&= C_{zx}{}^u C_{uv}{}^{x'} C_{yx'}{}^v \\
&= C_{zx}{}^u g_{uy} && \{\text{by def. } g_{uy}\} \\
&= C_{zxy} && \{\text{by definition}\}
\end{aligned}$$

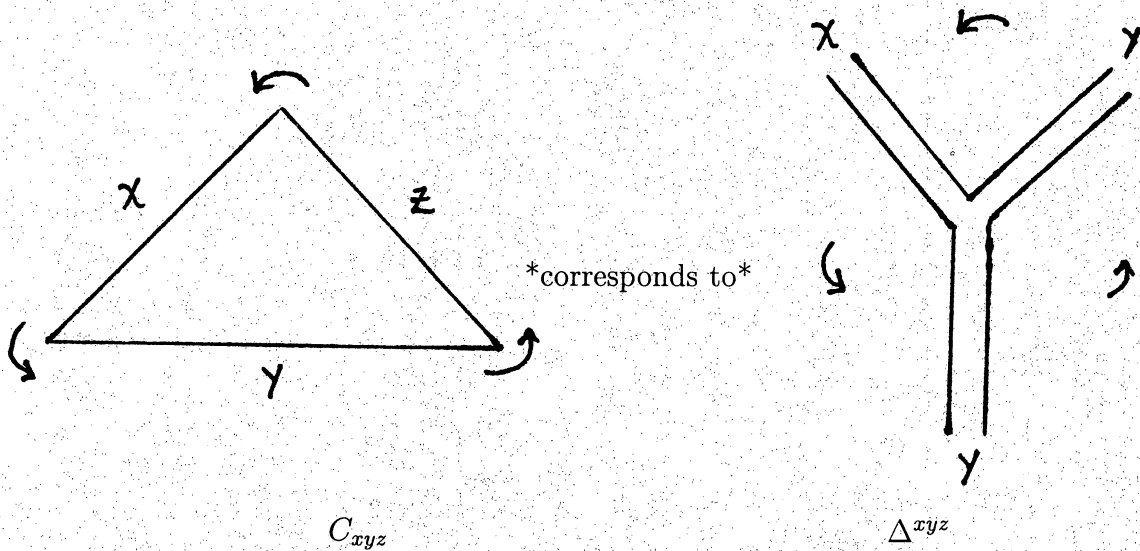
Hence,  $C_{xyz} = C_{yzx} = C_{zxy}$ .

This completes the proof of theorem 2.37.

## 2.4 Dual Formation

In this section we describe an equivalent approach to constructing a topological lattice field theory using thickened *trivalent graphs* instead of triangles. The information derived here will prove to be relevant in the construction of our three dimensional TLFT in the next chapter.

Given any triangulation of a 2-manifold we may define its dual by associating a vertex to every face, and connecting them across edges of the original triangulation. In order to help distinguish the original triangulation from its dual, we thicken the lines of the dual lattice. Under this duality, the weights  $C_{xyz}$  become weights  $\Delta^{xyz}$ :



**Figure 2.64** *Trivalent graph corresponding to face weights*

And the gluing operator  $g^{xy}$  becomes the gluing operator  $h_{xy}$ .

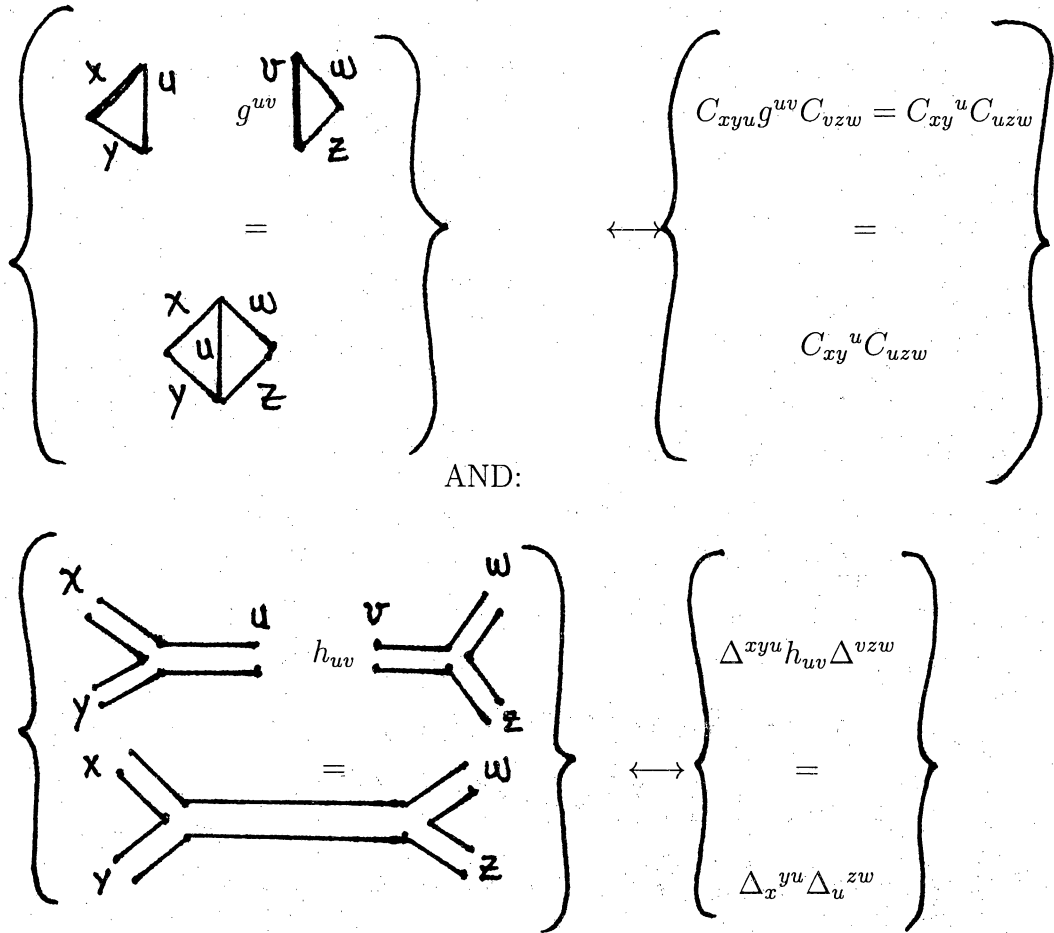
$$g^{xy} \longleftrightarrow h_{xy}$$

glues edges of  
adjacent triangles

glues lines emanating  
from vertices of adjacent  
trivalent vertices

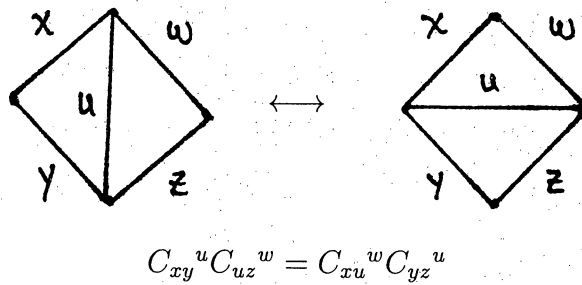


So, for example, an elementary gluing operation in both the original and dual formations may be illustrated as follows:

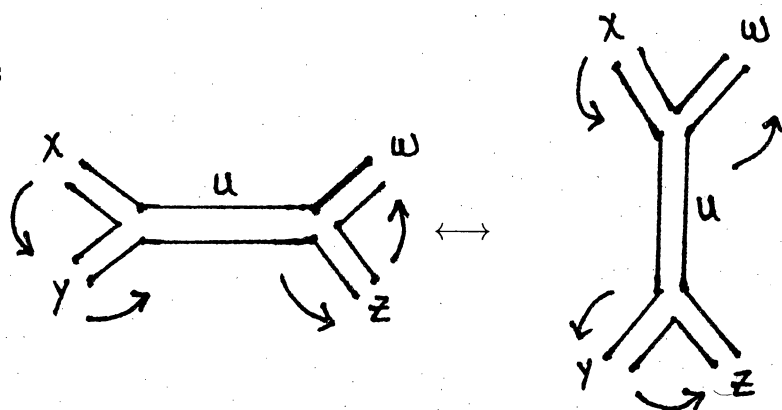


**Figure 2.65** *Gluing operation in both formulations*

In the dual formulation, 2 – 2 invariance



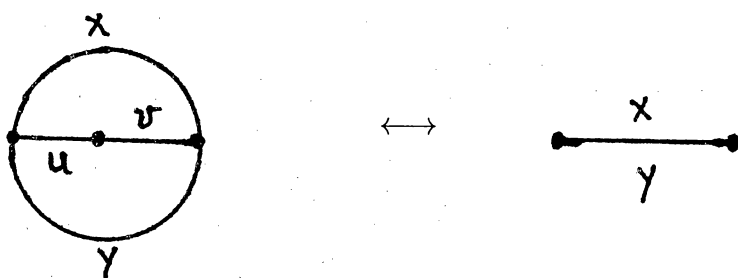
becomes



$$\Delta_x^{yu} \Delta_u^{zw} = \Delta_x^{uw} \Delta_u^{yz} \quad (2.66)$$

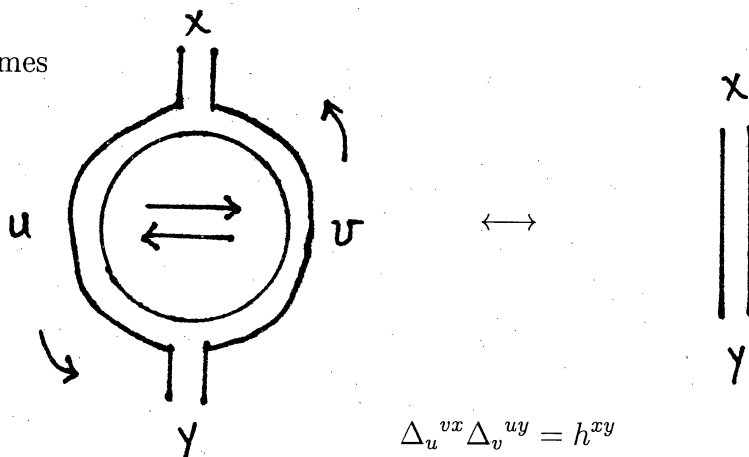
Figure 2.67 2-2 invariance

while bubble invariance



$$C_{xu}^v C_{yv}^u = g_{xy} \quad (2.68)$$

becomes



$$\Delta_u^{vx} \Delta_v^{uy} = h^{xy} \quad (2.69)$$

Figure 2.70 Bubble invariance

(This picture explains the terminology “bubble move”).

In two dimensions these two formulations are equivalent, so we may consider one or the other. But in three dimensions, as we shall see, we must couple these two structures together in a compatible manner, and this leads directly to Hopf algebras.

## Chapter 3

# Three Dimensional Chung-Fukuma-Shapere State Sum Invariant

### 3.1 3-D Definitions, Weighting Rules and Partition Function

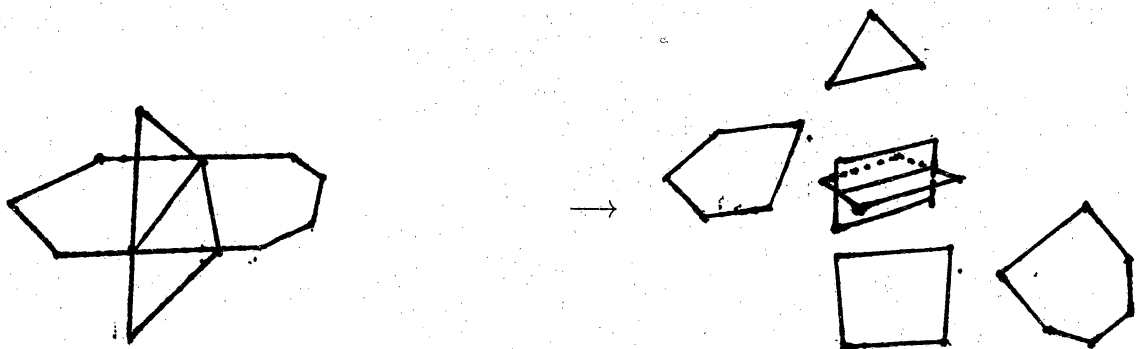
We extend the FHK concepts to Chung/Fukuma/Shapere theory (CFS) [CFS94] by extending our lattice field theory to three dimensions. As in the two dimensional case, we begin with a lattice. In usual approaches to three dimensional lattice field theories the faces of the lattice would be glued together, but CFS choose to glue along *hinges* instead, in order to preserve as much of the previous formalism as possible.

**Definition 3.1** A *lattice* ( $L$ ) is a collection of polygonal faces with edges glued together along one dimensional hinges.

**Definition 3.2** A *hinge* is a meeting of three or more edges (an open neighborhood of the line along which faces meet). (See Fig. 3.3)

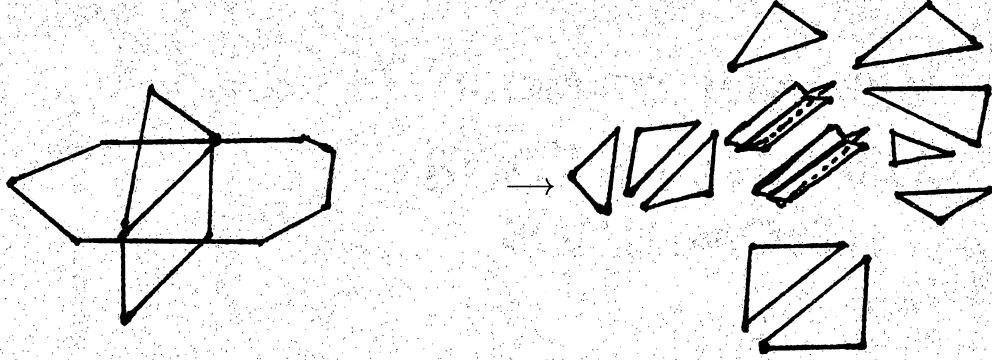
In constructing a three dimensional topological field theory we will color each edge of each face with a color  $x$  from our index set  $X$ . Then we will have to define a *hinge weight* because in three dimensions the edges of more than two faces can meet.

Consider the following example of the decomposition of an arbitrary three dimensional face/hinge structure.



**Figure 3.3** *Decomposition into polygonal faces and 4-valent hinge*

This reduces further into triangular faces and trivalent hinges:



**Figure 3.4** *Triangular decomposition*

The weighting rules we are about to introduce will be invariant under this subdivision.

In order to determine a complete set of weights for arbitrary faces and hinges we must specify the following rules in detail in the following subsections:

- 3.1.1 weights for triangles
- 3.1.2 weights for 3-hinges
- 3.1.3 gluing rules for connecting triangles
- 3.1.4 gluing rules for connecting 3-hinges
- 3.1.5 gluing rules for connecting triangles to 3-hinges

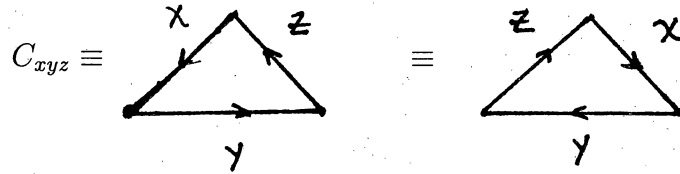
Then we will define the partition function as the product of all triangular weights and 3-hinge weights, with color indices contracted via our gluing rules.

### 3.1.1 Weighting Rules for Triangles

For all triangles in the lattice colored with  $x, y, z \in X$  associate a complex number  $C_{xyz}$  with cyclic symmetry. The weighting rule for faces is a map:

$$C : X \times X \times X \longrightarrow \mathbb{C}$$

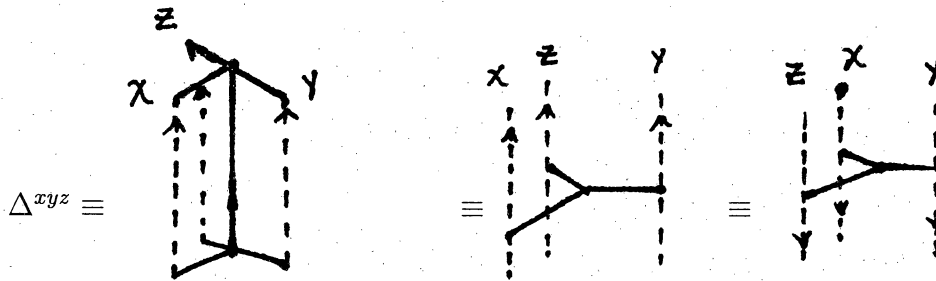
In the two dimensional case it was unnecessary to indicate the orientation of our triangular faces because they were embedded in 2-space. In the three dimensional case all 3-manifolds are assumed to be oriented, and gluing rules must respect this orientation. The problem is that in this higher dimension we are unsure which side of the triangle we are dealing with, so it becomes necessary to indicate the orientation of the faces with arrows on the edges.



**Figure 3.5** *Triangle weight*

### 3.1.2 Weighting Rules for 3-Hinges

The hinges, which are used to join three faces at one common edge, are composed of three infinitesimally thin strips whose outer edges are colored with elements from an index set. The hinge labelling is oriented in a counterclockwise direction when the arrows on the edges are directed upward. (See Fig. 3.6)



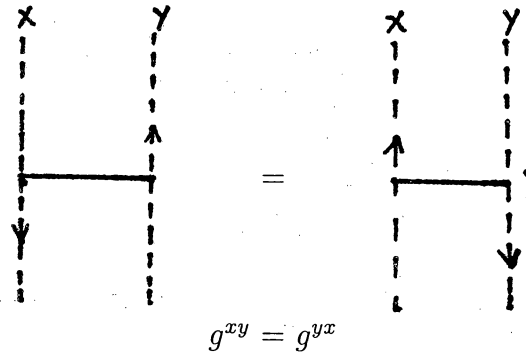
**Figure 3.6** *Hinge weights indicating that  $\Delta^{xyz} = \Delta^{zyx}$ , when the second sketch is read counterclockwise, and the third clockwise*

### 3.1.3 Gluing Triangles to Triangles

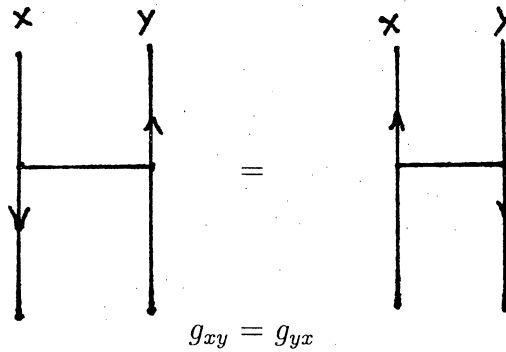
We recall that the face gluing operator  $g^{xy}$  glues triangular faces together (raises indices of  $C_{xyz}$ ). We now consider a graphical representation of the gluing operator and its inverse operator (metric) in three dimensions.

We will indicate hinge edges with dotted lines in order to distinguish them from triangle edges. Then the dotted lines will have raised indices and solid lines will have lowered indices associated to them.

In order to ensure that triangles are glued together with the appropriate orientations (so as to maintain the orientation of the original manifold) the face gluing operator  $g^{xy}$  (respectively  $g_{xy}$ ) must be represented by two oppositely oriented dotted (respectively solid) lines, as shown in Figures 3.7 and 3.8.



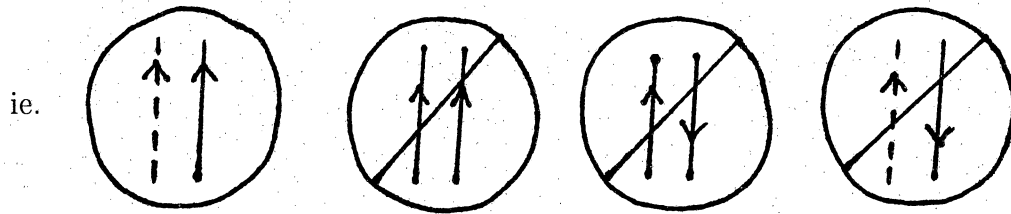
**Figure 3.7** *Graphical representation of the gluing operator*



**Figure 3.8** *Graphical representation of the inverse gluing operator*



With this convention, only dotted edges and solid edges with the same orientation are glued together. (See Fig. 3.9)



**Figure 3.9** *Gluing restrictions*

The corresponding algebraic operation is just the usual summation convention on repeated indices. (See Fig. 3.10)

$$\sum_x \equiv \begin{array}{c} x \\ \uparrow \\ \uparrow \end{array} \begin{array}{c} x \\ \uparrow \\ \uparrow \end{array} \equiv \begin{array}{c} x \\ \downarrow \\ \downarrow \end{array} \begin{array}{c} x \\ \downarrow \\ \downarrow \end{array} \equiv \begin{array}{c} x \\ \uparrow \\ \uparrow \end{array} \begin{array}{c} x \\ \uparrow \\ \uparrow \end{array}$$

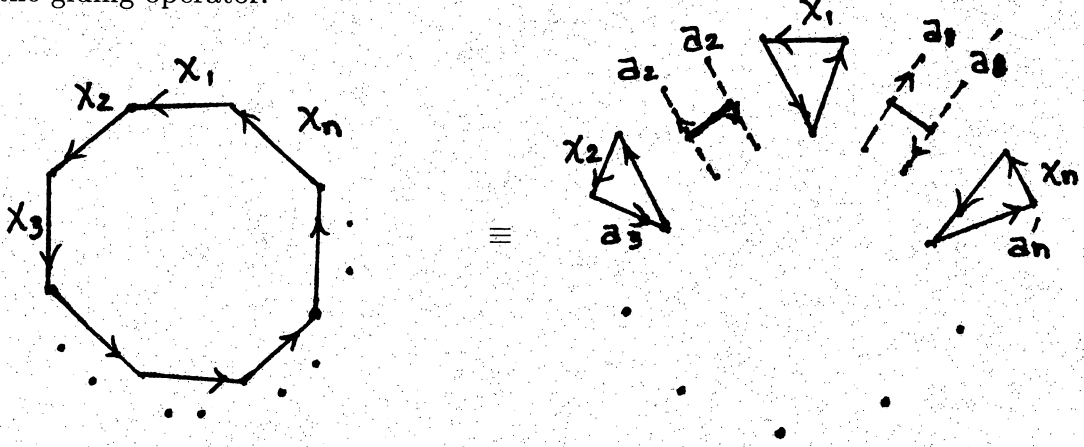
**Figure 3.10** *Summation convention on glued edges*

For an example of face gluing with these rules see Figure 3.11.

$$C_{xy}^u \quad C_{uzw} \quad = \quad C_{xyu} \quad g^{uv} \quad C_{vzw}$$

**Figure 3.11** *Algebraic code for 3d face gluing*

Given an arbitrary polygonal face, we may compute its weight just as we did in the two dimensional case, by triangulating it and gluing the internal triangles with the gluing operator.



$$\begin{aligned}
 C_{x_1 x_2 \dots x_n} &\equiv C_{a_1 x_1 a_2} g^{a_2 a'_2} C_{a'_2 x_2 a_3} \dots g^{a_n a'_n} C_{a'_n x_n a'_1} g^{a'_1 a_1} \\
 &= C_{a_1 x_1}^{a_2} C_{a_2 x_2}^{a_3} \dots C_{a_n x_n}^{a_1}
 \end{aligned}$$

**Figure 3.12** *Gluing an arbitrary polygonal face*

The polygonal weight will be independent of the particular triangulation chosen, provided we require that the weights  $C_{xyz}$  and the inverse gluing operator (metric)  $g_{xy}$  satisfy precisely the two equations, (2.27) and (2.31), that guaranteed topological invariance in the two dimensional case, namely

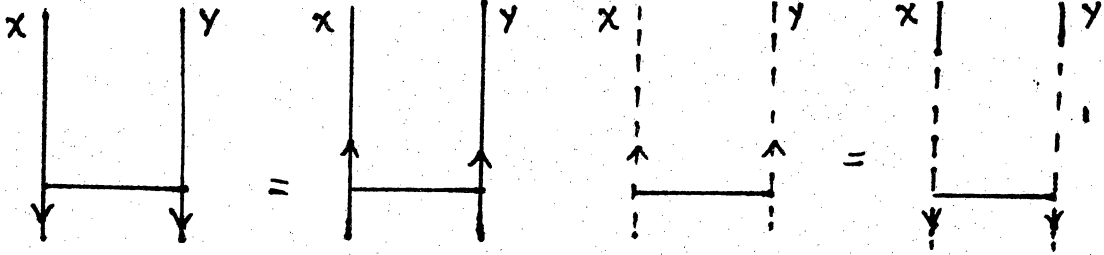
$$C_{xy}^u C_{uz}^w = C_{xu}^w C_{yz}^u \quad (3.13)$$

$$C_{xu}^v C_{yv}^u = g_{xy} \quad (3.14)$$

### 3.1.4 Gluing 3-hinges to 3-hinges

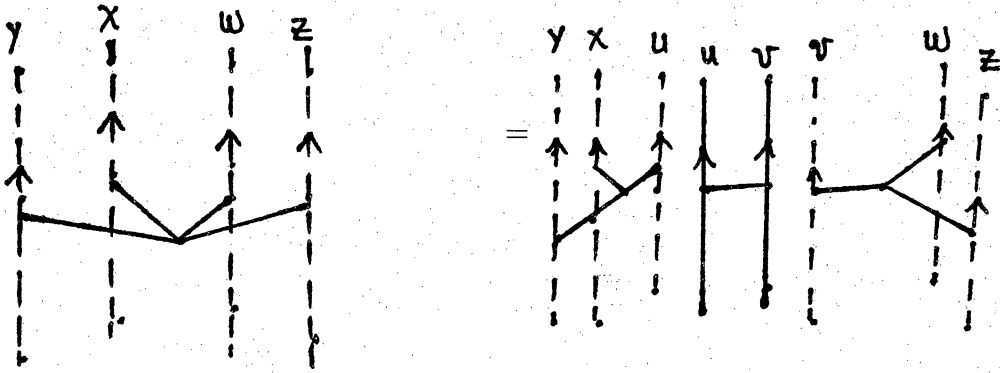
In this subsection we repeat the analysis of subsection 3.1.3 for hinges instead of for faces. To glue 3-hinges to 3-hinges we introduce the hinge gluing operator  $h_{xy}$  which raises and lower indices of the 3-hinge weight  $\Delta^{xyz}$ . Graphical representations of the

gluing operator  $h_{xy}$  and the inverse gluing operator (we call it the *cometric*)  $h^{xy}$  are as follows:



**Figure 3.15** Graphical representation of hinge gluing operators (a)  $h_{xy} = h_{yx}$  (b)  $h^{xy} = h^{yx}$

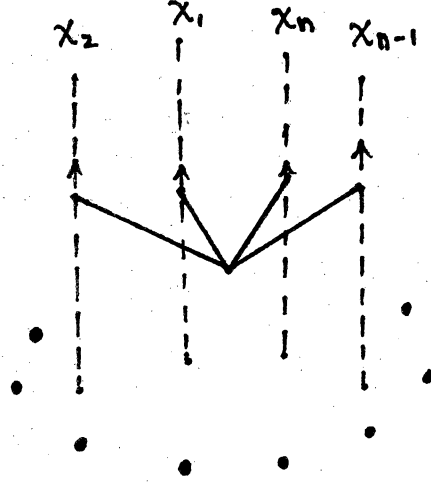
For example, we may glue two 3-hinges together to get a 4-hinge with weight  $\Delta^{xyzw}$ :



$$\begin{aligned}\Delta^{xyzw} &:= \Delta^{xyu} h_{uv} \Delta^{vzw} \\ &= \Delta^{xyu} \Delta_u^{zw}\end{aligned}$$

**Figure 3.16** Four hinge weight  $\Delta^{xyzw}$

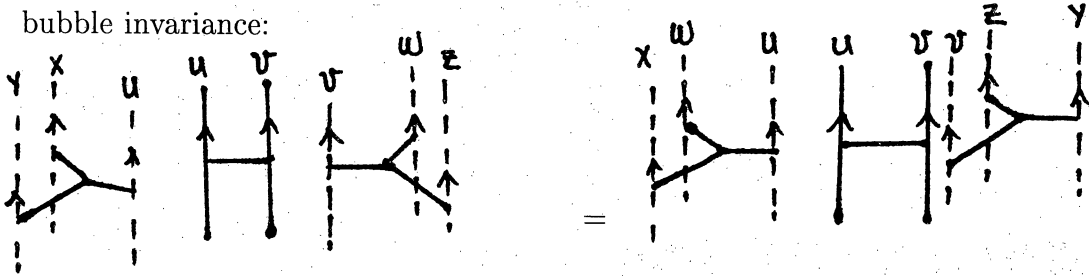
As before, we may extend this construction to arbitrary n-hinges. Such a hinge can be decomposed into a product of 3-hinges as depicted below:



**Figure 3.17** *Decomposition of  $\Delta^{x_1 x_2 \dots x_n}$  into  $\Delta_{a_1}^{x_1 a_2} \Delta_{a_2}^{x_2 a_3} \dots \Delta_{a_n}^{x_n a_1}$*

As previously, we require that the weight of the  $n$ -hinge be independent of the decomposition into 3-hinges chosen. In the plane perpendicular to the  $n$ -hinge this is equivalent to imposing 2-dimensional topological invariance for the trivalent graphs from section 2.4. (See Equations 2.66 and 2.68) Specifically, we demand that the 3-hinge weights  $\Delta^{xyz}$  and the cometric  $h_{xy}$  satisfy the dual versions of 2-2 and

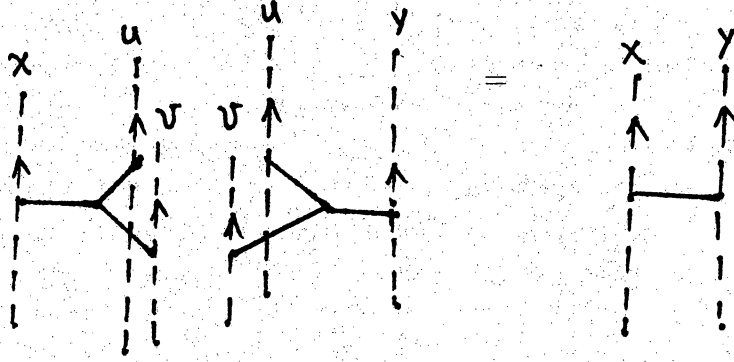
bubble invariance:



$$\Rightarrow \begin{aligned} \Delta_{xyu} \Delta_u^{zw} &= \Delta_{wxu} \Delta_u^{yz} \\ \Delta_x^{yu} \Delta_u^{zw} &= \Delta_x^{uw} \Delta_u^{yz} \end{aligned}$$

$$\Delta_x^{yu} \Delta_u^{zw} = \Delta_x^{uw} \Delta_u^{yz} \quad (3.18)$$

**Figure 3.19** *Dual 2-2 move*

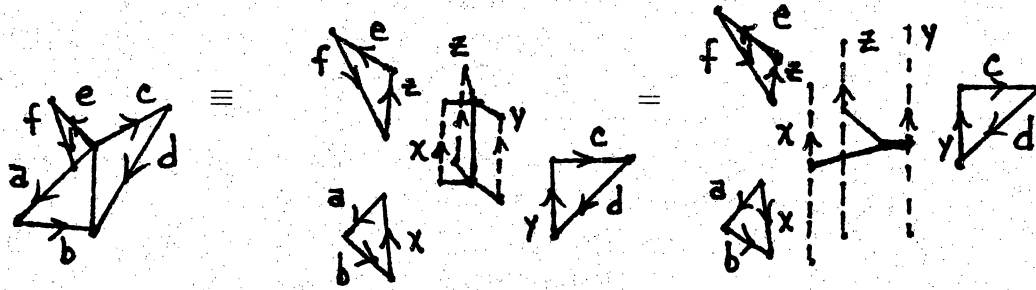


$$\Delta_v^{ux} \Delta_u^{vy} = h^{xy} \quad (3.20)$$

**Figure 3.21** *Dual bubble move*

### 3.1.5 Gluing triangles to 3-hinges

To finish our construction we must explain how to glue 3-hinges to triangles. There are two cases, depending upon whether the arrows on the triangle edges and hinge edges agree or not. In the first case the arrows are in the *same* direction.

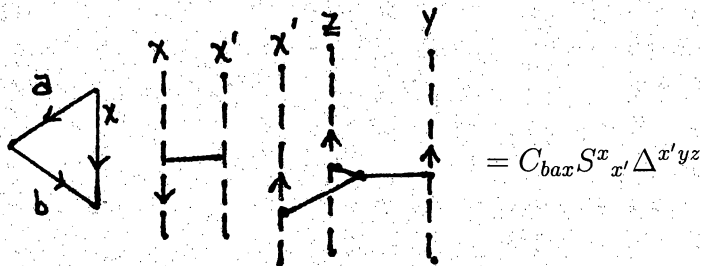


**Figure 3.22** *Triangles glued to a 3-hinge,  $C_{abx}C_{cdy}C_{efz}\Delta^{xyz}$*

In this case we merely connect the appropriate indices from each edge. In the example above we get  $C_{abx}C_{cdy}C_{efz}\Delta^{xyz}$  for the weight of the three-faced structure on the left.

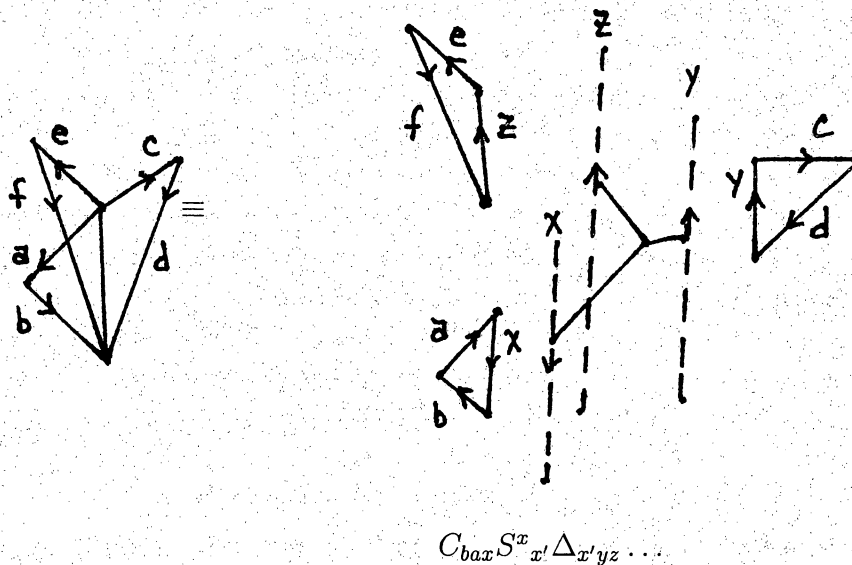
In the second case the arrows of face edge and hinge edge to be joined are in *opposite* directions. To carry out this operation we must have a way of flipping the

direction of the arrow on a hinge. This is accomplished by means of the *arrow changing operator*  $S^x_y$ . To be consistent with our diagrammatic notation, the arrow changing operator  $S^x_{x'}$  is represented by a dotted and solid line with arrows in opposite directions. (See Fig. 3.23)



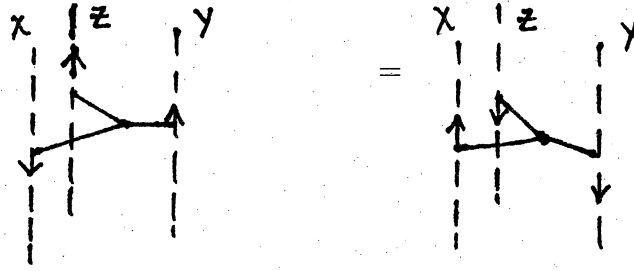
**Figure 3.23** The action of the arrow changing operator

A configuration requiring the use of the arrow changing operator is illustrated in Figure 3.24:



**Figure 3.24** A configuration requiring the arrow changing operator

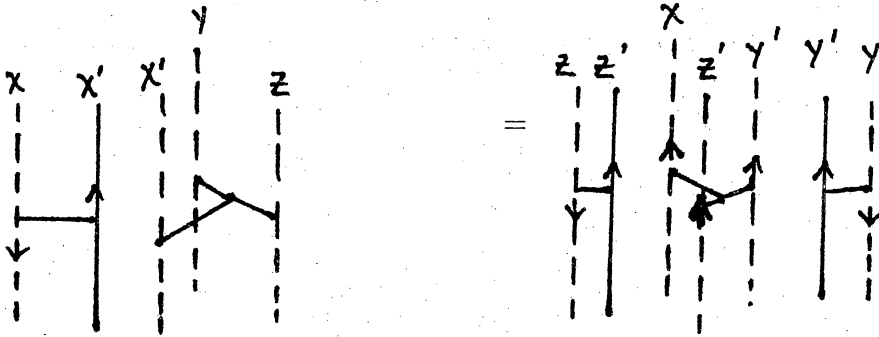
Since the following hinges should have the same weights



**Figure 3.25** *Identical hinge weights*

we require the following constraints on  $S^x_y$  and  $\Delta^{xyz}$ . (See Fig. 3.27)

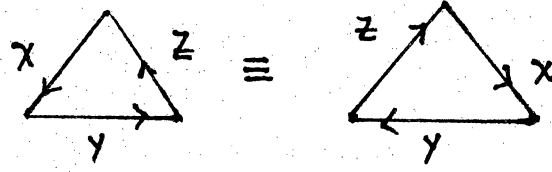
$$S^x_{x'} \Delta^{x'yz} = S^z_{z'} \Delta^{xz'y'} S^y_{y'} \quad (3.26)$$



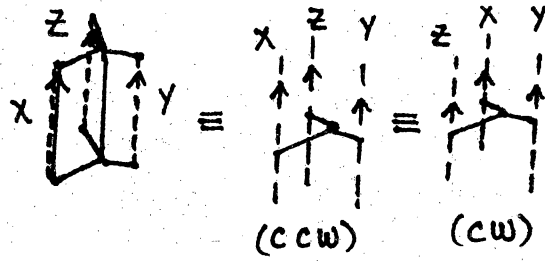
**Figure 3.27** *Constraints on  $S^x_y$  and  $\Delta^{xyz}$*

In summary, the following five weighting rules are the fundamental ingredients in the construction of a three dimensional lattice field theory:

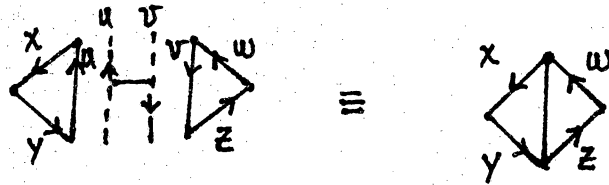
$C_{xyz}$  (triangle wt.)



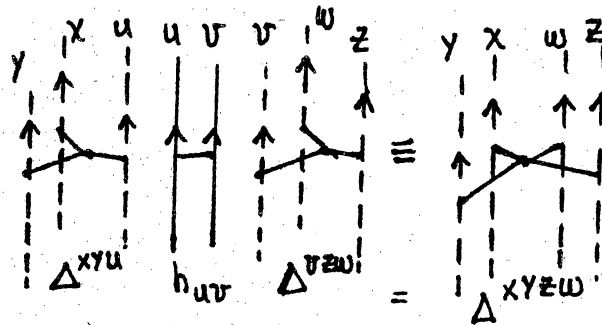
$\Delta^{xyz}$  (hinge wt.)



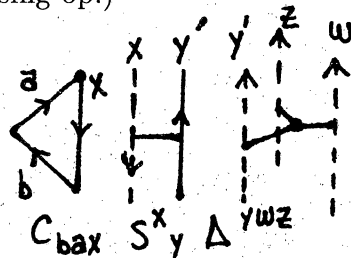
$g^{xy}$  (face gluer)



$h_{xy}$  (hinge gluer)



$S_y^x$  (arrow reversing op.)



**Figure 3.28** Five weighting rules for 3d LFT

The partition function for our three dimensional lattice field theory (LFT) is



given schematically by the expression:

$$Z(L) = \mathcal{N} \prod_{f:\text{faces}} \prod_{h:\text{hinges}} \prod_{\langle x,y \rangle} C_{a_1 a_2 \dots a_n}(f) \Delta^{b^1 b^2 \dots b^l}(h) S^x_y(e)$$

where  $\mathcal{N}$  is a normalization factor,  $\langle x, y \rangle$  indicates product over glued edges with arrow reversed, as necessary, and  $C$  and  $\Delta$  are defined in terms of the triangular decomposition of  $k$ -gonal faces and  $l$ -hinges described above, subject to the consistency conditions:

1.  $C_{xy}^u C_{uz}^w = C_{xu}^w C_{yz}^u$  (Eqn (2.27) 2-2 invariance)
2.  $C_{xu}^v C_{yv}^u = g_{xy}$  (Eqn (2.31) bubble invariance)
3.  $\Delta_x^{yu} \Delta_u^{zw} = \Delta_x^{uw} \Delta_u^{yz}$  (Eqn (3.18) dual 2-2 invariance)
4.  $\Delta_v^{ux} \Delta_u^{vy} = h^{xy}$  (Eqn (3.20) dual bubble invariance)
5.  $S^x_{x'} \Delta^{x'yz} = S^z_{z'} S^y_{y'} \Delta^{xz'y'}$  (Eqn (3.26) hinge arrow op. constraint)

The partition function  $Z(L)$  is not yet a topological invariant of the manifold on which it is defined. In the next section we develop the proper algebraic framework for the theory. This will enable us to find the additional constraints required for  $Z(L)$  to be a topological invariant.

## 3.2 Algebraic and Coalgebraic Structure

In this section we will show how the LFT data define algebra and coalgebra structures with certain properties. Recall that in the two dimensional case we constructed an algebra, which we will now call  $H$ , over  $\mathbb{C}$ , with a basis element for each element of the index set  $X$ :

$$H = \oplus_{x \in X} \mathbb{C} \phi_x. \quad (3.29)$$

And we defined multiplication on the algebra  $H$  via a map  $m$ :

$$m : H \otimes H \longrightarrow H \text{ via}$$

$$m(\phi_x \otimes \phi_y) \equiv \phi_x \cdot \phi_y := C_{xy}{}^z \phi_z \quad (3.30)$$

$$\text{where } C_{xy}{}^z := C_{xyz'} g^{z'z}$$

The constraints (2.28) and (2.32) imply that the algebra, so defined, is associative and semisimple. In terms of the map  $m$ , the associativity condition may be written:

$$m \circ (1_H \otimes m)(\phi_x \otimes \phi_y \otimes \phi_z) = m \circ (m \otimes 1_H)(\phi_x \otimes \phi_y \otimes \phi_z) \quad (3.31)$$

Also recall that invariance under the cone move implies the existence of a unit element  $u$  in our algebra (section 2.3). The unit satisfies:

$$u : \mathbb{C} \ni 1_{\mathbb{C}} \longmapsto u(1) = \underbrace{u^x \phi_x}_{1_H} \in H$$

Recollect that the defining equation for the unit in chapter two was (and still is):

$$u^x C_{xy}{}^z = \delta_y{}^z = u^x C_{yx}{}^z \quad (2.41)$$

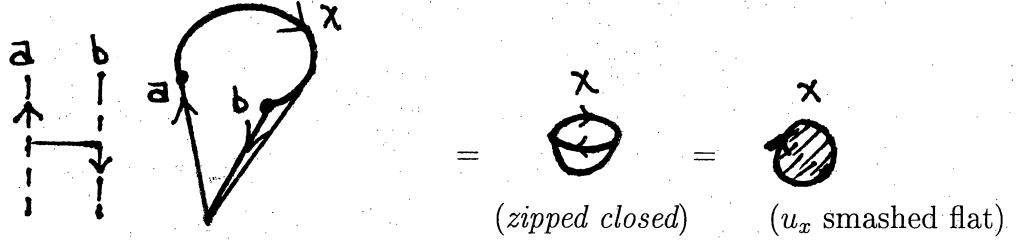
$$\text{with } u_x := C_{xa}{}^a \text{ and } u^x := g^{xy} u_y \quad (2.42)$$

### 3.2.1 Graphical representation of $u_x$

We may derive a graphical representation of  $u_x$  which will become useful to us in upcoming sections. From (2.2) we find

$$u_x = C_{xb}{}^b = C^b{}_{xb} = g^{ab} C_{axb} \quad (3.32)$$

Graphically, the right side is a triangle with two edges glued together as shown.



**Figure 3.33** *Graphical representation of  $u_x$*

So we see that  $u_x$  is represented as a 2-D disc with its boundary colored  $x$ .

Similarly, we may define an algebra  $\tilde{H} := \oplus_{x \in X} \mathbb{C} \tilde{\phi}^x$ , and a multiplication operator  $\tilde{m}$  on  $\tilde{H}$ :

$$\tilde{m} : \tilde{H} \otimes \tilde{H} \longrightarrow \tilde{H}$$

$$\tilde{m}(\tilde{\phi}^y \otimes \tilde{\phi}^z) := \Delta_x{}^{yz} \tilde{\phi}^x \quad (3.34)$$

The dual analogues of the 2-2 and bubble invariance (equations (3.18) and (3.20)) which are required for invariance under decomposition of 3-hinges, imply that  $\tilde{H}$  is associative.

$$(\tilde{m} \circ (1_{\tilde{H}} \otimes \tilde{m}))(\tilde{\phi}^x \otimes \tilde{\phi}^y \otimes \tilde{\phi}^z) = (\tilde{m} \circ (\tilde{m} \otimes 1_{\tilde{H}}))(\tilde{\phi}^x \otimes \tilde{\phi}^y \otimes \tilde{\phi}^z) \quad (3.35)$$

$\tilde{H}$  contains a unit as well:

$$\tilde{u} : \mathbb{C} \ni 1_{\mathbb{C}} \longmapsto \underbrace{\tilde{u}(1)}_{1_{\tilde{H}}} = \epsilon_x \tilde{\phi}^x \in \tilde{H} \quad (3.36)$$

where

$$\epsilon_x = h_{xy} \Delta_u^{uy} \quad (3.37)$$

There is a natural identification of  $\tilde{H}$  with the dual vector space to  $H$ . In this identification the multiplication  $\tilde{m}$  corresponds to *comultiplication*  $\Delta$  on  $H$ , and the hinge weights  $\Delta_x^{yz}$  act as the co-structure constants:

$$\Delta : H \longrightarrow H \otimes H \text{ via}$$

$$\Delta(\phi_x) := \Delta_x^{yz} \phi_y \otimes \phi_z \quad (3.38)$$

The condition of *coassociativity*, which follows by duality from associativity for  $\tilde{m}$  in  $\tilde{H}$ , is expressed by:

$$(\Delta \otimes 1_H) \circ \Delta(\phi_w) = (1_H \otimes \Delta) \circ \Delta(\phi_w) \quad (3.39)$$

Duality also directly implies that our coalgebra is *cosemisimple* and that it contains a counit  $\epsilon$  which satisfies the following condition:

$$\epsilon : H \ni \phi_x \longmapsto \epsilon(\phi_x) = \epsilon_x \in \mathbb{C}$$

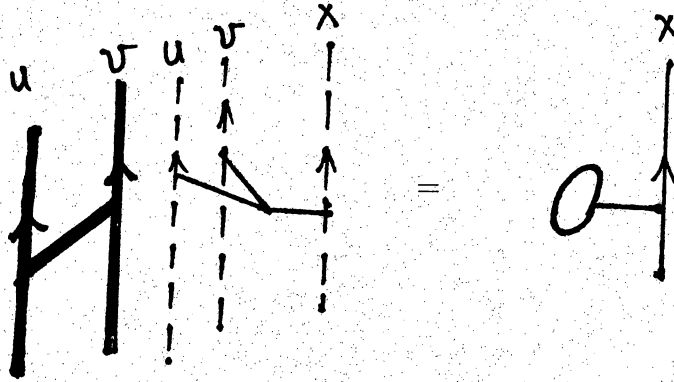
$$\Delta_x^{yz} \epsilon_z = \delta_x^y = \epsilon_z \Delta_x^{zy} \quad (3.40)$$

where

$$\epsilon_x := h_{xy} \Delta_u^{uy} = \Delta_u^u{}_x = \Delta^u_{xu} \quad (3.41)$$

### 3.2.2 Graphical representation of $\epsilon_x$

We defined  $\epsilon_x$  to be  $\epsilon_x := \Delta_u^u{}_x$ . From this definition we may derive a graphical representation of the counit  $\epsilon_x$  as we did for the unit  $u_x$ . (Keep in mind that dotted lines correspond to raised indices and solid lines correspond to lowered indices.)



$$\epsilon_x := \Delta_u^u{}_x = h_{uv} \Delta^{vu}{}_x = \epsilon_x \quad (3.42)$$

**Figure 3.43** *Counit  $\epsilon_x$  in graphical representation*

So the counit  $\epsilon_x$  is represented graphically as an oriented line with a bubble blowing wand attached.

Summarizing the algebras we have introduced in the three dimensional section we have:

<u>TYPE</u>	<u>VEC. SPACE/UNIT</u>	<u>MULT</u>
ALGEBRA ( $H, m, u$ ) Data: ( $C_{xyz}, g^{xy}$ )	$H := \oplus_{x \in X} \mathbb{C}\phi_x$ $u(1) \cdot \phi = \phi = \phi \cdot u(1)$ where $u(1) = u^x \phi_x$	$m : H \otimes H \longrightarrow H$ $m(\phi_x \otimes \phi_y) := \phi_x \cdot \phi_y$ $:= C_{xy}{}^z \phi_z$ where $C_{xy}{}^z := C_{xyz'} g^{z'z}$
DUAL ALGEBRA ( $\tilde{H}, \tilde{m}, \tilde{u}$ ) Data: ( $\Delta^{xyz}, h_{xy}$ )	$\tilde{H} := \oplus_{x \in X} \mathbb{C}\tilde{\phi}^x$ $\tilde{u}(1) \cdot \phi = \phi = \phi \cdot \tilde{u}(1)$ where $\tilde{u}(1) = \epsilon_x \tilde{\phi}^x$	$\tilde{m} : \tilde{H} \otimes \tilde{H} \longrightarrow \tilde{H}$ $\tilde{m}(\tilde{\phi}^y \otimes \tilde{\phi}^z) := \tilde{\phi}^y \cdot \tilde{\phi}^z$ $:= \Delta_x{}^{yz} \tilde{\phi}^x$ where $\Delta_x{}^{yz} := h_{xx'} \Delta^{x'yz}$
COALGEBRA ( $H, \Delta, \epsilon$ ) Data: ( $\Delta^{xyz}, h_{xy}$ )	$H := \oplus_{x \in X} \mathbb{C}\phi_x$ $\Delta_x{}^{yz} \epsilon_z = \delta_x{}^y = \epsilon_z \Delta_x{}^{zy}$ where $\epsilon(\phi_x) = \epsilon_x$	$\Delta : H \longrightarrow H \otimes H$ $\Delta(\phi_x) := \Delta_x{}^{yz} \phi_y \otimes \phi_z$ where $\Delta_x{}^{yz} := h_{xx'} \Delta^{x'yz}$

Invariance of faces and hinges under subdivision implies the algebras are associative and semisimple, and the coalgebra is coassociative and cosemisimple.

Recall that an equivalent lattice theory may be defined on the dual lattice  $\tilde{L}$  in which *hinges become faces* and *faces become hinges*. The structure constants  $C_{xy}{}^z$  and  $\Delta_z{}^{xy}$  simply exchange places and the algebra/coalgebra of the lattice determine the coalgebra/algebra structure of the dual lattice, respectively.

### 3.3 Topological Invariance and Correspondence to Hopf Algebra

In prior sections we have demonstrated that invariance of faces and hinges under subdivision implies that our algebra  $(H, m, u)$  is associative and semisimple and our coalgebra  $(H, \Delta, \epsilon)$  is coassociative and cosemisimple. In this section we will show that the requirement of topological invariance of our LFT implies that the algebra  $(H, m, u)$  and coalgebra  $(H, \Delta, \epsilon)$  combine with the arrow-reversing operator  $S$  (antipode) to form a Hopf algebra with involutory antipode. [S69]

The main theory of this chapter is

**Theorem 3.44** *The set of three dimensional topological lattice field theories with data  $(C_{xyz}, g^{xy}, \Delta^{xyz}, h_{xy}, S^x_y)$  is in one to one correspondence with the set of Hopf algebras  $(H, m, u, \Delta, \epsilon, S)$  with involutive antipode.*

**Remark:** The statement of the theorem is not precisely the same as that in [CFS94]. In [CFS94] the authors require that the antipode take a particular form (given in Equation (3.3.44) below). As we shall see, however, the specific form of the antipode follows from the requirement that it be involutive, so the extra hypothesis is not needed.

*Proof:* The outline of the proof is as follows. In Step 1 we introduce two new local moves in three dimensions, the *hinge move* and the *3D cone move*, and demand that  $Z(L)$  be invariant under both. Then we will show that (a) invariance under the hinge move implies that the collection  $(H, m, u, \Delta, \epsilon, \cdot)$  is a bialgebra, and (b) invariance under the 3D cone move implies that the arrow-changing operator  $S$  is an involutive antipode, thereby making  $(H, m, u, \Delta, \epsilon, S)$  into a Hopf algebra with antipode satisfying  $S^2 = 1$ . In Step 2 we show that a Hopf algebra with involutive antipode gives rise to a 3D TLFT. Finally, in Step 3 we show that no additional

constraints (beyond the hinge and 3D cone moves ) are required to ensure that our LFT be topologically invariant.

**STEP 1.a.** For  $(H, m, u, \Delta, \epsilon)$  to be a bialgebra we must show  $m$  and  $u$  are coalgebra morphisms with respect to  $\Delta$  and  $\epsilon$ , or, equivalently,  $\Delta$  and  $\epsilon$  are algebra morphisms with respect to  $m$  and  $u$ . These conditions are expressed algebraically as follows:

$$\Delta \circ m = (m \otimes m) \circ (1 \otimes \tau \otimes 1) \circ (\Delta \otimes \Delta) \quad (3.45)$$

$$\Delta \circ u = u \otimes u \quad (3.46)$$

$$\epsilon \circ m = \epsilon \otimes \epsilon \quad (3.47)$$

$$\epsilon \circ u = 1 \quad (3.48)$$

where the *twist map*  $\tau$  is defined via  $\tau : H \otimes H \ni \phi_a \otimes \phi_b \mapsto \phi_b \otimes \phi_a \in H \otimes H$ . In the standard basis  $\{\phi\}$  these equations read

$$C_{xy}{}^z \Delta_z{}^{ab} = \Delta_x{}^{pq} \Delta_y{}^{rs} C_{pr}{}^a C_{qs}{}^b \quad (3.49)$$

$$u^x \Delta_x{}^{yz} = u^y u^z \quad (3.50)$$

$$C_{xy}{}^z \epsilon_z = \epsilon_x \epsilon_y \quad (3.51)$$

$$\epsilon_x u^x = 1 \quad (3.52)$$



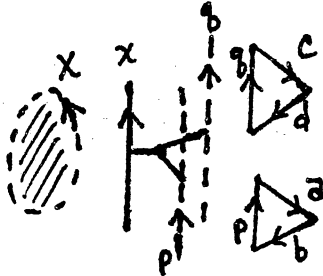
To prove, for example, that (3.45) and (3.49) are equivalent, we apply both sides of (3.41) to a basis:

$$\begin{aligned}
\Delta \circ m(\phi_x \otimes \phi_y) &= (m \otimes m) \circ (1 \otimes \tau \otimes 1) \circ (\Delta \otimes \Delta)(\phi_x \otimes \phi_y) \\
\Leftrightarrow \Delta(\phi_x \cdot \phi_y) &= (m \otimes m) \circ (1 \otimes \tau \otimes 1)(\Delta_x^{pq} \phi_p \otimes \phi_q \otimes \Delta_y^{rs} \phi_r \otimes \phi_s) \\
\Leftrightarrow \Delta(C_{xy}^z \phi_z) &= (m \otimes m) \circ (1 \otimes \tau \otimes 1)(\Delta_x^{pq} \Delta_y^{rs} \phi_p \otimes \phi_q \otimes \phi_r \otimes \phi_s) \\
\Leftrightarrow C_{xy}^z \Delta \phi_z &= (m \otimes m) \circ (\Delta_x^{pq} \Delta_y^{rs} \phi_p \otimes \phi_r \otimes \phi_q \otimes \phi_s) \\
\Leftrightarrow C_{xy}^z \Delta_z^{ab} \phi_a \otimes \phi_b &= \Delta_x^{pq} \Delta_y^{rs} \phi_p \cdot \phi_r \otimes \phi_q \cdot \phi_s \\
&= \Delta_x^{pq} \Delta_y^{rs} C_{pr}^a \phi_a \otimes C_{qs}^b \phi_b \\
&= \Delta_x^{pq} \Delta_y^{rs} C_{pr}^a C_{qs}^b \phi_a \otimes \phi_b
\end{aligned}$$

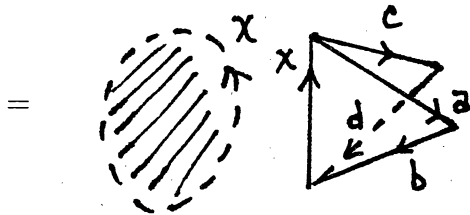
□

We prove Equation(3.50) diagrammatically as follows. For clarity of the manipulations, we attach two triangles to the hinge whose weight is  $\Delta_x^{pq}$  and then detach them at the end.

Let  $u^x \Delta_x^{pq}$  act on  $C_{pab}$  and  $C_{qcb}$ , in other words, attach triangles  $C_{pab}$  and  $C_{qcd}$  to  $u^x$  and hinge  $\Delta_x^{pq}$ .

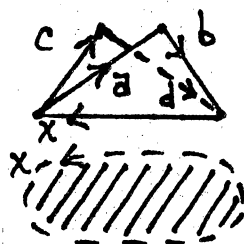


$$(u^x \Delta_x^{pq} C_{pab} C_{qcd})$$



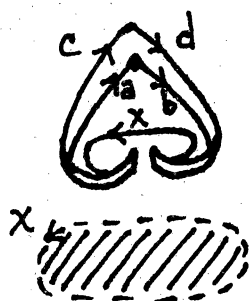
faces attached  
to hinge

=



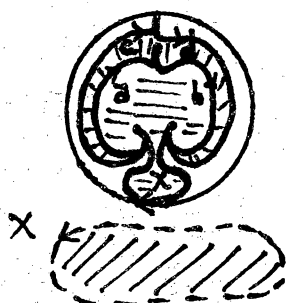
rotate

=



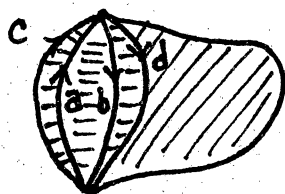
wrap bottom  
corners together

=



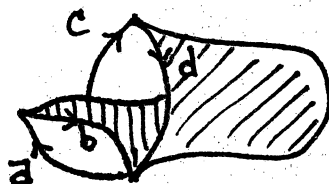
continue wrapping

=



attach  $u^x$  cap

=



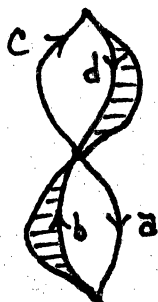
pull out side (b)

=



continue pulling

=



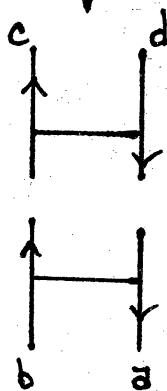
inner cup pulled out

=



smashed flat

=



$(g_{ab}g_{cd})$

3-D version of (2.36)

=



$$\begin{aligned}
&= \text{Diagram of two triangles sharing a vertex, with edges labeled } a, b, c, d \text{ and } p, q. \\
&= (u^p C_{pab} u^q C_{qcd})
\end{aligned}$$

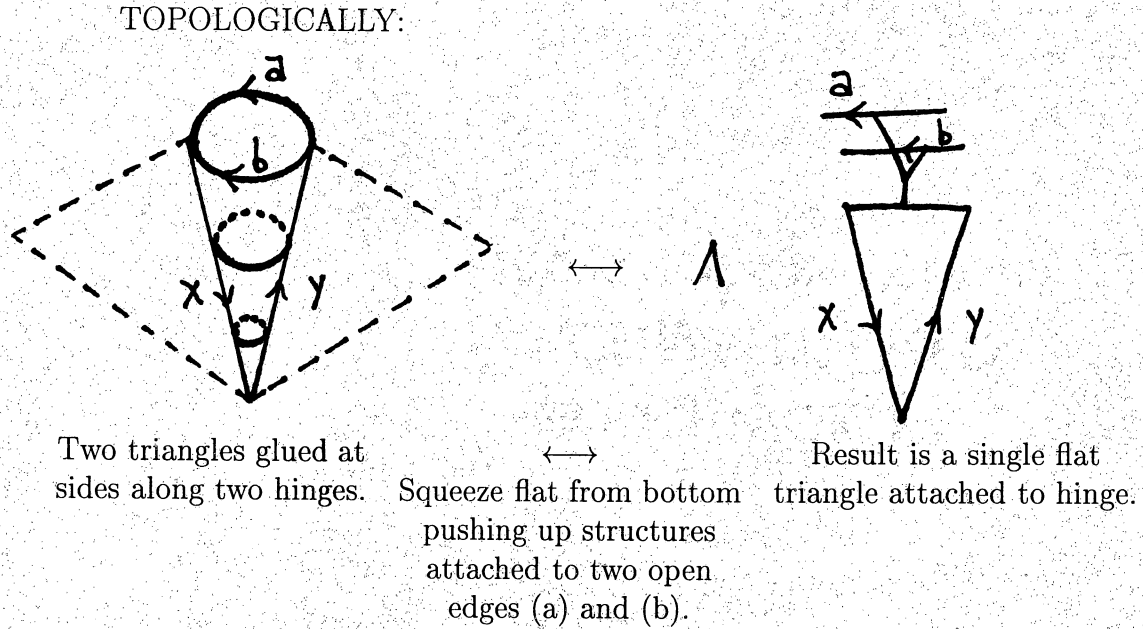
**Figure 3.53** Graphical proof of Equation (3.50)  $u_x \Delta_x^{yz} = u^y u^z$

Thus

$$u^x \Delta_x^{pq} C_{pab} C_{qcd} = g_{ab} g_{cd} = u^p C_{pab} u^q C_{qcd} \quad (3.54)$$

As Equation(3.54) holds for all triangles, Equation (3.50) also holds. Equation (3.51) follows by duality.

Next, we introduce a new move, called the *hinge move*, and demand that our theory be invariant under it. This will provide us with a proof of Equation (3.49). The move itself derives from a topology-preserving transformation that takes two triangles glued to each other along two hinges, and collapses them homotopically to a single triangle plus a hinge.



ALGEBRAICALLY:

$$\Delta_x^{pq} \Delta_y^{rs} C_{apr} C_{bqs} = \Lambda C_{xyz} \Delta_{ba}^z \quad (3.55)$$

**Figure 3.56** *Hinge Move*

where numerical factor  $\Lambda$  is introduced to account for the number of three dimensional cells lost in this operation.

We would like to derive the bialgebra condition (3.49) from (3.55). To do so we first introduce a new operator  $T$ :

$$T^x_y := h^{xz} g_{zy} \quad (3.57)$$

and a numerical constant  $\Lambda_0$ :

$$\Lambda_0 := \epsilon_x T^x_y u^y = \epsilon^x u_x \quad (3.58)$$

The second equality in (3.58) follows because  $h^{xy}$  acts on hinges and therefore on  $\epsilon_x = \Delta_u^u{}_x$ , while  $g_{xy}$  acts on triangles and therefore on  $u^y = C^y{}_a{}^a$ . Specifically

$$\begin{aligned} \epsilon_x T^x_y u^y &= \epsilon_x h^{xz} g_{zy} u^y && \{\text{by def}\} \\ &= \epsilon^z g_{zy} u^y && \{\text{apply } h^{xz} *\} \\ &= \epsilon^z u_z && \{\text{apply } g_{zy} *\} \end{aligned}$$

The hinge move equation (3.55) implies a restriction on the operator  $T$ :

$$T^a{}_r T^b{}_s \Delta_y{}^{rs} = \Lambda T^z{}_y \Delta_z{}^{ba} \quad (3.59)$$

which can be seen as follows:

$$\begin{aligned}
u^x(\Delta_x^{pq}\Delta_y^{rs}C_{apr}C_{bqs}) &= u^x(\Lambda C_{xyz}\Delta^z{}_{ba}) && \{\text{Eq (3.55)}\} \\
\Leftrightarrow u^p u^q \Lambda_y^{rs} C_{apr} C_{bqs} &= \Lambda u^x C_{xyz} \Delta^z{}_{ba} && \{\text{Eq (3.50)}\} \\
\Leftrightarrow \underbrace{u^p C_{pra} u^q C_{qsb}} \Delta_y^{rs} &= \Lambda \underbrace{u^x C_{xyz}} \Delta^z{}_{ba} \\
\Leftrightarrow g_{ra} g_{sb} \Delta_y^{rs} &= \Lambda g_{yz} \Delta^z{}_{ba} && \{\text{by def } g_{xy}\} \\
\Leftrightarrow h^{a'a} h^{bb'} (g_{ra} g_{sb} \Delta_y^{rs}) &= h^{aa'} h^{bb'} (\Lambda g_{yz} \Delta^z{}_{ba}) \\
\Leftrightarrow h^{a'a} g_{ar} h^{bb'} g_{bs} \Delta_y^{rs} &= \Lambda g_{yz} \underbrace{h^{aa'} h^{bb'}}_{ba} \Delta^z{}_{ba} \\
\Leftrightarrow T^{a'}{}_r T^{b'}{}_s \Delta_y^{rs} &= \Lambda g_{yz} \Delta^{zb'a'} && \{\text{by (3.57)}\} \\
\Leftrightarrow &= \Lambda g_{yz} h^{zz'} \Delta_{z'}{}^{b'a'} \\
\Leftrightarrow &= \Lambda h^{z'z} g_{zy} \Delta_{z'}{}^{b'a'} \\
\Leftrightarrow &= \Lambda T^{z'}{}_y \Delta_{z'}{}^{b'a'} && \{\text{by (3.57)} \square\}
\end{aligned}$$

Starting from (3.55) we may write

$$\begin{aligned}
\Delta_x^{pq}\Delta_y^{rs}C_{pra}C_{qsb} &= \Lambda C_{xyz}\Delta^z{}_{ba} \\
\Leftrightarrow \Delta_x^{pq}\Delta_y^{rs}C_{pr}{}^m C_{qs}{}^n g_{ma}g_{nb} &= \Lambda C_{xy}{}^u g_{uz} h^{zt} \Delta_{tba} \\
\Leftrightarrow \Delta_x^{pq}\Delta_y^{rs}C_{pr}{}^m C_{qs}{}^n g_{ma}g_{nb} h^{ac} h^{bd} &= \Lambda C_{xy}{}^u T^t{}_u \Delta_t{}^{dc} \\
\Leftrightarrow \Delta_x^{pq}\Delta_y^{rs}C_{pr}{}^m C_{qs}{}^n T^c{}_m T^d{}_n &= \Lambda C_{xy}{}^u T^t{}_u \Delta_t{}^{dc}
\end{aligned}$$

Equation (3.59) gives

$$\Lambda T^t{}_u \Delta_t{}^{dc} = T^c{}_m T^d{}_n \Delta_u{}^{mn}$$

so we get

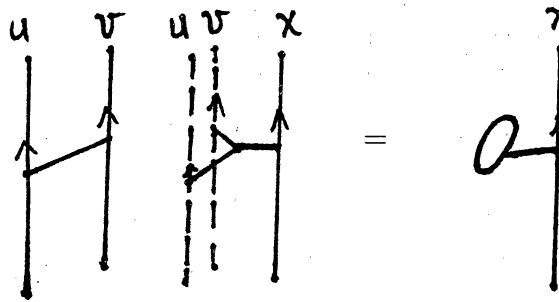
$$\Delta_x^{pq}\Delta_y^{rs}C_{pr}{}^m C_{qs}{}^n T^c{}_m T^d{}_n = C_{xy}{}^u \Delta_u{}^{mn} T^c{}_m T^d{}_n \quad (3.60)$$

As this equation holds for all  $T$  operators, Equation (3.49) follows.

Thus far we have demonstrated three of the four conditions required for the quintet  $(H, m, u, \Delta, \epsilon)$  to be a bialgebra. The fourth condition (3.52) is proved as follows:

$$\begin{aligned}
& u^y \epsilon_b (\Delta_x^{pq} \Delta_y^{rs} C_{pr}^a C_{qs}^b) = u^y \epsilon_b (C_{xy}^z \Delta_z^{ab}) \\
\Leftrightarrow & u^y \Delta_y^{rs} C_{qs}^b \epsilon_b \Delta_x^{pq} C_{pr}^a = u^y C_{y^z}^x \Delta_z^{ab} \epsilon_b \\
\Leftrightarrow & u^r u^s \epsilon_q \epsilon_s \Delta_x^{pq} C_{pr}^a = \delta_x^z \delta_z^a \\
\Leftrightarrow & u^r C_{r^p}^a \Delta_x^{pq} \epsilon_q u^s \epsilon_s = \delta_x^z \delta_z^a \\
\Leftrightarrow & \delta_p^a \delta_x^p u^s \epsilon_s = \delta_x^a \\
\Leftrightarrow & \delta_x^a u^s \epsilon_s = \delta_x^a \\
\Leftrightarrow & \delta_x^a u^s \epsilon_s = \delta_x^a \\
\Leftrightarrow & u^s \epsilon_s = 1
\end{aligned}$$

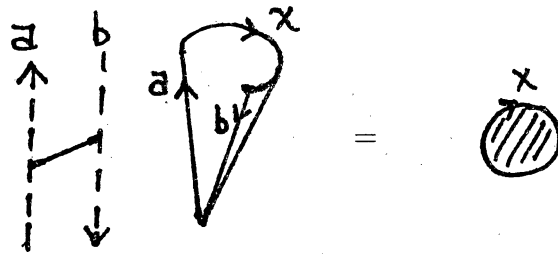
**STEP 1b.** Next we show that the arrow-reversing operator  $S$  is indeed the antipode of a Hopf algebra  $(H, m, u, \Delta, \epsilon, S)$  by considering a lattice configuration in which two edges of a triangle are glued along a hinge, and imposing invariance under a local move (called the *3D cone move*) that removes such a triangle. We first recall the graphical representations of  $\epsilon_x$  (Figure 3.61) and  $u^x$  (Figure 3.62).



$$\Delta_u^u x = \epsilon_x$$

**Figure 3.61** The counit  $\epsilon_x$

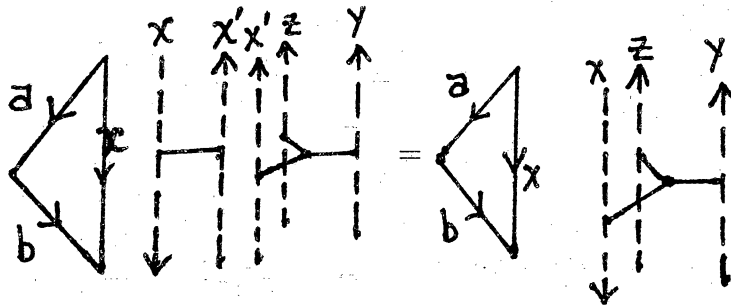




$$C_{xb}^b = u_x.$$

**Figure 3.62** *The unit  $u_x$*

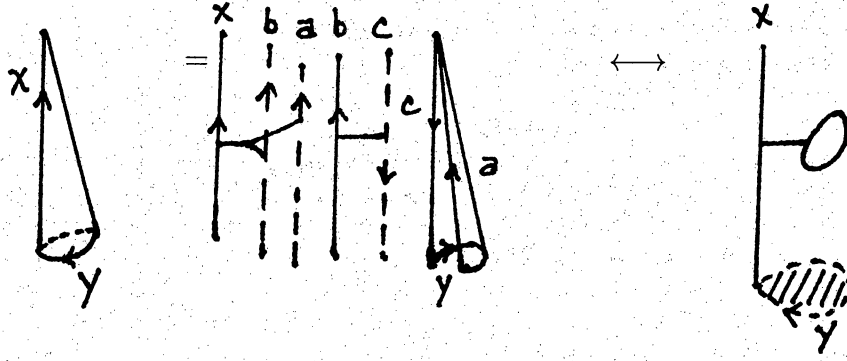
We also recollect how the arrow-reversing operator  $S$  works.



$$C_{bax} S_{x'}^x \Delta^{x'yz}$$

**Figure 3.63** *The action of the arrow-changing operator*

The 3D cone move is represented in Figure (3.64).



$$\Delta_x^{ab} S_b^c C_{ac}^y = u^y \epsilon_x$$

**Figure 3.64** *The 3D cone move*

Reading the diagram of Figure (3.64) we arrive at the 3D cone equation

$$\Delta_x^{ab} S_b^c C_{ac}^y = u^y \epsilon_x \quad (3.65)$$

By adjusting the orientation of the edges and imposing invariance under three similar cone moves we produce the following three variations of Equation (3.65):

$$\Delta_x^{ab} S_a^c C_{cb}^y = u^y \epsilon_x \quad (3.66)$$

$$\Delta_x^{ab} S_b^c C_{ca}^y = u^y \epsilon_x \quad (3.67)$$

$$\Delta_x^{ab} S_a^c C_{bc}^y = u^y \epsilon_x \quad (3.68)$$

(See corresponding Figures 3.69 to 3.71 below.)

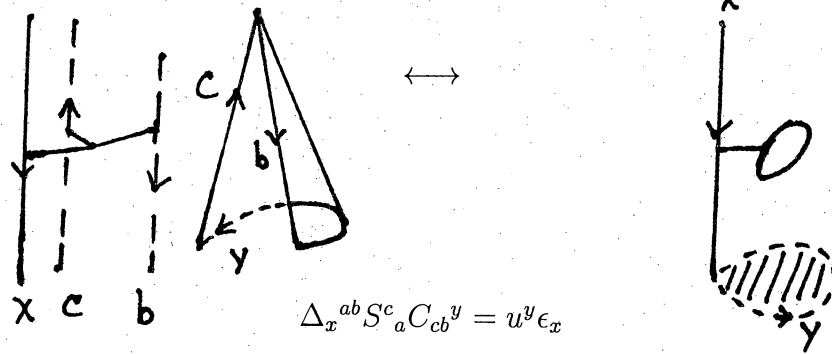


Figure 3.69 Cone move: Variation 2

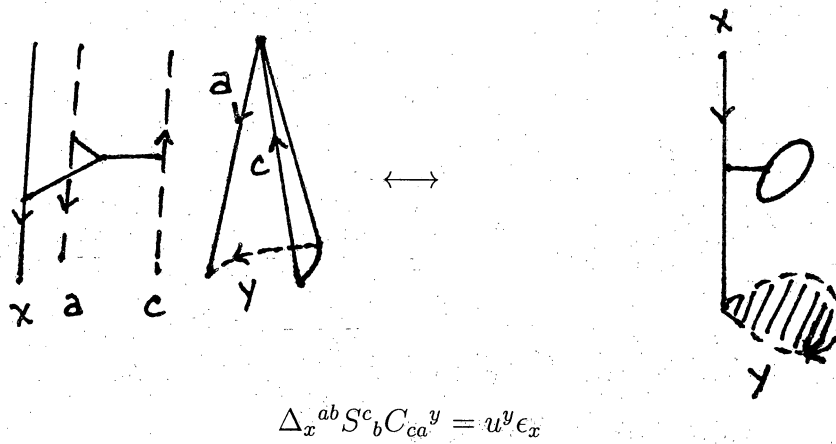


Figure 3.70 Cone move: Variation 3

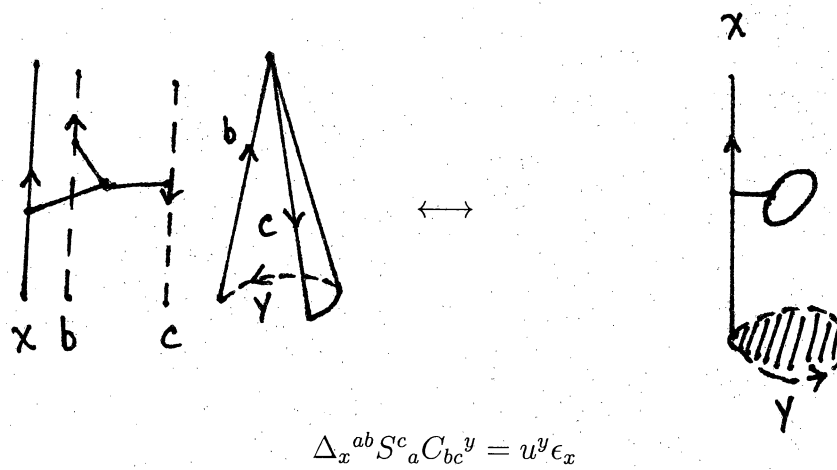


Figure 3.71 Cone move: Variation 4

We are attempting to demonstrate that our bialgebra  $(H, m, u, \Delta, \epsilon)$  is more than just a bialgebra. If we can show that the arrow direction changing operator  $S$  corresponds to a certain antipode defining axiom we will have established that the bialgebra is indeed a Hopf algebra.

The antipode of a Hopf algebra is defined to be the convolution inverse of the identity. This definition is expressed in the defining axiom for the antipode:

**Definition 3.72** Let  $(H, m, u, \Delta, \epsilon)$  be a bialgebra.

If linear map  $S : H \longrightarrow H$  satisfies

$$m \circ (1 \otimes S) \circ \Delta = m \circ (S \otimes 1) \circ \Delta = u \circ \epsilon$$

then  $(H, m, u, \Delta, \epsilon, S)$  is a *Hopf algebra with antipode  $S$* .

The antipode  $S$  is defined in the basis  $\{\phi_x : x \in X\}$  to be  $S(\phi_x) := S^y_x \phi_y$ . The condition of the antipode being involutive is expressed in the property  $S^2 = 1$ .

The claim is that the first two cone equations (3.65) and (3.66) are equivalent to  $S$  being an antipode, while the second two equations (3.67) and (3.68) are equivalent to the antipode being involutive. Our defining axiom for the antipode (Definition 3.72), when expressed in terms of the same basis becomes:

$$\begin{aligned} m \circ (1 \otimes S) \circ \Delta(\phi_x) &= m \circ (1 \otimes S)(\Delta_x^{ab} \phi_a \otimes \phi_b) \\ &= \Delta_x^{ab} m \circ (1 \otimes S)(\phi_a \otimes \phi_b) \\ &= \Delta_x^{ab} m(\phi_a \otimes S^c_b \phi_c) \\ &= \Delta_x^{ab} S^c_b m(\phi_a \otimes \phi_c) \\ &= \Delta_x^{ab} S^c_b C_{ac}^y(\phi_y) \\ &= u^y \epsilon_x(\phi_y) && \text{\{by Eq (3.65)\}} \\ &= u \circ \epsilon(\phi_x) && \text{\{by Def 3.72\}} \end{aligned}$$

from which we may conclude that

$$m \circ (1 \otimes S) \circ \Delta(\phi_x) = u \circ \epsilon(\phi_x) \tag{3.73}$$

The other equality in Definition (3.72) is derived by:

$$\begin{aligned}
m \circ (S \otimes 1) \circ \Delta(\phi_x) &= m \circ (S \otimes 1)(\Delta_x^{ab} \phi_a \otimes \phi_b) \\
&= \Delta_x^{ab} m \circ (S \otimes 1)(\phi_a \otimes \phi_b) \\
&= \Delta_x^{ab} m(S_a^c \phi_c \otimes \phi_b) \\
&= \Delta_x^{ab} S_a^c m(\phi_c \otimes \phi_b) \\
&= \Delta_x^{ab} S_a^c C_{cb}^y(\phi_y) \\
&= u^y \epsilon_x(\phi_y) && \{\text{by Eq (3.66)}\} \\
&= u \circ \epsilon(\phi_x)
\end{aligned}$$

implying that

$$m \circ (S \otimes 1) \circ \Delta = u \circ \epsilon \quad (3.74)$$

We have thus established that invariance under the 3D cone move (Equation (3.65) and (3.66)) implies that the arrow-reversing operator  $S$  is the antipode for the Hopf algebra  $(H, m, u, \Delta, \epsilon, S)$ . It remains to show that  $S^2 = 1$ . It is easier to do this using Sweedler's notation (see, *e.g.*, [K95] pp. 52-54). First, we note that the cone equations (3.67) and (3.68) are written in basis-free notations as

$$m \circ (S \otimes 1) \circ \tau \circ \Delta = u \circ \epsilon \quad (3.75)$$

and

$$m \circ (1 \otimes S) \circ \tau \circ \Delta = u \circ \epsilon \quad (3.76)$$

In Sweedler's notation Equation (3.75) becomes

$$\sum_{(x)} S(x'') x' = \epsilon(x) 1 \quad (3.77)$$

while (3.76) is written

$$\sum_{(x)} x'' S(x') = \epsilon(x) 1 \quad (3.78)$$

Since the antipode of a Hopf algebra is unique, we only need to show that  $S^2$  is the convolution inverse to  $S$ . But as the antipode is also an algebra antimorphism ([K95], Theorem III.3.4, p. 52), we have, using (3.77),

$$\begin{aligned} (S \star S^2)(x) &= \sum_{(x)} S(x') S^2(x'') = S\left(\sum_{(x)} S(x'') x'\right) = S(\epsilon(x)1) = \epsilon(x)S(1) \\ &= \epsilon(x)1 \end{aligned} \tag{3.79}$$

A similar argument shows that  $S^2 = 1$  implies (3.77) and (3.78), and we are finished with Step 1.

**STEP 2.** Next we show that, given a Hopf algebra  $(H, m, u, \Delta, \epsilon, S)$  with involutive antipode we may construct a 3D TLFT with data  $(C_{xyz}, g^{xy}, \Delta^{xyz}, h_{xy}, S^x_y)$ . As before, we construct the metric and cometric via

$$g_{xy} := C_{xa}{}^b C_{yb}{}^a \tag{3.80}$$

$$h^{xy} := \Delta_a{}^{bx} \Delta_b{}^{ay} \tag{3.81}$$

Using these, we define the triangle and hinge weights as follows:

$$C_{xyz} := g_{zz'} C_{xy}{}^{z'} \tag{3.82}$$

$$\Delta^{xyz} := h^{xx'} \Delta_{x'}{}^{yz} \tag{3.83}$$

and associativity and coassociativity of the algebra and coalgebra imply that these weights are cyclically symmetric. Equations (3.80), (3.81), (3.82), and (3.83) ensure that the theory is invariant under arbitrary two dimensional decompositions of polygons and multihinges. The involutivity of the antipode implies (see below) that

the algebra and coalgebra are semisimple and cosemisimple, respectively, so that the metric and cometric are nondegenerate.

We must show that the hinge and 3D cone move equations hold. The last part of the proof of Step 1b, which is reversible, shows that the antipode property of  $S$  gives the cone move equations (3.65) and (3.66), while equations (3.67) and (3.68) follow from the fact that the antipode is involutive. So all that remains is to show that the hinge equation (3.55) follows from our construction.

Let us define

$$u_x := C_{xy}^y \quad (3.84)$$

and

$$\epsilon^x := \Delta_y^{yx} \quad (3.85)$$

Observe that

$$C_{xy}^z u_z = C_{xy}^z C_{zw}^w = C_{xz}^w C_{yw}^z = g_{xy} \quad (3.86)$$

where we used associativity and the definition of the metric. Similarly

$$\epsilon^x \Delta_x^{pq} = \Delta_y^{yx} \Delta_x^{pq} = \Delta_y^{xq} \Delta_x^{yp} = h^{pq} \quad (3.87)$$

where we used coassociativity and the definition of the cometric.<sup>1</sup>

**Theorem 3.88** (*Larson and Radford [LR88]*) *Let  $H$  be a Hopf algebra with involutive antipode. Then  $u_x$  is a left and right integral (and, dually,  $\epsilon^x$  is a left and right cointegral).*

---

<sup>1</sup>It happens that  $u_x = g_{xy} u^y$  and  $\epsilon^x = h^{xy} \epsilon_y$ , but at this stage we do not want to make any assumptions about the nondegeneracy of the metric or cometric.

In our notation this means we have the following equations:

$$\Delta_x^{pq} u_p = u_x u^q \quad (3.89)$$

$$\Delta_x^{pq} u_q = u_x u^p \quad (3.90)$$

$$\epsilon^a C_{ab}{}^c = \epsilon_b \epsilon^c \quad (3.91)$$

$$\epsilon^b C_{ab}{}^c = \epsilon_a \epsilon^c \quad (3.92)$$

where  $u^x$  and  $\epsilon_x$  are the ordinary unit and counit, respectively. Multiplying (3.89) by  $\epsilon^x$  and using (3.58) and (3.87) yields the following equation:

$$h^{pq} u_p = \Lambda_0 u^q \quad (3.93)$$

Now, recall the bialgebra condition (3.49):

$$C_{xy}{}^z \Delta_z{}^{ab} = \Delta_x{}^{pq} \Delta_y{}^{rs} C_{pr}{}^a C_{qs}{}^b$$

If we multiply the left hand side of this equation by  $\epsilon^x u_a$  we get (using (3.88), (3.91), and (3.93))

$$C_{xy}{}^z \Delta_z{}^{ab} \epsilon^x u_a = \epsilon_y \epsilon^z \Delta_z{}^{ab} u_a = \epsilon_y h^{ab} u_a = \Lambda_0 \epsilon_y u^b \quad (3.94)$$

while the right hand side gives (using (3.57), (3.86), and (3.87))

$$\Delta_x{}^{pq} \Delta_y{}^{rs} C_{pr}{}^a C_{qs}{}^b \epsilon^x u_a = h^{pq} \Delta_y{}^{rs} g_{pr} C_{qs}{}^b = \Delta_y{}^{rs} T_r{}^q C_{qs}{}^b \quad (3.95)$$

Equating both sides yields



$$u^b \epsilon_y = \Delta_y^{rs} \left( \frac{1}{\Lambda_0} T_r^q \right) C_{qs}^b \quad (3.96)$$

Similar reasoning shows that

$$u^b \epsilon_y = \Delta_y^{rs} \left( \frac{1}{\Lambda_0} T_s^q \right) C_{rq}^b \quad (3.97)$$

Comparing (3.96) and (3.97) with (3.65) and (3.66) we see that  $T^a_b/\Lambda_0$  is (by uniqueness) the antipode  $S^a_b$  of our Hopf algebra. That is, we have proved

**Theorem 3.98** (*Kuperberg [Ku91]*) *Let  $(H, m, u, \Delta, \epsilon, S)$  be a Hopf algebra with antipode satisfying  $S^2 = 1$ . Then*

$$S^a_b = \frac{1}{\Lambda_0} T^a_b \quad (3.99)$$

where  $T^a_b$  and  $\Lambda_0$  are defined by Equations (3.57) and (3.58), respectively.

We must now show that the antipode  $S$  functions as the arrow-reversing operator of our TLFT. To do so we must show that the consistency condition (3.26) is satisfied. Using the fact ([K95], Theorem III.3.4, p. 52) that the antipode  $S$  of a Hopf algebra is also a coalgebra antimorphism:

$$(S \otimes S) \circ \tau \circ \Delta = \Delta \circ S \quad (3.100)$$

we get Equation (3.26) immediately:

$$\begin{aligned} & (S \otimes S) \circ \tau \circ \Delta(\phi_y) &= \Delta \circ S(\phi_y) \\ \Leftrightarrow & (S \otimes S) \circ \tau(\Delta_y^{rs} \phi_r \otimes \phi_s) &= \Delta(S_y^z \phi_z) \\ \Leftrightarrow & \Delta_y^{rs} (S \otimes S)(\phi_s \otimes \phi_r) &= S_y^z \Delta(\phi_z) \\ \Leftrightarrow & \Delta_y^{rs} (S^b_s \phi_b \otimes S^a_r \phi_a) &= S_y^z \Delta_z^{ba} \phi_b \otimes \phi_a \end{aligned}$$

which implies

$$S^a_r S^b_s \Delta_y^{rs}(\phi_b \otimes \phi_a) = S_y^z \Delta_z^{ba}(\phi_b \otimes \phi_a) \quad (3.101)$$

From Equation (3.101) and Definition 3.98 together with Theorem (3.98) we may write

$$\begin{aligned}
S^a{}_b S^b{}_s \Delta^{xrs} &= S^a{}_r S^b{}_s h^{xy} \Delta_y{}^{rs} \\
&= h^{xy} (S^z{}_y \Delta_z{}^{ba}) \\
&= h^{xy} S^z{}_y h_{zz'} \Delta^{z'ba} \\
&= \frac{1}{\lambda_0} h^{xy} T^z{}_y h_{zz'} \Delta^{z'ba} \\
&= \frac{1}{\lambda_0} h^{xy} h^{zw} g_{wy} h_{zz'} \Delta^{z'ba} \\
&= \frac{1}{\lambda_0} T^x{}_w \Delta^w{}_{z'} \Delta^{z'ba} \\
&= S^x{}_w \Delta^{wba}
\end{aligned}$$

Which is Equation (3.26).

Using the fact that the antipode is a coalgebra antimorphism we may substitute (3.99) into (3.100) and, evaluating in the standard basis (as in the calculation following (3.100)), immediately derive (3.59). Then reversing the argument in Step 1a we get the hinge equation (3.55). Lastly, we observe that, as the antipode is invertible in any finite dimensional Hopf algebra, the determinant of the left hand side of (3.99) is nonzero. (This also follows from  $S^2 = 1$ .) Hence the determinant of the operator  $T$  is nonzero, and so the determinants of  $g_{ab}$  and  $h^{ab}$  are nonzero, which is to say that involutivity of the antipode implies that our Hopf algebra is semisimple and cosemisimple.

This completes the proof of Step 2.

### STEP 3)

In this step we will show that no additional constraints are required (beyond hinge and 3-D cone moves) to ensure that our LFT is topologically invariant.

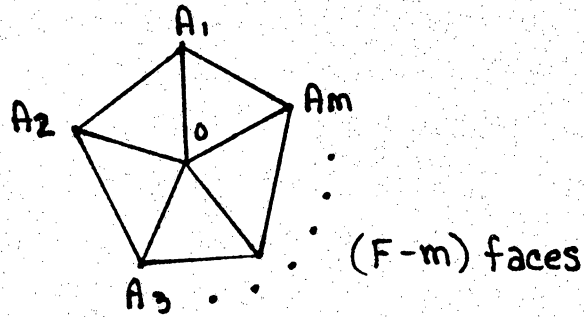
Stating our goal formally we want to prove:

**Theorem 3.102** *We can generate any local deformation of a 3-D lattice by a sequence of hinge moves, cone moves, and face subdivision moves.*

We begin with our manifold  $M$  which we subdivide into two distinct polyhedral lattices,  $L$  and  $L'$ . In part A) of our proof of Theorem 3.102 we will modify them so that at least three triangles always meet at any vertex of any polyhedron. In part B) we will chop up the resulting polyhedra into tetrahedra and relate the topologically equivalent lattices via bubble moves and (2,3) moves. The final products will be two topologically equivalent tetrahedral lattices,  $\Gamma$  and  $\Gamma'$ , acquired by a sequence of the two moves indicated above. Finally, in part C), we will demonstrate that with the tetrahedral decomposition of our lattice Theorem 3.102 follows directly.

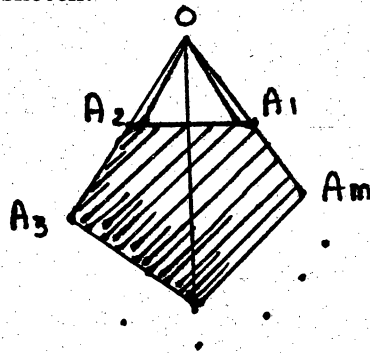
To accomplish our objective in part A) we will simply sketch the procedure for modifying our topologically equivalent lattices. Triangulating all the polygonal faces in  $L$  and  $L'$ , we next eliminate single triangles that have two edges meeting at a hinge, as well as all pairs of triangles that share two common edges. To eliminate these problematic triangles we use the hinge and the 3-D cone moves. This procedure will result in the modified triangulations  $\tilde{L}$  and  $\tilde{L}'$ , both of which will have the property that any vertex of any polyhedron will always be the meeting place of at least three triangles.

For part B) we will demonstrate that the hinge and face sub-division moves are sufficient to decompose each resulting polyhedron into tetrahedra. We begin with a polyhedron,  $P$ , where at least three faces meet. (See Figure 3.103) Let  $F$  represent the number of total faces in  $P$ . We isolate one vertex  $0$  on our polyhedron, and we indicate the number of triangular faces that meet at  $0$  by the variable  $m$ , where  $m \geq 3$ .



**Figure 3.103** Polyhedron  $P$ , where we have shown  $m$  faces and suppressed  $(F - m)$  faces, for a total of  $F$  faces

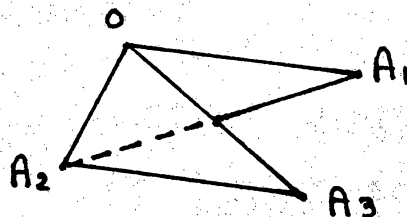
To better visualize the three dimensional structure of our lattice we will raise the vertex position in our sketch:

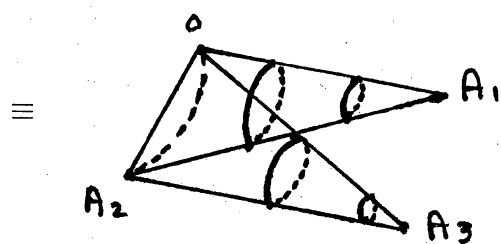


**Figure 3.104** Polyhedron  $P$  with vertex  $0$  raised

In order to acquire a valid tetrahedral decomposition of our polyhedron  $P$  we perform the following four steps:

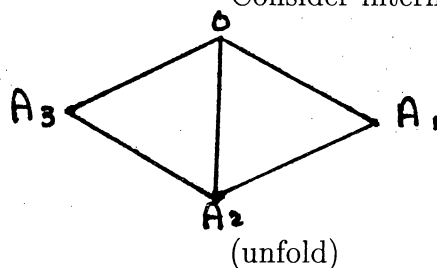
Step B-I. Using induction on the number of faces  $F$  in our polyhedron  $P$ , we first consider two adjacent triangles that meet at vertex  $0$ , triangle  $\triangle 0A_1A_2$  and triangle  $\triangle 0A_2A_3$ , and demonstrate how they can be topologically manipulated into a single tetrahedron:



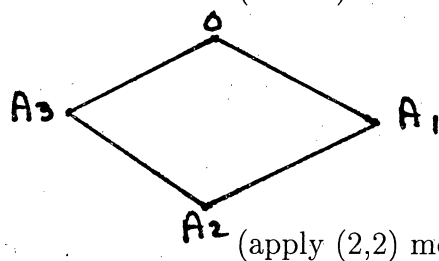


{by upcoming Cor 3.116

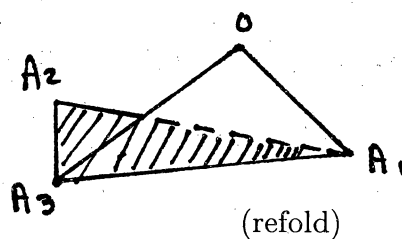
Consider internal  $\triangle$ 's:



(unfold)

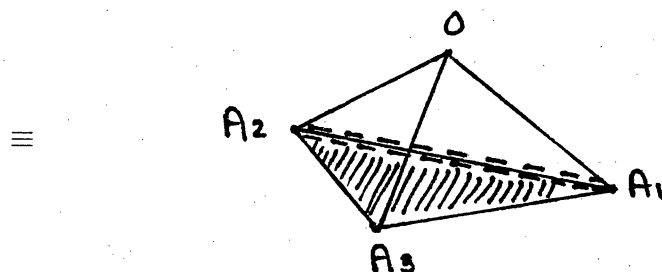


(apply (2,2) move)



(refold)

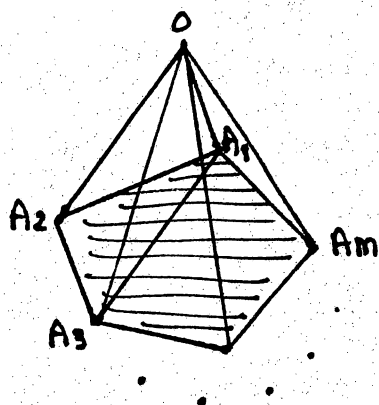
re-insert results:



**Figure 3.105** Forming a tetrahedron from two adjacent faces of  $P$  at vertex 0

Step B-II. Now we repeat the process on successive pairs of adjacent triangles; triangle  $\triangle 0A_1A_k$  and triangle  $\triangle 0A_kA_{k+1}$ , for  $k = 3, 4, \dots, m - 1$ . In Figure 3.105 we

carefully describe how the process consumes adjacent vertices. The final result will be  $m - 2$  interior tetrahedra:



1st tetra consumes  $0, A_1, A_2, A_3$ .

2nd tetra consumes  $0, A_1, A_3, A_4$ .

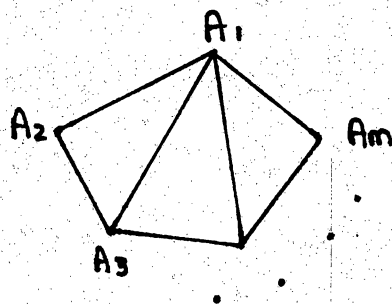
$(m - 3)th$  tetra consumes  $0, A_1, A_{m-2}, A_{m-1}$ .

$(m - 2)th$  tetra consumes  $0, A_1, A_{m-1}, A_m$ .

**Figure 3.106** Forming  $(m - 2)$  tetrahedra from polyhedron  $P$

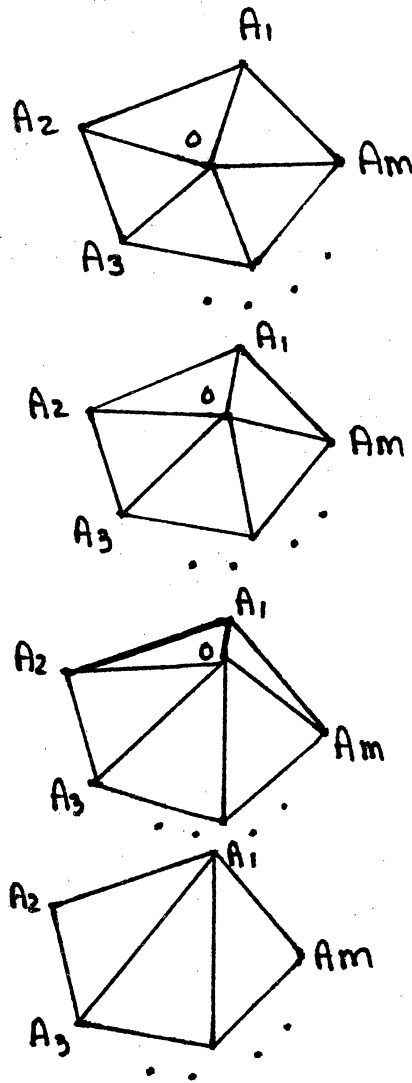
In the above sketch we note that each vertex where three edges meet can be consumed twice in this process (with the exception of vertices  $A_1$  and  $A_m$ , which are each consumed once), while the vertices where  $m$  faces meet (vertices  $0$  and  $A_1$ ) are consumed  $m - 2$  times. Since we do not have sufficient vertices remaining to form an  $(m - 3)th$  tetrahedron we stop at the  $(m - 2)th$  tetrahedron, noting that our original  $m$  triangles comprise the external faces of the interior tetrahedra.

Step B-III. We next remove our  $(m - 2)$  interior tetrahedra as follows:



**Figure 3.107** Modified polyhedron  $P$ , where we have shown  $(m - 2)$  faces and suppress  $(F - m)$  faces, for a total of  $(F - 2)$  faces in  $P$ .

In removing the  $(m - 2)$  tetrahedra we lost the vertex  $0$ . This reduces our faces by two as demonstrated below:



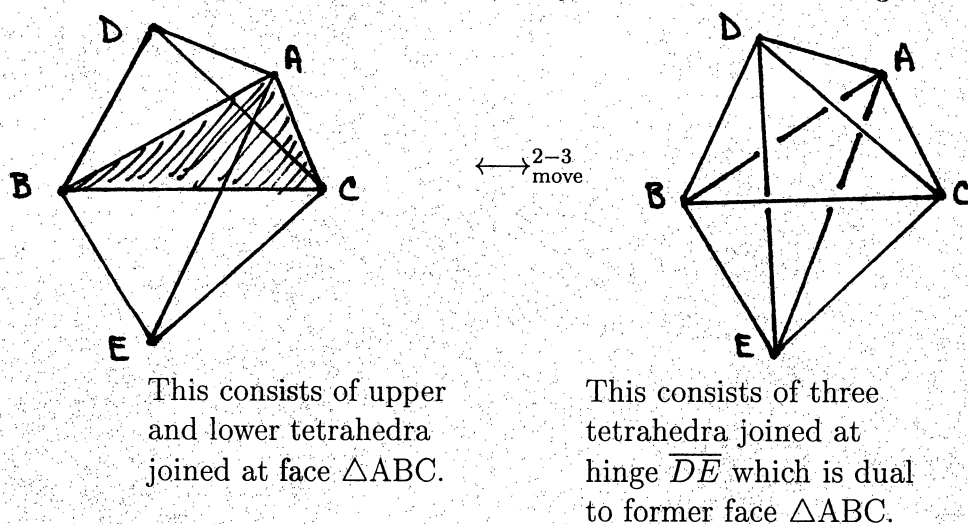
**Figure 3.108** Removing  $(m - 2)$  tetrahedra from polyhedra  $P$

Step B-IV. We repeat the face reducing process described above. Upon each application we reduce the faces by two until we achieve four faces, a *tetrahedron*. Note that our polyhedral 3-cells must all be contractible for this process to work. The result is that a tetrahedral decomposition of the polyhedron  $P$  has been obtained, completing part B) of our proof of Theorem 3.102.

We recall that in part A) we started with two topologically equivalent lattices  $L$  and  $L'$ . We modified them into our ‘good’ triangulations  $\tilde{L}$  and  $\tilde{L}'$ , where at least three triangles always met at any vertex. In part B) we demonstrated that  $\tilde{L}$  and  $\tilde{L}'$  could be decomposed, in general, into tetrahedral lattices. We will now prove in part C) that our two *tetrahedralized* lattices  $\tilde{L}$  and  $\tilde{L}'$  are topologically equivalent, just as their predecessors  $L$  and  $L'$  were. We accomplish our task by further decomposing  $\tilde{L}$  and  $\tilde{L}'$  into two topologically equivalent tetrahedral lattices  $\Gamma$  and  $\Gamma'$ .

By a three dimensional version of Alexander’s theorem any two topologically equivalent tetrahedral lattices are related by a sequences of special local lattice moves, specifically the three dimensional 2-3 and bubble moves. Therefore, if we can demonstrate that our lattice  $\tilde{L}$  can be manipulated into our lattice  $\tilde{L}'$ , using these two moves, we will have shown that they are topologically equivalent. But first we must conceptualize the meaning of these two basic moves in three dimensions.

The three dimensional 2-3 move takes two tetrahedra joined at a common face and transforms it into three tetrahedra joined at a common edge.



**Figure 3.109** *The three dimensional 2-3 move*

To better visualize our topologically equivalent three cells we separate the tetrahedra:



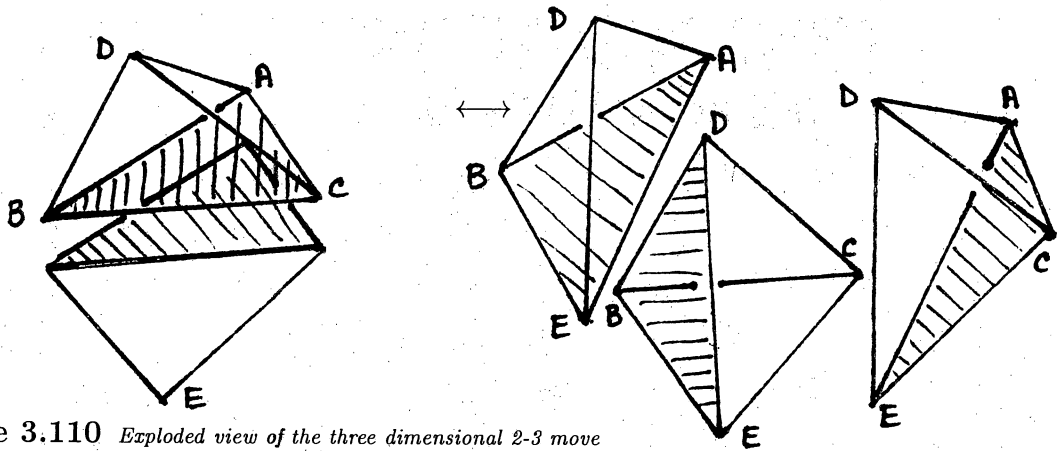
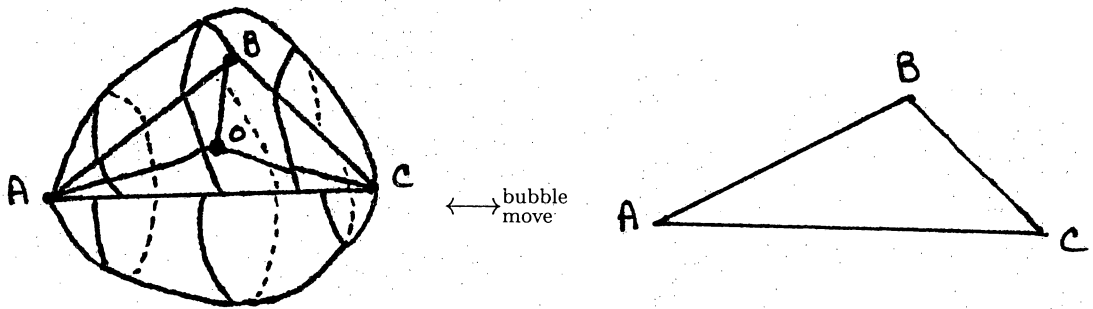


Figure 3.110 Exploded view of the three dimensional 2-3 move

The three dimensional bubble move takes two tetrahedra which share three common faces and transforms them into a single triangular face.

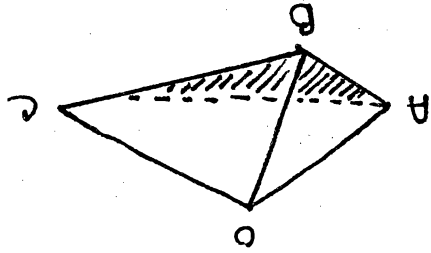


This consists of two  
tetrahedra sharing three  
faces:  $\triangle ABO$ ,  $\triangle BCO$   
 $\triangle ACO$ .

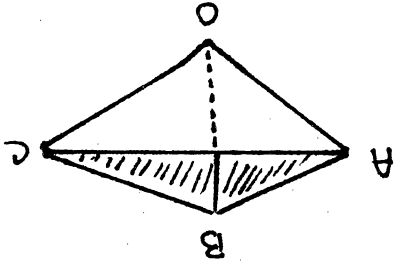
This is a single face.

Figure 3.111 Three dimensional bubble move

Since this move is much more abstract and difficult to view in three dimensions, we will sketch a brief topological description of the transformation. We begin by separating the two tetrahedra (bubbles) and collapsing them into triangles.

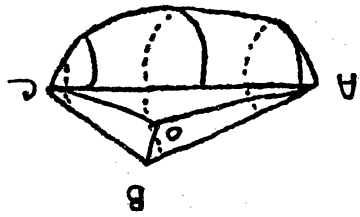


(bottom)  
pull vertex up

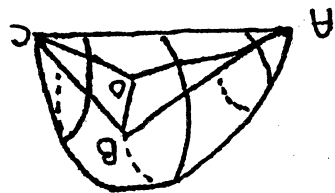


(top)  
pull vertex down

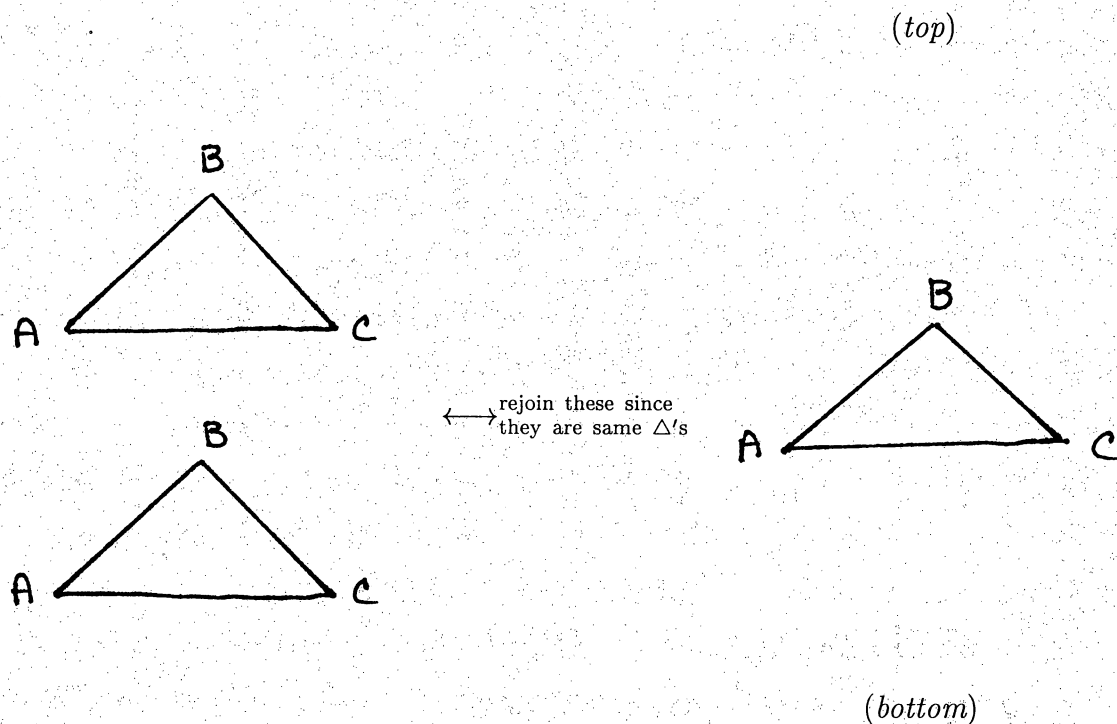
(separate)



(bottom)



(top)



(smash each flat)

**Figure 3.112** *Topological detail of the 3-D bubble move*

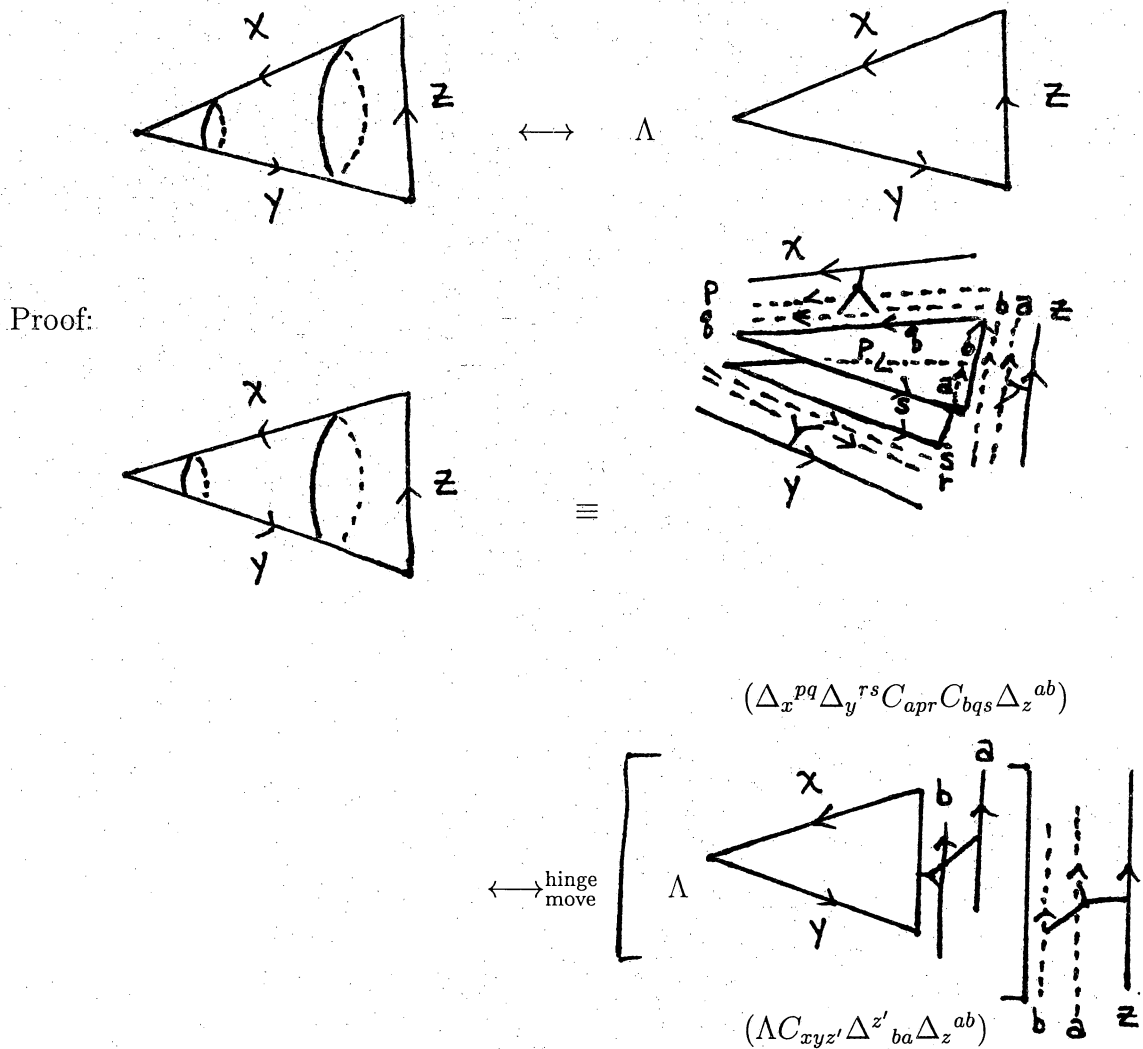
Our detailed descriptions of the three dimensional 2-3 and bubbles moves (Figures 3.110 and 3.112) are motivation for the upcoming full blown proofs of the these moves. (Theorems 3.119 and Corollary 3.115)

For the remainder of part C) of our proof of Theorem 3.102 we will derive the bubble and 2-3 moves for three dimensions and prove various corollaries of each. As we work through these derivations it will become clear that each of the moves are actually generated by a sequence of *hinge* and *face sub-division* moves. Hence, we will have demonstrated that the 2-3 and bubble moves interpolating between our two topologically equivalent tetrahedral lattices  $\Gamma$  and  $\Gamma'$  can be reduced to a sequence of hinge moves, which can in turn be incorporated into a sequence of

hinge, 3-D cone and face sub-division moves interpolating between our original topologically equivalent lattices  $L$  and  $L'$ . This will conclude our proof of Theorem 3.102.

The next lemma and corollary will prove invariance under the bubble move, assuming only that the hinge equation (3.55) is satisfied. Lemma 3.113 is a triangle reduction move. It takes two triangular faces joined at three edges with hinges, and transforms them into a single face with a numerical factor of  $\Lambda$

**Lemma 3.113** *Triangle Reduction Move*



$$\begin{aligned}
&= \Lambda \quad \begin{array}{c} \text{Diagram 1: A triangle with vertices } x \text{ (top), } y \text{ (bottom-left), and } z \text{ (bottom-right). Arrows point from } x \text{ to } y, y \text{ to } z, \text{ and } z \text{ to } x. \end{array} \\
&= \Lambda \quad \begin{array}{c} \text{Diagram 2: A triangle with vertices } x \text{ (top), } y \text{ (bottom-left), and } z \text{ (bottom-right). Arrows point from } x \text{ to } y, y \text{ to } z, \text{ and } z \text{ to } x. \end{array} \\
&\quad (\Lambda C_{xyz})
\end{aligned}$$

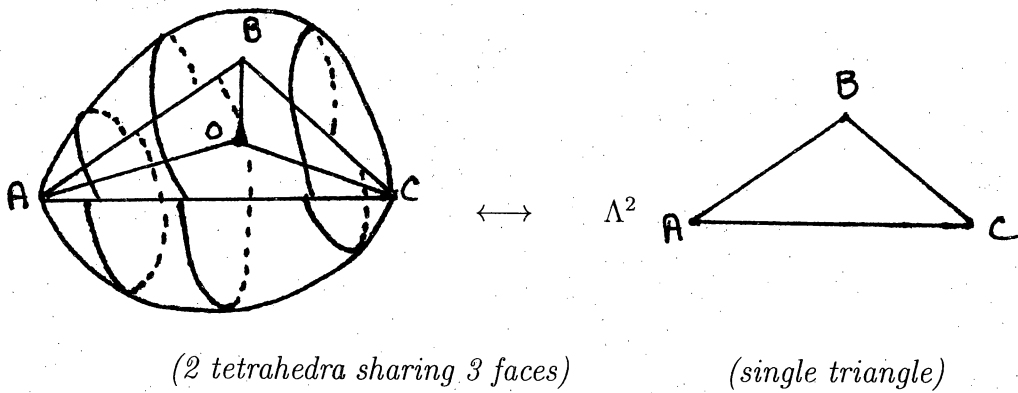
□

Therefore, the triangle reduction move can be represented in the equation:

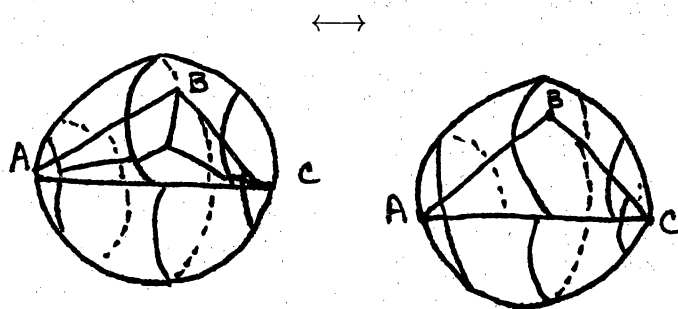
$$\Delta_x^{pq} \Delta_y^{rs} C_{apr} C_{bqs} \Delta_z^{ab} = \Lambda C_{xyz'} \Delta^{z'}_{ba} \Delta_z^{ab} = \Lambda C_{xyz} \quad (3.114)$$

The three dimensional bubble move follows directly as a corollary of Lemma 3.113.

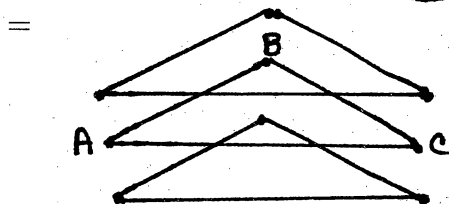
**Corollary 3.115** *Bubble Move*



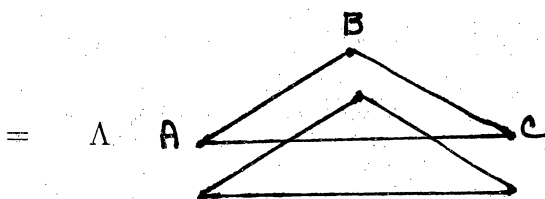
Proof:



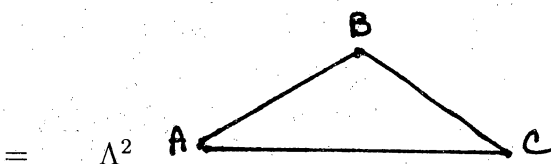
2-dim'l 1-3 move  
on inner triangle



Top 2  $\triangle$ 's hinged  
at 3 edges, while  
bottom 2  $\triangle$ 's  
hinged at 3 edges.



apply Lma 3.113 to top

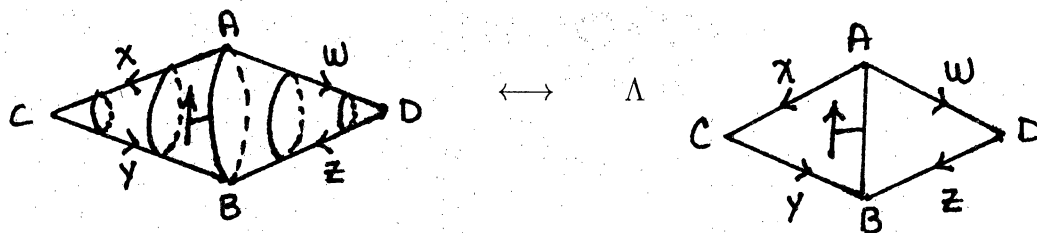


apply lma again

□

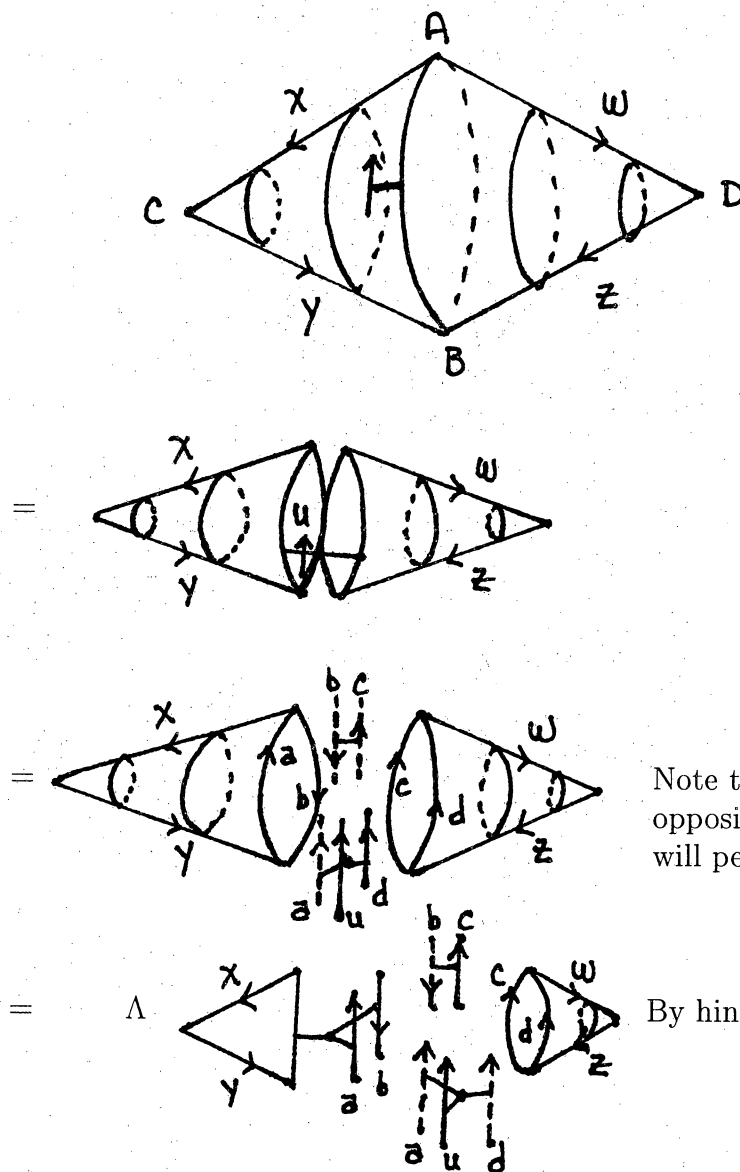
Having demonstrated the bubble move we now proceed to illustrate the 2-3 move. The plan is to develop a new move (Corollary 3.116 of Lemma 3.113) which will reduce four triangular faces to two. Then we will use this move to develop another new move (Lemma 3.117) which will reduce four triangular faces to three, and a similar move (Lemma 3.118) that increases three triangular faces to four. Finally we will use all of these to show that the three dimensional 2-3 move can be derived under the assumption that the hinge equation is satisfied.

**Corollary 3.116** *Four Triangles to Two*



Note that the two front triangles are connected by a 3-hinge operator along the solid edge  $\overline{AB}$ . The two rear triangles are connected by a 2-hinge operator along the dotted edge  $\overline{AB}$ .

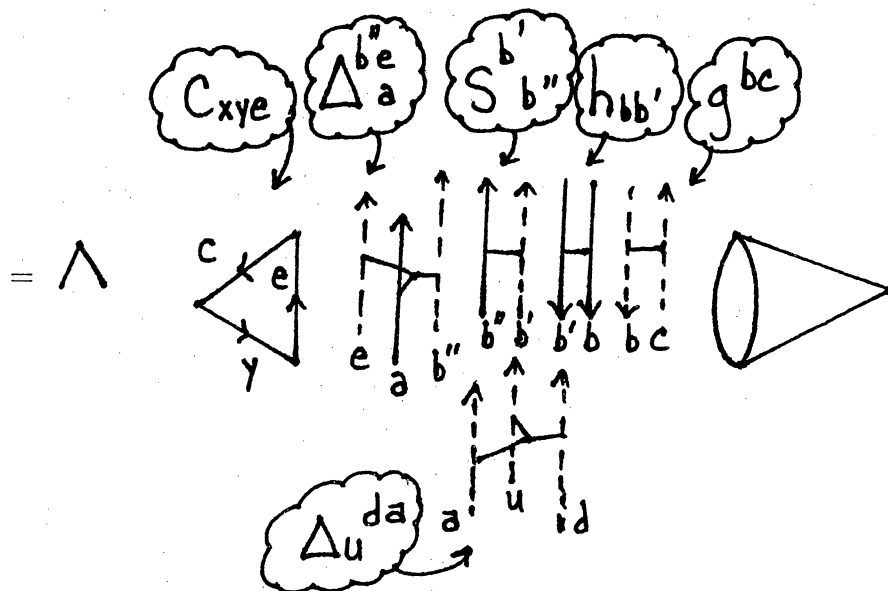
Proof:



Note that sides  $a, b$  are in opposite directions, as we will perform a hinge move.

By hinge move of Fig. 3.56

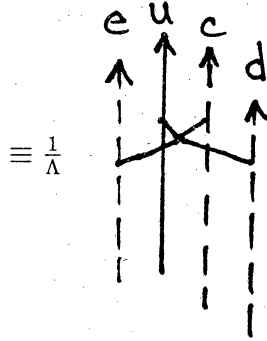
To better understand what is occurring on the inside of our structure we expand our sketch to the following exploded perspective:



Now we diverge for a moment to isolate and algebraically simplify only the hinges and gluing operators, which yields :



$$\begin{aligned}
\Delta_u^{da} \Delta^{b''e}_a (S^{b'}_{b''}) h_{bb'} g^{bc} &= \delta_u^{da} \Delta^{b''e}_a \left( \frac{1}{\Lambda} T^{b'}_{b''} \right) h_{bb'} g^{bc} \\
&= \Delta_u^{da} \Delta^{b''e}_a \left( \frac{1}{\Lambda} h^{b'w} g_{wb''} \right) h_{bb'} g^{bc} \quad \{\text{by def of T}\} \\
&= (\Delta_u^{da} \frac{1}{\Lambda}) [g^{bc} \Lambda^{b''e}_a h^{b'w} g_{wb''} h_{bb'}] \\
&= (\Delta_u^{da} \frac{1}{\Lambda}) [g^{bc} g_{wb''} \underbrace{h^{wb'} h_{b'b}}_{\Delta^{b''e}_a}] \\
&= (\Delta_u^{da} \frac{1}{\Lambda}) [g^{bc} g_{wb''} (\delta^w_b) \Delta^{b''e}_a] \\
&= (\Delta_u^{da} \frac{1}{\Lambda}) [\underbrace{g^{bc} g_{bb''}}_{\Delta^{b''e}_a}] \\
&= (\Delta_u^{da} \frac{1}{\Lambda}) [(\delta^{c''}_b) \Delta^{b''e}_a] \\
&= (\Delta_u^{da} \frac{1}{\Lambda}) [\Delta^{ce}_a] \\
&= \frac{1}{\Lambda} \Delta_u^{da} \Delta_a^{ce} \\
&= \frac{1}{\Lambda} \Delta_u^{dce}
\end{aligned}$$



Now we insert the results of our divergence back into our proof, replacing the original collection of hinges and gluing operators with our derived four hinge:

$$= \Lambda$$

$$= \Lambda C_{xye} \left( \frac{1}{\Lambda} \Delta_u^{dce} \right)$$

algebraically

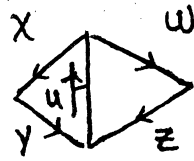
$$= C_{xye} (\Delta_u^{dce})$$

$$=$$

$$=$$

glue together with hinge

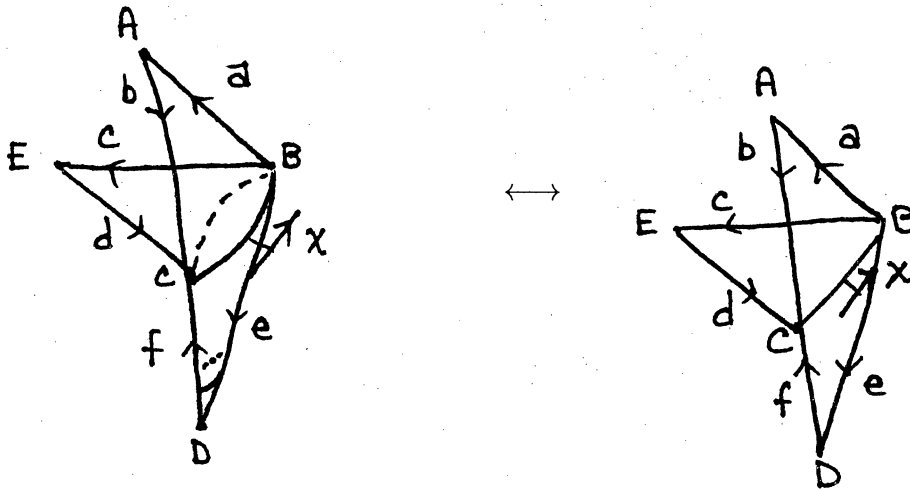
=  $\Lambda$



by Lemma 3.113

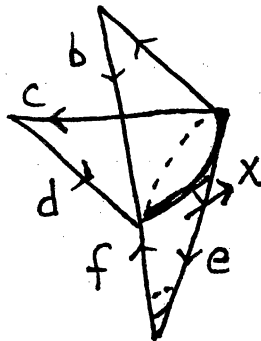
□

**Lemma 3.117** *Four Triangles to Three*

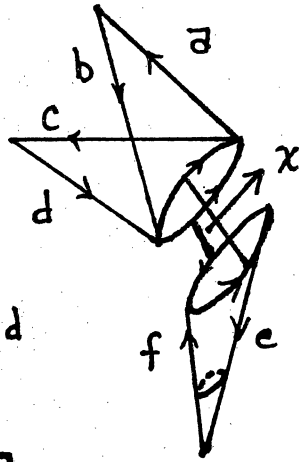


Note that for the sketch on the right the rear triangle  $BCD$  connects to  $BCE$  by a 2-hinge operator along the dotted edge  $\overline{BC}$ . The front triangle  $BCD$  connects to  $BCA$  by a 3-hinge operator along the solid edge  $\overline{BC}$ .

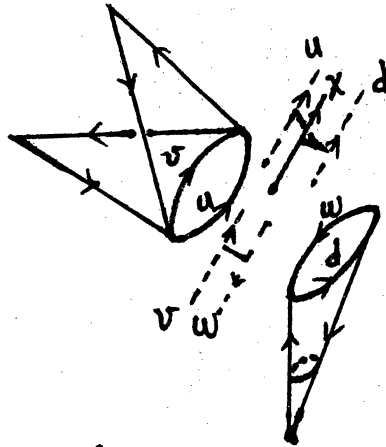
Proof:



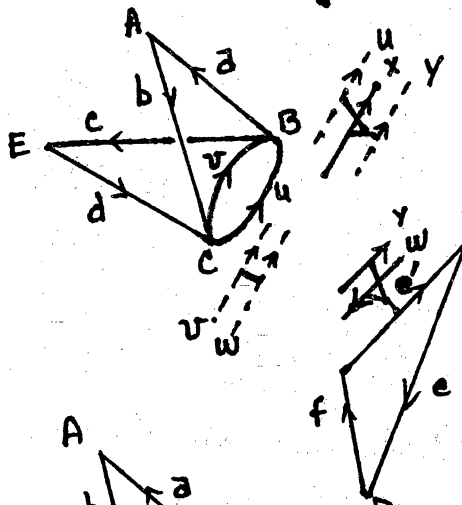
=



=

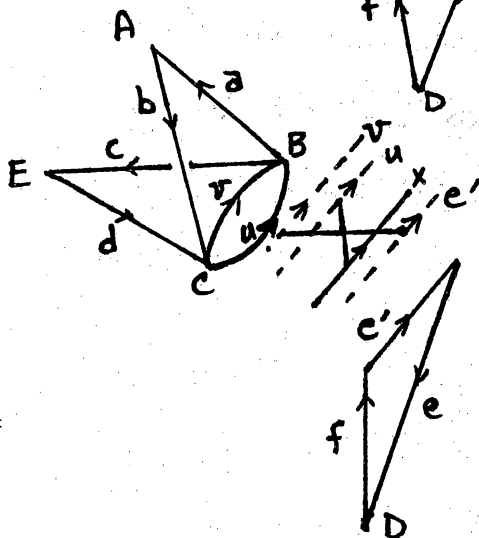


=  $\Lambda$



by hinge move of Fig 3.56

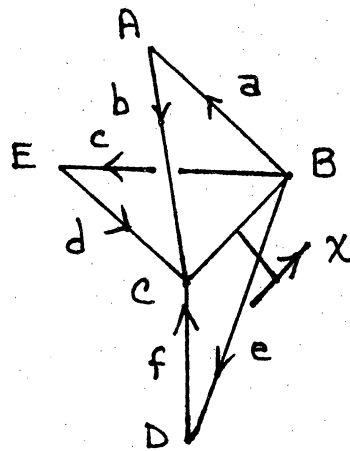
=



4-hinge eliminates  $\Lambda$

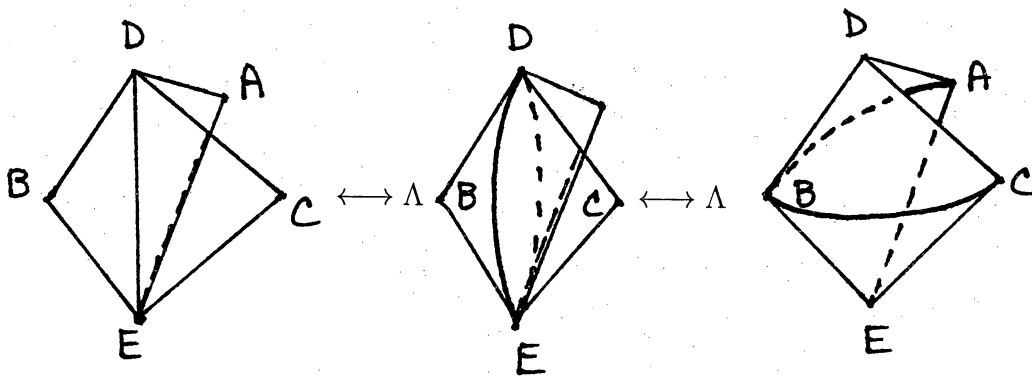
as in proof of Cor 3.116

=



join faces to hinge  $\square$

**Lemma 3.118** *Three Triangles to Four*



3  $\triangle$ 's

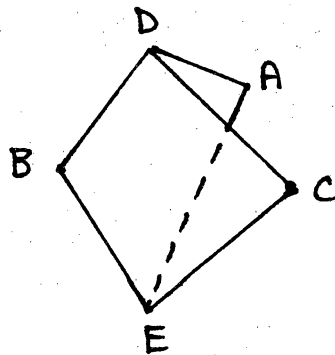
sideways cone

4  $\triangle$ 's

with 3-hinge

and faces

Proof:



=

(C\_{abv}C\_{efw}C\_{cdz}\Delta^{vzw})

decompose along 3-hinge

=

correct directions on  
hinges with  $S$  operators

$$(C_{abv}C_{efw}C_{cdz}\Delta^{vz'w'}S_{z'}^zS_{w'}^w)$$

$$= C_{abv}C_{efw}C_{cdz}\Delta^{vz'w'}(S^{-1})_{z'}^{z'}(S^{-1})_{w'}^{w'}$$

(where  $S = S^{-1}$  because our antipode is involutory.)

$$= C_{abv}C_{efw}C_{cdz}\Delta^{vz'w'}(\Lambda h_{yz'}g^{zy})(\Lambda h_{xw'}g^{wx})$$

(This step is true because  $S_{z'}^z = \frac{h^{zy}g_{yz'}}{\Lambda}$  implies that  $(S^{-1})_{z'}^z = \Lambda h_{yz'}g^{zy}$ .)

$$\begin{aligned}
&= C_{abv} C_{efw} C_{cdz} \Lambda^2 (\Delta^{vz'w'} h_{yz'} h_{xw'}) g^{zy} g^{wx} \\
&= C_{abv} C_{efw} C_{cdz} \Lambda^2 \Delta^v_{yx} g^{zy} g^{wx} \quad \{\text{by hinge operators}\}
\end{aligned}$$

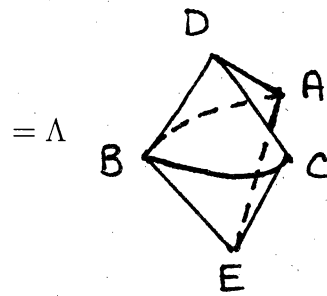
$$= \Lambda^2$$

$$= \Lambda^2 \Lambda^{-1}$$

by hinge move

$$= \Lambda$$

glue

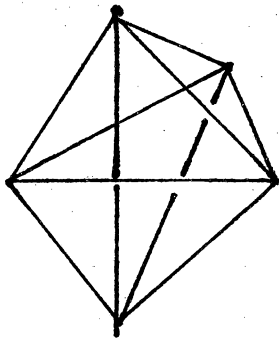


2-2 move on  
front and rear  $\triangle$ 's

□

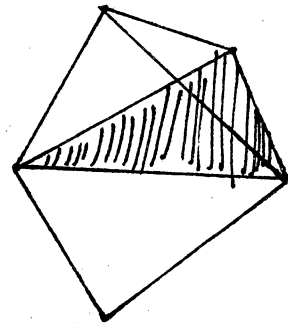
And finally using the three-to-four face move (Lemma 3.118), the four-to-two face move (Corollary 3.116), and the four-to-three face move (Lemma 3.117) we are in a position to prove the three dimensional 2-3 move:

### Theorem 3.119 2-3 MOVE



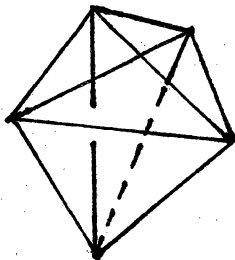
*3 tetrahedra sharing common edge DE*

$\longleftrightarrow \Lambda^2$



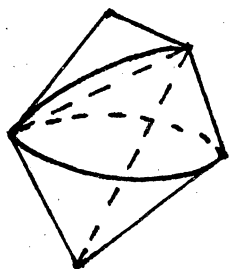
*2 tetrahedra sharing common face ABC*

Proof



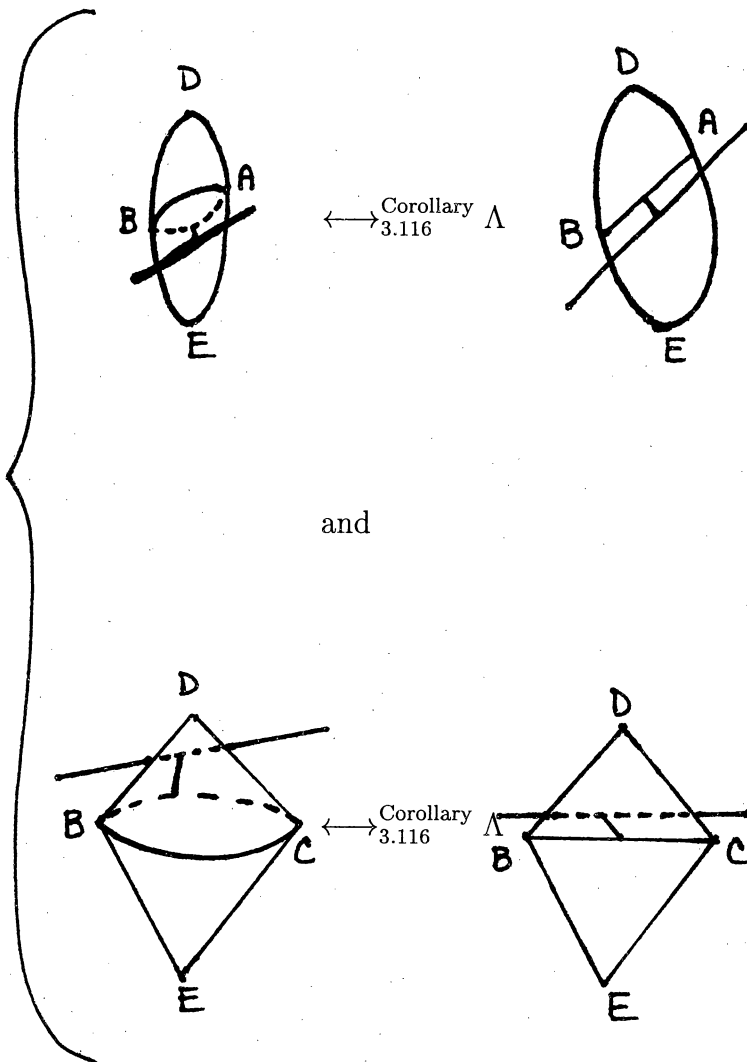


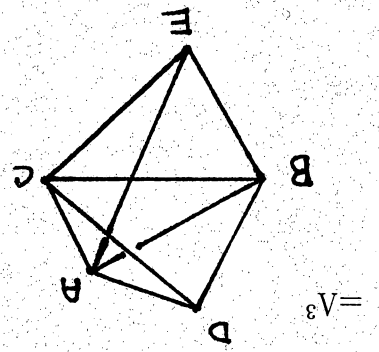
$=\Lambda$



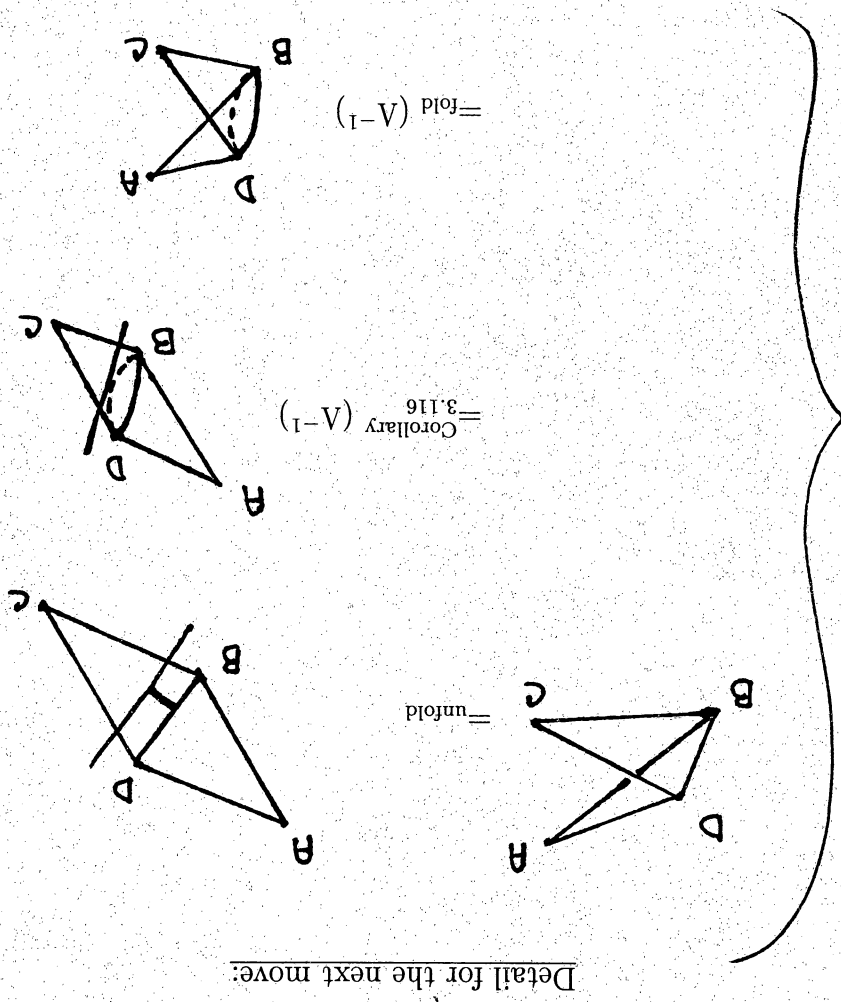
(by Lemma 3.118)

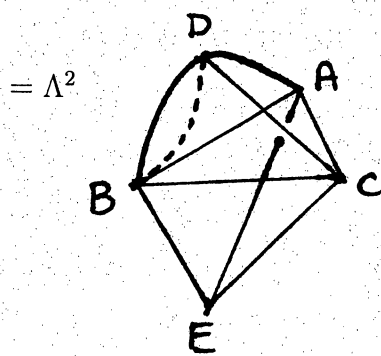
Detail for the next move:



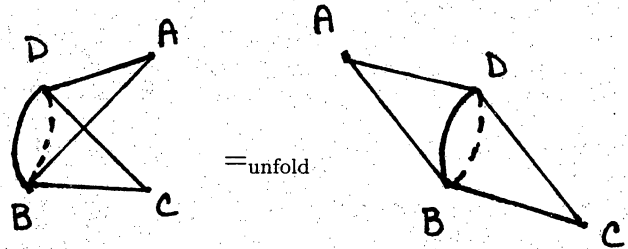


100

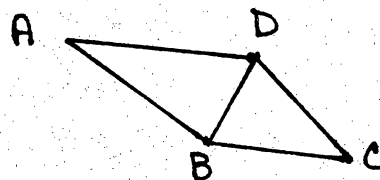




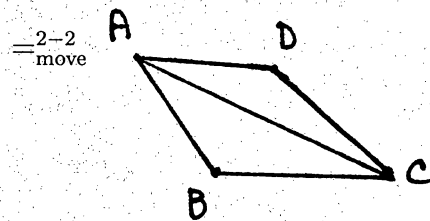
Detail for the next move:

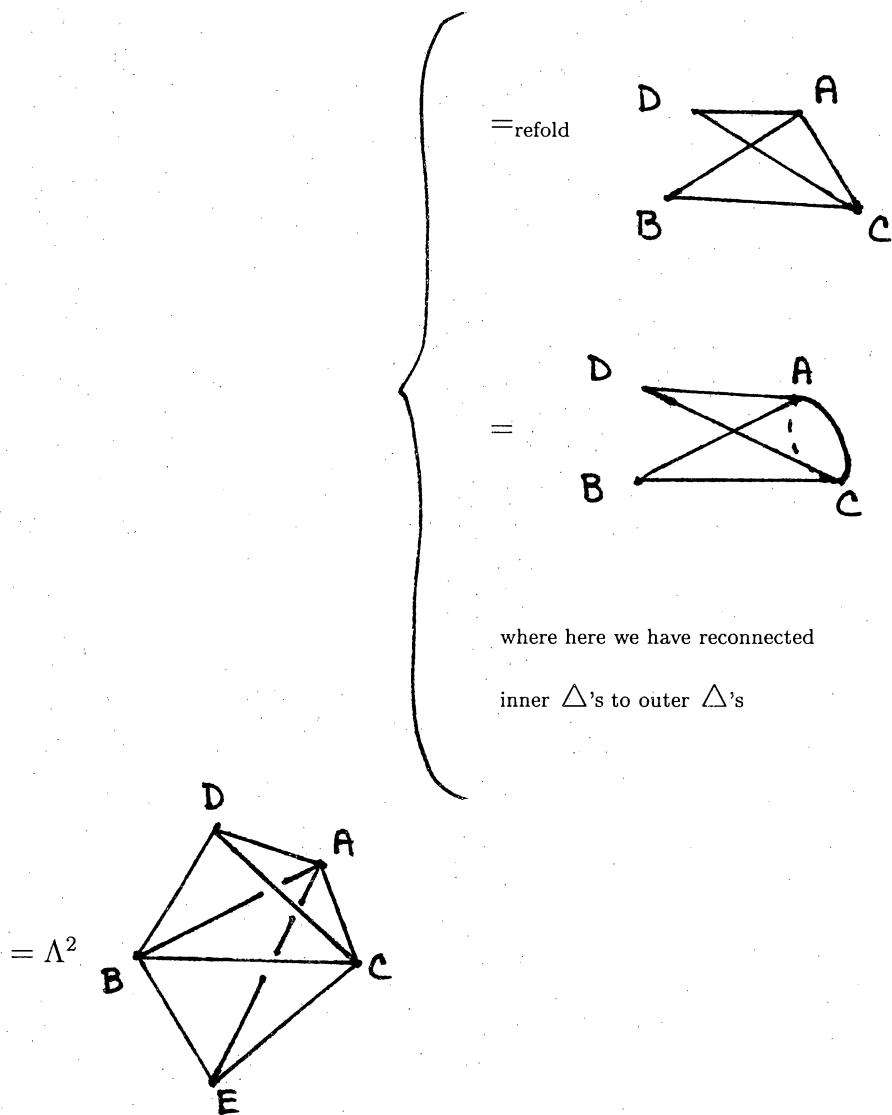


(Now consider the inner  $\triangle$ 's only)



gluing with 2 -hinges





Before this last move we had an inflation along edge  $\overline{BD}$ , whereas now we have an inflation along  $\overline{AC}$ . We note the following detail of this modification:

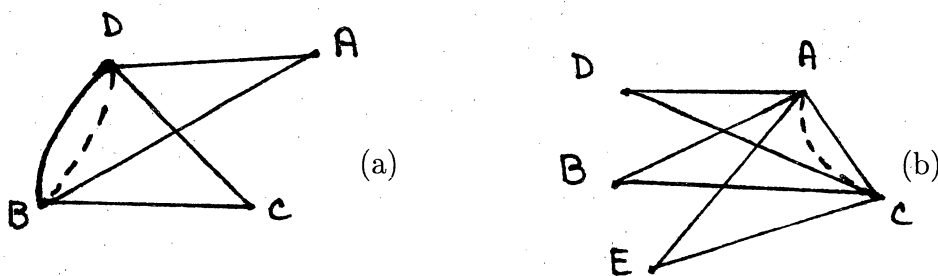
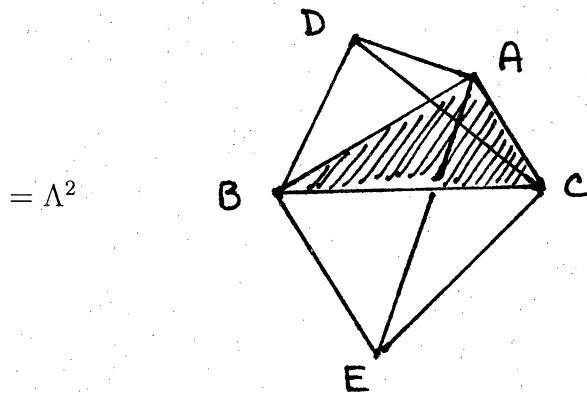


Figure 3.120 Detail of inflation move

In going from (a), an inflation along an edge where two faces meet, to (b), an

inflation along an edge where three faces meet, we now have the cone with two faces adjoined at the top (as described in Lemma 3.117). Therefore, applying Lemma 3.117 to the last figure we complete our proof.



**Figure 3.121** *Two tetrahedra sharing a common face ABC*

□

This concludes step 3, and hence the proof for theorem 3.44.

## Chapter 4

# Turaev-Viro (Kauffman-Lins) State Sum Invariant

In this chapter we present the Kauffman-Lins (KL) variant [Kau94] of the Turaev-Viro (TV) [TV92] state sum invariant of three manifolds. The original state sum of Turaev and Viro was constructed using the algebraic properties of what are now called *quantum 6j symbols*, whose properties follow from the representation theory of the quantum group  $U_q(sl(2))$  when  $q = e^{i\pi/r}$  is a root of unity [KR89]. As with the CFS invariant considered in Chapter 3, the TV invariant is obtained from a compact manifold  $M$  by constructing a triangulation  $Y$  and coloring the edges of  $Y$  with colors from a color set  $X = \{1, 2, \dots, r-2\}$ . To every 3-simplex of the triangulation  $Y$  Turaev and Viro associate a quantum 6j symbol

$$\left\{ \begin{array}{ccc} a & b & c \\ d & e & f \end{array} \right\}$$

where  $(a, d)$ ,  $(b, e)$ , and  $(c, f)$  are opposite edges of the tetrahedron. Multiplying these together with suitable weights and summing over all possible colorings of  $Y$  yields the state sum  $TV_M$ .

The crucial point is that, as Turaev and Viro show, their state sum  $TV_M$  is independent of the choice of triangulation. They show this by appealing to Alexander's theorem. As we noted before, Alexander's original theorem requires a

possibly infinite set of different moves to relate one triangulation to another. But while Chung, Fukuma, and Shapere use the result of Steen and Varsted to reduce these to a finite set of generating moves, Turaev and Viro pass to the dual complex (“special spines”) and prove that only a finite set of generating moves, called the *Matveev-Piergallini* moves ([Mat88] [Pier88]) are required there. Demonstration of the invariance of their state sum thus reduces to consideration of the behaviour of  $TV_M$  under three special moves, call the *lune move*, the *Y-move*, and the *bubble move*. Miraculously, invariance under these three moves is guaranteed by properties of the quantum 6j symbols.

Kauffman and Lins develop a version of the TV invariant based upon what they call the “tangle theoretic Temperley-Lieb algebra”. This approach, which we outline below, provides a direct, combinatorial, and knot theoretic understanding of the recoupling theory of  $U_q(sl(2))$ , upon which the invariance properties of the TV state sum rest. Kauffman and Lins also use the Matveev-Piergallini moves on special spines to demonstrate invariance of their state sum. Although they constructed their invariant to be simply a different presentation of the TV invariant, the equivalence between the two was later demonstrated formally by Piunikhin [Piu92].

We begin in Section 4.1 by recalling some elementary knot theory, including a brief discussion of the Kauffman bracket, which constitutes the foundation upon which everything else rests. After recalling the definitions of tangles and braids in Section 4.2 and the braid group in Section 4.3, we introduce the Temperley-Lieb algebra in Section 4.4 and its tangle-theoretic interpretation. To represent the recoupling theory of  $U_q(sl(2))$  graphically we next discuss the tangle-theoretic interpretation of the Jones-Wenzl projectors in Section 4.5, followed by an exposition of the  $q$ -symmetrizer in Section 4.6. introduction to the various components which make up our Kauffman-Lins tangle-theoretic version of the TV

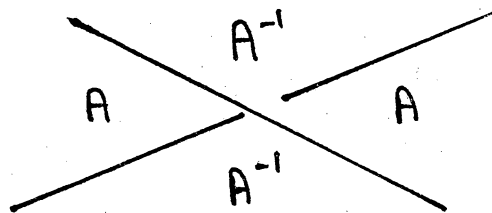
partition function in Section 4.7, and in Section 4.8 we sketch the specific moves our partition function will be required to satisfy in order to insure topological invariance. Section 4.9 follows with a tangle-theoretic interpretation of the 3-vertex. We offer a brief In Section 4.10 we explicitly define the theta net and tetrahedral net, and illustrate their relevance for computations. Finally, in Section 4.10 we define the state sum in this context and demonstrate its invariance under the Matveev-Piergallini moves.

The advantage of the Kauffman-Lins approach to the subject is that it is almost entirely elementary, but deceptively so because underlying everything is the sophisticated representation theory of the quantum group  $U_q(sl(2))$ . To see the connection between this and the work of Kauffman and Lins the reader is urged to consult the monograph of Carter, Flath, and Saito [CFS95]. The tangles used in the KL approach can be viewed as *q-spin networks*, a generalization of Penrose's *spin networks* [Pen71], which were first introduced by Roger Penrose as a way of recovering the properties of spacetime from the quantum mechanical rules for addition of angular momenta.



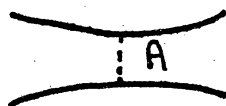
## 4.1 Knot Theory and Bracket Polynomial Basics

In this section we recall some elementary facts about the Kauffman bracket model for the Jones polynomial [Kau94]. Within a knot diagram we may have various under and overcrossings of strands. Kauffman's bracket is defined using a notion of 'smoothing' of a crossing as follows. We first label the different regions about the strands. If we walk upon an understrand toward a crossing the region to our left is labeled  $A$ , with the righthand region being labeled  $A^{-1}$ .

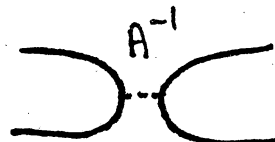


**Figure 4.1** *Labeling of a crossing*

For the above labeled crossing we have two different smoothings:



$A$ -smoothing joins  $A$  regions



$A^{-1}$ -smoothing joins  $A^{-1}$  regions

**Figure 4.2** *Smoothings of a crossing*

It is convenient to leave the label  $A$  or  $A^{-1}$  to indicate which smoothing has been performed.

The *Kauffman bracket* is a function from unoriented link diagrams to Laurent polynomials in a single variable  $A$  satisfying the two properties illustrated in the following figure, where  $d = -(A^2 + A^{-2})$  and it is understood that the pictures in the figure stand for a small part of the knot diagram  $D$ .

$$\langle \bigcirc D \rangle = d \langle D \rangle \quad (4.3)$$

$$\langle \text{crossing} \rangle = A \langle \text{smoothing 1} \rangle + A^{-1} \langle \text{smoothing 2} \rangle \quad (4.4)$$

**Figure 4.5** *Recursion relations for the bracket*

Following Kauffman [Kau94] we choose to normalize the bracket by setting  $\langle \phi \rangle = 1$ , where  $\phi$  is the empty knot (see Figure 4.6).

$$\langle \rangle = 1$$

**Figure 4.6** *The normalization of the bracket.*

In that case the value of the bracket of the unknot is  $d$ .

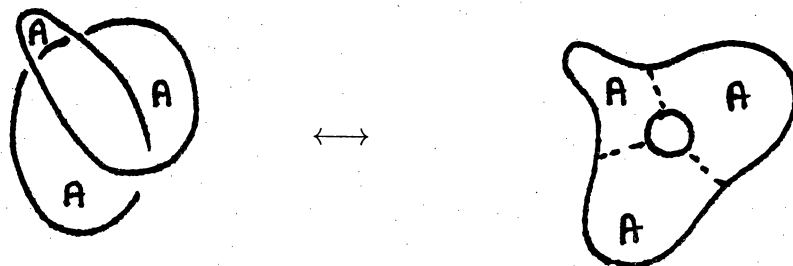
To calculate the Kauffman bracket of a knot we introduce the notion of the *state* of a diagram.

**Definition 4.7** A *state*  $S$  of a knot diagram  $D$  is a choice of smoothing at each crossing.

**Definition 4.8**  $\langle D|S \rangle$  denotes the product of the resulting labels in  $A$  after smoothing the knot diagram  $D$  into state  $S$ .

**Definition 4.9**  $\| S \|$  represents the number of disjoint Jordan curves in the state  $S$  of knot diagram  $D$ .

**Example 4.10** Given the diagram  $D$  for the trefoil knot, label the  $A$  regions, find the  $A$ -smoothing state and determine  $\| S \|$  for the state.



**Figure 4.11** *The  $A$ -smoothing state for the trefoil*

Since there are two disjoint Jordan curves for the above state,  $\| S \| = 2$ .

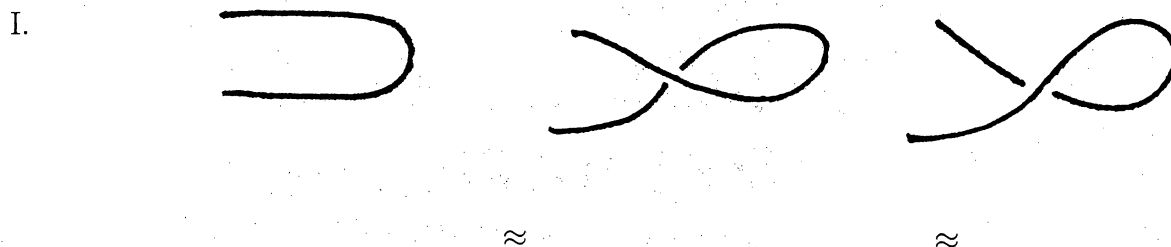
It follows that the Kauffman bracket of a knot diagram may be expressed as a sum over all states of the diagram.

$$\langle D \rangle := \sum_S \langle D | S \rangle d^{\| S \|} \quad (4.12)$$

where  $d = -A^2 - A^{-2}$ , and the bracket of the empty knot is defined to be  $\langle \phi \rangle := 1$ .

Recall that two diagrams  $D$  and  $D'$  represent the same link in three dimensions if and only if one can be transformed into the other by a sequence of *Reidemeister moves*.

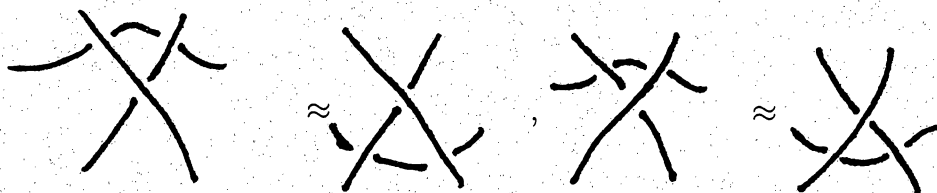
**Definition 4.13** *The Reidemeister Moves* for knot or link diagrams depicted below change the graphical structure of the diagram while leaving the topological type of the embedding of the corresponding knot or link the same.



II.



III.

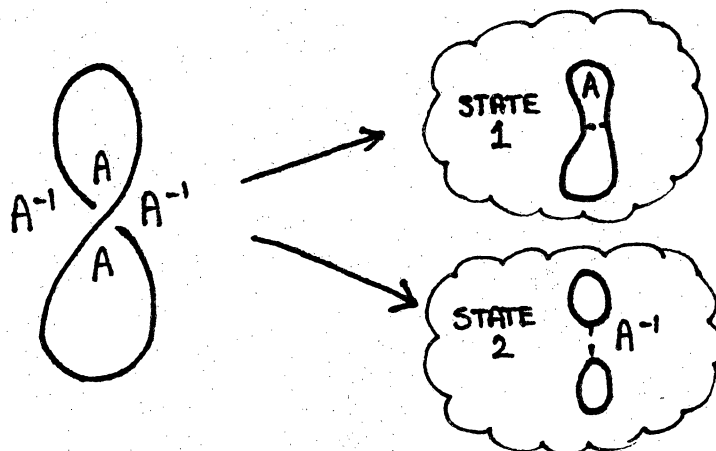


**Figure 4.14** *The three Reidemeister moves.*

If the two link diagrams  $D$  and  $D'$  are related by a sequence using only Reidemeister moves of types II and III, the links are said to be *regular isotopic*, whereas if the move of type I is needed the two links are *ambient isotopic*. It is easy to see [Kau87] that the bracket is invariant under moves of type II and III and so yields an invariant of regular isotopy.

The Kauffman bracket is not an ambient isotopy link invariant, as can be seen in the following example (although it is an ambient isotopy invariant of *framed* links).

**Example 4.15** Given: The unknot  $K$  with a twist.



**Figure 4.16** *The unknot with a twist*

Find: The bracket polynomial of  $K$ .

$$\begin{aligned}
 \langle \text{8} \rangle &= \sum_s \langle \text{8} \setminus s \rangle d^{\|s\|} \\
 &= Ad^1 + A^{-1}d^2 \\
 &= -\frac{d}{A^3} \quad \square
 \end{aligned}$$

**Figure 4.17** *The bracket of a twist*

Although it is not needed in what follows, we note in passing that the Kauffman bracket does provide us with an invariant of *oriented* links, which is essentially equivalent to the *Jones polynomial* [J83]. To each crossing in the diagram  $D$  of an oriented link  $L$  we may associate a sign  $\epsilon = \pm 1$  according to the following right hand rule: grasp the upper strand with your right hand; if your fingers curl in the direction of the lower strand, assign the crossing an  $\epsilon = +1$ , otherwise give it an  $\epsilon = -1$  assignment.

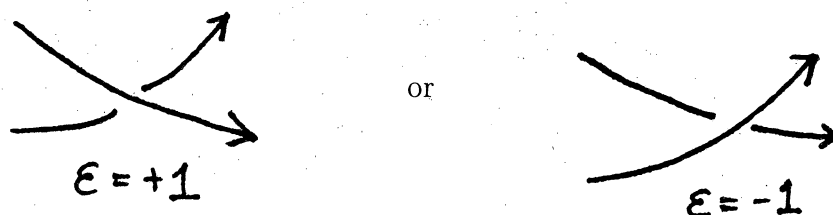


Figure 4.18 *The sign of a crossing*

The *writhe*  $w(D)$  of the diagram  $D$  of the oriented link  $L$  is just the sum of the signs of all the crossings. The Jones polynomial, an ambient isotopy invariant of oriented links, is given by

$$V(L) = (-A^{-3})^{w(D)} \langle D \rangle / \langle \bigcirc \rangle \quad (4.19)$$

where  $\bigcirc$  represents the unknot and  $A = t^{-1/4}$ .

## 4.2 Tangles and Braids

Consider two collections of  $n$  points in  $\mathbb{R}^3$ . Label the points of each set with the numbers from 1 to  $n$ , and add the names ‘input’ to the first set and ‘output’ to the second. Connect every pair of points with a curve (‘strand’) so that all the curves are disjoint. The resulting configuration is called a *tangle*. If each strand connects one input point to one output point the tangle is called a *braid*. It is convenient to arrange the input and output points in increasing order in opposing parallel rows in the plane and to confine the strands to a rectangular box whose top and bottom sides contain the output and input points, respectively.

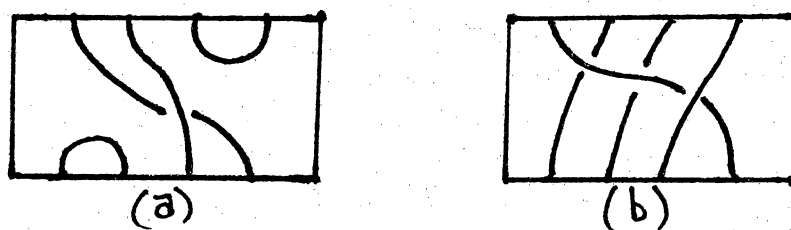


Figure 4.20 A tangle (a), and a braid (b)

Two tangles are ambient isotopic if there is an ambient isotopy from one to the other keeping the input and output points fixed and keeping the strands within the box.

Given a tangle  $x$ , we may form its *closure*  $\bar{x}$  by connecting the input and output points with ‘parallel’ strands that induce no new crossing, as shown ibelow.

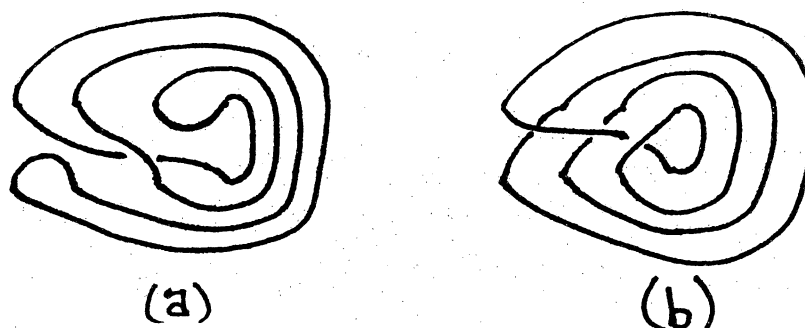


Figure 4.21 The closure of the tangles in Figure 4.20

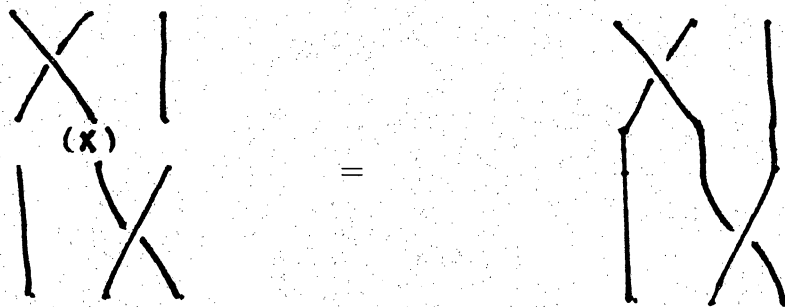
There is a close connection between braids and links, given by *Alexander's Theorem*

**Theorem 4.22** (*Alexander*) *Each link in  $\mathbb{R}^3$  is ambient isotopic to the closure of some braid.*



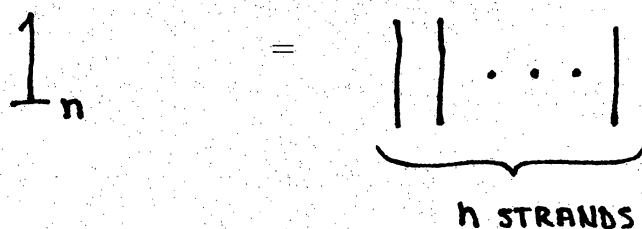
### 4.3 The Braid Group

The collection of all ambient isotopy equivalence classes of braids with  $n$  strands forms an infinite group, called the *Artin braid group on  $n$  strands*, denoted  $B_n$ . The product  $bb'$  of two braids  $b$  and  $b'$  is simply concatenation: identify the output strands of  $b'$  with the input strands of  $b$ .



**Figure 4.23** *The product of two braids in  $B_3$*

The identity element of the group is the braid with all parallel strands.



**Figure 4.24** *The identity element of  $B_n$*

Every braid in  $B_n$  can be written as a product of the  $n - 1$  *elementary braids* or *generators*  $\sigma_1, \sigma_2, \dots, \sigma_{n-1}$  and their inverses  $\sigma_1^{-1}, \sigma_2^{-1}, \dots, \sigma_{n-1}^{-1}$ . The  $i^{\text{th}}$  elementary braid  $\sigma_i$  connects the  $i^{\text{th}}$  input point to the  $(i + 1)^{\text{th}}$  output point and *vice versa*, as shown below.

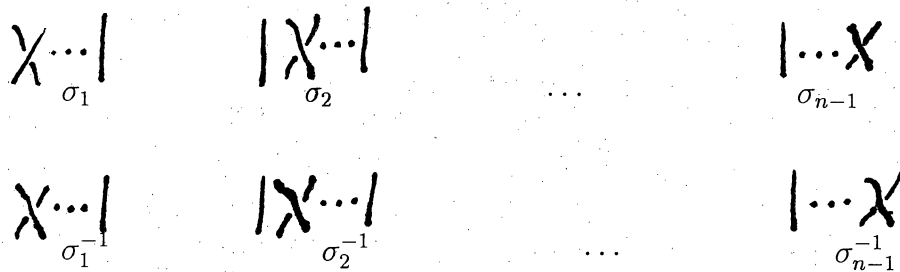
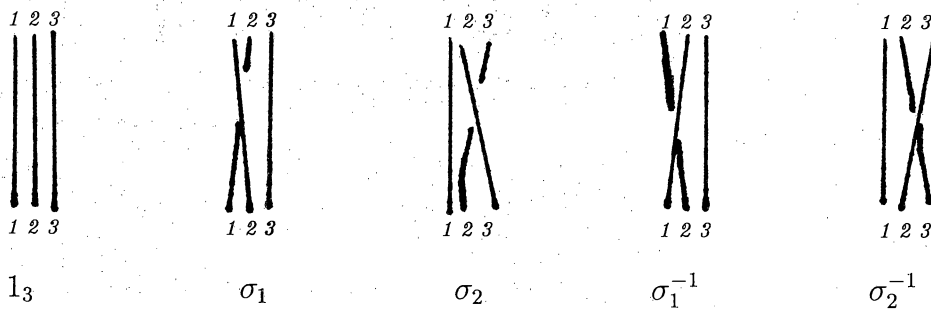


Figure 4.25 The generators of  $B_n$  and their inverses

The generators of the braid group on three strands  $B_3$  are:

Example 4.26 .



An arbitrary braid is given by a ‘word’, namely a concatenation of the ‘letters’ consisting of the elementary braids. For example, the braid word  $\sigma_1^{-1}\sigma_2\sigma_1^{-1}\sigma_2\sigma_1^{-1}\sigma_2$  is illustrated in Figure 4.27.

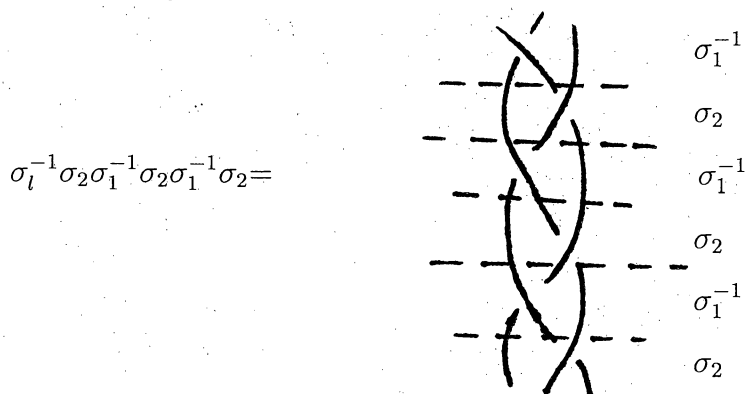


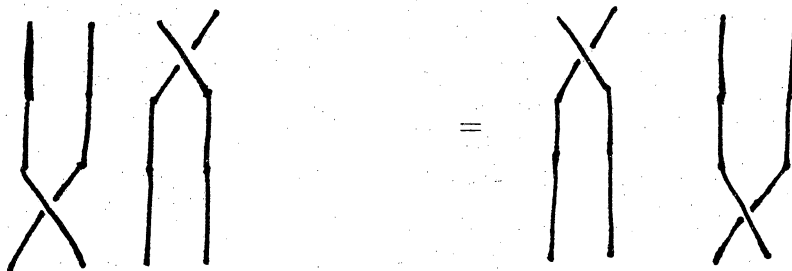
Figure 4.27 A braid word in  $B_3$

One may use the elementary braids and their inverses to give a presentation of the braid group in terms of the generators above and the following relations.

$$\sigma_i \sigma_j = \sigma_j \sigma_i \quad |i - j| > 1 \quad (4.28)$$

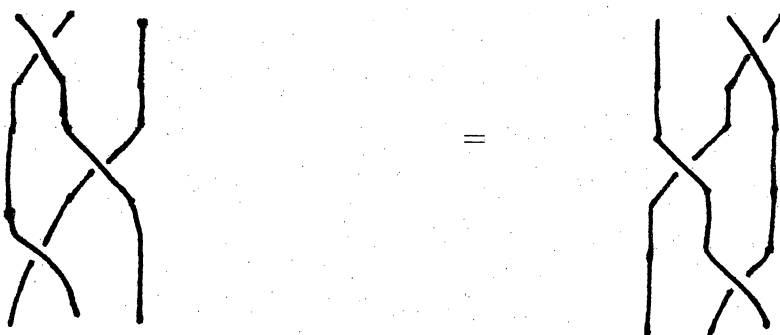
$$\sigma_i \sigma_{i+1} \sigma_i = \sigma_{i+1} \sigma_i \sigma_{i+1} \quad (4.29)$$

To illustrate these relations the example below demonstrates (4.28) in  $B_3$ , which is simply the Reidemeister move of type III.



**Figure 4.30** *Demonstration of (4.28) in  $B_3$ ,  $\sigma_1 \sigma_3 = \sigma_3 \sigma_1$*

The following example demonstrates the second braid relation (4.29) in  $B_3$ .

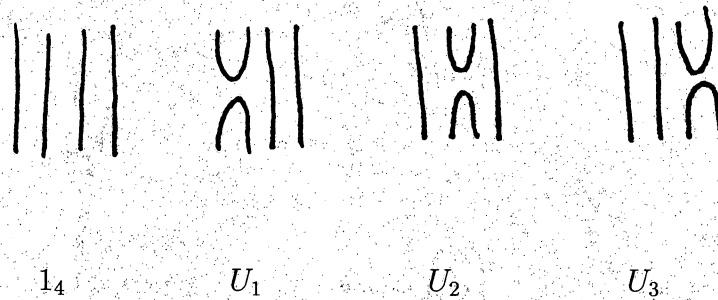


**Figure 4.31** *Demonstration of (4.29) in  $B_3$ ,  $\sigma_1 \sigma_2 \sigma_1 = \sigma_2 \sigma_1 \sigma_2$*

Note that  $S_n$ , the permutation group on  $n$  letters is just the quotient of the braid group modulo the relations  $\sigma_i^2 = 1$ .

## 4.4 The Temperley-Lieb Algebra

We define  $U_i$ , the  $i^{\text{th}}$  elementary tangle on  $n$  strands, to be the tangle obtained from the identity braid by connecting the  $i^{\text{th}}$  and  $(i+1)^{\text{th}}$  input together and the  $i^{\text{th}}$  and  $(i+1)^{\text{th}}$  output together.



**Figure 4.32** The identity tangle together with the elementary tangles on 4 strands

Using the same rule for multiplication as in the braid group (that is, concatenation),

$$U_1 U_2 = \frac{U_1}{U_2} = \text{diagram} = \text{diagram}$$

The diagram on the left shows the concatenation of  $U_1$  and  $U_2$ . The top part is  $U_1$  (cups and caps on strands 1 and 2), and the bottom part is  $U_2$  (cups and caps on strands 2 and 3). The middle strand (strand 2) has a cup from the top part and a cap from the bottom part, which cancel each other out. The resulting diagram on the right shows a single cup and cap on strands 1 and 2, with strand 3 remaining parallel.

**Figure 4.33** Example of multiplication of 4 strand tangles

we observe the following identities hold

## ABSTRACT RELATIONS    4 STRAND EXAMPLE

1.  $U_i^2 = dU_i$
  
2.  $U_i U_{i+1} U_i = U_i$
  
3.  $U_i U_j = U_j U_i$  for  $|i - j| > 1$

**Figure 4.34** *Temperley-Lieb algebra identities*

where  $d$  is defined below.

Let  $A$  be an indeterminate, and let  $\tilde{\mathbb{Z}}[A, A^{-1}]$  denote the ring of Laurent polynomials in  $A$  with integral coefficients. By  $\tilde{\mathbb{Z}}[A, A^{-1}]$  we mean the set of rational functions of the form  $P/Q$  with  $P, Q \in \tilde{\mathbb{Z}}[A, A^{-1}]$ . The *Temperley-Lieb algebra*  $T_n$  is the free additive algebra over  $\tilde{\mathbb{Z}}[A, A^{-1}]$  with multiplicative generators  $1_n, U_1, U_2, \dots, U_{n-1}$  and the relations of Figure 4.34 above. So the elements in Figure 4.32, for example, are the *generators* of the 4 strand Temperley-Lieb algebra  $T_4$ . We choose  $d = -(A^2 + A^{-2})$ ; it is clear that  $d$  commutes with all the elements of  $T_n$ , so it can be treated like a scalar. What is not so clear is that the diagrammatics of the elementary tangles encodes precisely the relations of the Temperley-Lieb algebra.

There exists an intimate connection between the Jones polynomial and the tangle-version of the T-L algebra. The Jones polynomial is actually defined via a representation of the Artin braid group  $B_n$  into the T-L algebra. There is, indeed, an underlying representation  $\rho$  from  $B_n$  into abstract  $T_n$  that produces a correspondence between elementary braids and the abstract basis elements  $U_i$  of  $T_n$ . We now begin our investigation of representation  $\rho$ .

## SMOOTHINGS OF $B_n$

Let us consider the two types of smoothings, state 1 and state 2 as described in Section 4.1, of elementary braids of  $B_n$ . We investigate the relationship between tangles in Figure 4.32 and the bracket evaluation of elementary braids and their closures. Recalling that the bracket of a knot diagram requires smoothings of the internal crossings, it becomes evident that the bracket state of the closure of a braid depends upon smoothings of braid crossings. Our demonstration begins using  $\sigma_2$ , and  $\sigma_2^{-1}$ , in the three strand basis for  $B_3$  of Example 4.26.

*Horizontal Smoothings:*

$$H(\sigma_2) = H\left(\begin{array}{c} | \\ \diagdown \diagup \\ | \end{array}\right) = \begin{array}{c} | \\ \bigcup \\ | \end{array} = U_2 \text{ in Figure 4.32}$$

also

$$H(\sigma_2^{-1}) = H\left(\begin{array}{c} | \\ \diagup \diagdown \\ | \end{array}\right) = \begin{array}{c} | \\ \bigcap \\ | \end{array} = U_2 \text{ in Figure 4.32}$$

We may conclude that in general  $H(\sigma_i^{\pm}) = U_i$  in our set of elementary tangles (see Figure 4.32 for the 4 strand example) in an  $n$ -strand basis.

*Vertical smoothings:*

$$V(\sigma_2) = V\left(\begin{array}{c} \diagdown \diagup \\ | \end{array}\right) = ||| = 1_3 \text{ identity element in } B_3.$$

also

$$V(\sigma_2^{-1}) = V\left(\begin{array}{c} \diagup \diagdown \\ | \end{array}\right) = ||| = 1_3 \text{ identity element in } B_3.$$

We may conclude that in general  $V(\sigma_i^{\pm}) = 1_n$ , the identity element in  $B_n$ .

Recalling that the recursion property of the bracket in Section 4.1 requires that we perform state smoothings, the bracket of an elementary braid may be

$$\overline{V(\sigma_2)} = \overline{V(1 \times )} = \overline{|||} = \bigcirc = \overline{1_3}$$

*Closure of Vertical Smoothings:*

$$\overline{H(\sigma_2^{-1})} = \overline{H(1 \times )} = \overline{|| \cup} = \bigcirc = \overline{|| \cup} = \overline{U_2}$$

$$\overline{H(\sigma_2)} = \overline{H(1 \times )} = \overline{|| \cup} = \bigcirc = \overline{|| \cup} = \overline{U_2}$$

*Closure of Horizontal Smoothings:*

different smoothings performed above.

closure of smoothings of elementary braid elements. First we look at closures of the

Our goal here is to examine the bracket of a special knot, specifically the

with an bar drawn over the braid element,  $\bar{b}$ , we refer the reader back to Figure 4.21.

Before considering the *closure* of these types of smoothings, which we indicate

$$\langle \sigma_i^{-1} \rangle := A \langle U_i \rangle + A^{-1} \langle 1_n \rangle \quad (4.36)$$

and

$$\langle \sigma_i \rangle := A \langle 1_n \rangle + A^{-1} \langle U_i \rangle \quad (4.35)$$

the elementary tangles in Figure 4.32:

viewed as a localized horizontal/vertical smoothing action which will be related to

$$\overline{V(\sigma_2^{-1})} = \overline{V(\text{I} \times)} = \overline{|||} = \text{D} = \overline{1_3}$$

We conclude in general that  $\overline{H(\sigma_i^\pm)} = \overline{U_i}$  and  $\overline{V(\sigma_i^\pm)} = \overline{1_n}$ . In other words, closures of the states of braids correspond to closures of the tangles in Figure 4.32.

As with the bracket evaluation of the open braids (4.35) and (4.36), it is clear that the bracket state of any closed braid,  $\langle \bar{b} \rangle$ , is related to the strand closure of our elementary tangles.

$$\langle \bar{\sigma}_i \rangle = \langle \bar{\sigma}_i | A \text{ state} \rangle d^{||\overline{U_i}||} + \langle \bar{\sigma}_i | A^{-1} \text{ state} \rangle d^{||\overline{1_n}||} \quad (4.37)$$

Let us consider an example of the bracket of the closed braid  $\sigma_1$  in  $B_2$ .

Diagrammatically our  $\sigma_1$  is  $\times$ , which implies that its closure is

$$\overline{\sigma_1} = \text{D} . \quad (4.38)$$

Also in  $B_2$  we have the diagram for the elementary tangle  $U_1 =$ , which implies that

$$\overline{U_1} = \overline{\text{U}} = \text{D} . \quad (4.39)$$

The “A” smoothing state of  $\overline{\sigma_1}$  is

$$\text{D}^A = \overline{U_1} \quad (4.40)$$

while the identity braid in  $B_2$  is

$$1_2 = || \implies \overline{1_2} = \text{D} \quad (4.41)$$

The “ $A^{-1}$ ” smoothing state of  $\overline{\sigma_1}$  is



$$\begin{array}{c} A^{-1} \\ \text{---} \bigcirc \end{array} = \overline{1_2}. \quad (4.42)$$

With all the preliminaries in place, we begin our example.

**Example 4.43** The evaluation of  $\langle \overline{\sigma_1} \rangle$  in  $B_2$  is:

$$\begin{aligned} \langle \overline{\sigma_1} \rangle &= \langle \overline{\sigma_1} | A \text{ state} \rangle d^{\|\overline{U_1}\|} + \langle \overline{\sigma_1} | A^{-1} \text{ state} \rangle d^{\|\overline{1_2}\|} \\ &= \langle \begin{array}{c} \text{---} \bigcirc \end{array} \rangle d^{\|\begin{array}{c} \text{---} \bigcirc \end{array}\|} + \langle \begin{array}{c} \bigcirc \end{array} \rangle d^{\|\begin{array}{c} \bigcirc \end{array}\|} \\ &= \langle \overline{U_1} \rangle d^{\|\begin{array}{c} \text{---} \bigcirc \end{array}\|} + \langle \overline{1_2} \rangle d^{\|\begin{array}{c} \bigcirc \end{array}\|} \\ &= A d^{\|\begin{array}{c} \text{---} \bigcirc \end{array}\|} + A^{-1} d^{\|\begin{array}{c} \bigcirc \end{array}\|} \\ &= Ad + A^{-1}d^2 \\ &\quad - \frac{d}{A^3} \end{aligned}$$

Apparently our set of tangles in Figure 4.32 (for example) is becoming very important. We have expressed the bracket evaluation of elementary braid elements and the bracket of the closure of such in terms of these tangles. Having clearly established an association between the Artin braid group  $B_n$  and the set of tangles in Figure 4.32, let us now consider Jones' representation  $\rho$ .

### REPRESENTATION $\rho$

With our tangle-theoretic foundation appropriately constructed, we may now define our underlying representation from the braid group to the abstract T-L algebra.

The representation  $\rho : B_n \longrightarrow T_n$  is determined by:

$$\rho(\sigma_i) = AU_i + A^{-1}1_n \quad (4.44)$$

$$\rho(\sigma_i^{-1}) = A^{-1}U_i + A1_n. \quad (4.45)$$

Next, we define the trace from the  $r$ -strand tangle algebra  $T_r$  to the field of polynomials in  $A$  and  $A^{-1}$ .

**Definition 4.46** The *trace*,  $tr : T_r \longrightarrow \mathbf{Z}[A, A^{-1}]$ , is defined by:

- i)  $tr(x) = \langle \bar{x} \rangle$  where  $\langle \rangle$  is the Kauffman bracket.
- ii)  $tr(x + y) = tr(x) + tr(y)$ .

With this definition it follows that Kauffman's trace and Jones' trace coincide via the equation

$$tr\rho(b) = \langle \bar{b} \rangle \quad (4.47)$$

and both yield the Jones polynomial.

## 4.5 The Jones-Wenzl Projectors

We now define special idempotents in the Temperley-Lieb algebra and investigate some of their properties. Using these idempotents we will be able to define a trivalent vertex (related to the quantum 3j symbols giving the recoupling of two representations of  $U_q(sl(2))$ ) and (a version of) the quantum 6j symbols, both of which are the main ingredients in the definition of the KL invariant.

In this section we will inductively define a very special element  $f_i$  of the abstract Temperley-Lieb algebra which is called the Jones-Wenzl projector. Each  $f_i$  is actually the product of the generators of abstract  $T_n$ , extended linearly. Our special  $f_i$  are restricted by the following definition.

**Definition 4.48** For each  $k \in \{0, 1, \dots, n-1\}$ , provided  $A$  is chosen so that  $\Delta_1 \Delta_2 \dots \Delta_k \neq 0$ , we may define the  $k^{\text{th}}$  *Jones-Wenzl projector* recursively by

$$f_0 = 1_n \tag{4.49}$$

$$f_{k+1} = f_k - \mu_{k+1} f_k U_{k+1} f_k \tag{4.50}$$

where

$$\mu_1 = d^{-1} \tag{4.51}$$

$$\mu_{k+1} = (d - \mu_k)^{-1} \tag{4.52}$$

$$d = -A^2 - A^{-2} \quad (4.53)$$

$$U_i^2 = dU_i, \quad \forall i \quad (4.54)$$

**Example 4.55** In  $T_2$  the element  $f_1$  is given by

$$\begin{aligned} f_1 &= f_0 - \mu_1 f_0 U_1 f_0 \\ &= 1_2 - (d^{-1})(1_2)(U_1)(1_2) \\ &= 1_2 - d^{-1}(U_1) \\ &= 1_2 - \frac{1}{d}U_1 \end{aligned}$$

For each  $k \geq -1$  we define the polynomial function  $\Delta_n$  of degree  $n$  in  $d = -(A^2 + A^{-2})$  by the recursion

$$\Delta_n = d\Delta_{n-1} - \Delta_{n-2} \quad (4.56)$$

with the initial conditions  $\Delta_0 = 1$  and  $\Delta_{-1} = 0$ . Then  $\Delta_n$  is the  $n^{\text{th}}$  (renormalized) *Chebyshev polynomial* of the second kind.

**Lemma 4.57** ([W87]) *The Jones-Wenzl projectors satisfy the following properties:*

$$\text{i) } f_i^2 = f_i \text{ for } i = 0, 1, \dots, n-1 \quad (4.58)$$

$$\text{ii) } f_i U_j = U_j f_i = 0 \text{ for } j \leq i \quad (4.59)$$

$$\text{iii) } \text{tr}(f_{n-1}) = \Delta_n = \Delta_n(-A^2) \quad (4.60)$$

and

$$\mu_{k+1} = \Delta_k / \Delta_{k+1} \quad (4.61)$$

where  $\Delta_n(x) = (x^{n+1} - x^{-n-1}) / (x - x^{-1})$  is the  $n$ th Chebyshev polynomial

(For proof see [L91].)

We now offer an interesting and what will prove to be a most important proposition. Be forewarned that the element  $f$  in the following proposition must satisfy the properties in Lemma 4.57. Therefore,  $f$  in the proposition is actually  $f_{n-1}$  in disguise.

**Proposition 4.62** *There exists unique Jones Wentzl projector*

$f \in T_n$ ,  $f \neq 0$ , such that

- i)  $f^2 = f$
- ii)  $fU_i = U_i f = 0 \quad i=0,1,\dots,n-1$

Proof:

Existence:

Clearly, according to the required properties our  $f$  equals  $f_{n-1}$ , therefore we have existence by Lemma 4.57.

Uniqueness:

Let  $g \in T_n$ ,  $g \neq 0$ .

Let  $g^2 = g$  and  $gU_i = U_i g = 0$ , for  $i=0,1,\dots,n-1$ .

So  $g$  is a linear combination of products of our abstract  $T_n$  generators  $\{1_n, U_1, \dots, U_{n-1}\}$ .

Let  $U$  be the sum of products of  $U'_i$ s.

$$\text{ie. } U = b_1 U_1 + b_2 U_2 + b_3 U_3 + \dots + c_1 U_1 U_2 + c_2 U_1 U_3 + \dots$$

where each term includes at least one  $U_i$

Therefore, we may write  $g = a1_n + U$  for  $a \in \text{field}$ .

By our hypothesis,  $g^2 = g$ .

$$\implies (a1_n + U)(a1_n + U) = (a1_n + U)$$

$$\implies a^2 1_n + 2a1_n U + U^2 = (a1_n + U)$$

But since each term in  $U$  includes at least one  $U_i$ ,  $a^2 1_n$  must equal  $a1_n$ .

$$\implies a^2 = a$$

$$\implies a = 1$$

$$\implies g = 1_n + U.$$

By the same argument  $f$  in the statement of our proposition is:

$$f = 1_n + U'$$

Demonstrating that  $f$  and  $g$  are the same element:

$$\begin{aligned} f &= f + fU && \{by\ fU = 0 \\ &= f(1_n + U) \\ &= fg && \{by\ g = 1_n + U \\ &= (1_n + U')g && \{by\ f = 1_n + U' \\ &= 1_n g + U'g \\ &= 1_n g && \{by\ U'g = 0\ \text{in hypothesis} \\ &= g \end{aligned} \quad \square$$

When we view our algebra elements from their tangle-theoretic perspective it allows us to work with examples and proofs involving projectors in a more hands-on manipulative manner. For instance, consider the following example of property (ii) of Proposition 4.62 in the three strand Temperley-Lieb algebra.

**Example 4.63** In  $T_3$ :

$$f_0 = ||| \text{ and } U_1 = \bigcap^{\cup} |.$$

So, by Definition 4.48:

$$f_1 = f_0 - \mu_1 f_0 U_1 f_0 = ||| - \frac{1}{d} \bigcap^{\cup} |.$$

And

$$\begin{aligned} f_2 &= f_1 - \mu_2 f_1 U_2 f_1 \\ &= \left( ||| - \frac{1}{d} \bigcap^{\cup} | \right) - (d - d^{-1})^{-1} \left( ||| - \frac{1}{d} \bigcap^{\cup} | \right) \left( | \bigcap^{\cup} \right) \left( ||| - \frac{1}{d} \bigcap^{\cup} | \right) \\ &= ||| - \frac{1}{d} \bigcap^{\cup} | - (d - d^{-1})^{-1} \left( ||| - \frac{1}{d} \bigcap^{\cup} | \right) \left( | \bigcap^{\cup} - \frac{1}{d} \text{ (crossing) } \right) \\ &= ||| - \frac{1}{d} \bigcap^{\cup} | - (d - d^{-1})^{-1} \left[ | \bigcap^{\cup} - \frac{1}{d} \text{ (cup) } - \frac{1}{d} \text{ (cap) } + \frac{1}{d^2} \text{ (cup-cap) } \right] \end{aligned}$$

$$0 =$$

$${}_1U \left[ \frac{({}_1-p-p)p}{1} + \left( \frac{1-z^p}{1} + 1 \right) - 1 \right] =$$

$$U_1 f_2 = \bigcup \left[ \frac{p}{1} + \frac{(p-z^p)}{1} \right] - \bigcup \left[ \frac{p}{1} - \frac{({}_1-p-p)}{1} \right] - \bigcup \left[ \frac{p}{1} - \frac{p}{1} \right] =$$

Therefore


$$= ||| - \left[ \frac{p}{1} + \frac{({}_1-p-p)z^p}{1} \right] - \bigcup \left[ \frac{p}{1} - \frac{({}_1-p-p)}{1} \right] - \bigcup \left[ \frac{p}{1} - \frac{p}{1} \right] =$$



## 4.6 The $q$ -symmetrizer


We now define a special tangle, called a  $q$ -symmetrizer, which may be viewed as the quantum analogue of the *antisymmetrizer* of Penrose's spin network theory (see [Kau91]). The  $q$ -symmetrizer is the basic tool used in the diagrammatic approach to the recoupling theory of  $U_q(sl(2))$ . Although it is defined below to be an element of the braid group, we may use the representation defined in Section 4.4 (the Kauffman bracket) to view it as an element of the Temperley-Lieb algebra.

**Definition 4.64** Let  $S_n$  denote the symmetric group on  $n$  letters. The *length*  $l(\sigma)$  of  $\sigma \in S_n$  is the *minimal* number of adjacent transpositions required to write  $\sigma$  (non-uniquely) as a product of adjacent transpositions.

**Definition 4.65** For any permutation  $\sigma \in S_n$  we define  to be the  $n$ -tangle obtained from any *minimal presentation* of  $\sigma$  in which each transposition is replaced by a *positive* braid generator  $\sigma_i^+$ .

**Example 4.66** Given: Permutation

$$\sigma = \begin{pmatrix} 1 & 2 & 3 \\ 3 & 1 & 2 \end{pmatrix} = (132)$$

Find: 

Write  $\sigma$  as product of transpositions:

$$(132)$$

$$=(23)(12)$$

$$= \begin{pmatrix} 1 & 2 & 3 \\ 1 & 3 & 2 \end{pmatrix} \begin{pmatrix} 1 & 2 & 3 \\ 2 & 1 & 3 \end{pmatrix}$$

Replace transpositions with corresponding elementary braids,  $\sigma_2$  and  $\sigma_1$  in

$B_3$ :

$$= \left( \begin{array}{c} | \text{X} \end{array} \right) \left( \begin{array}{c} \text{X} | \end{array} \right)$$

Multiply via concatenation:

$$= \frac{\text{X} |}{| \text{X}}$$

The result is the minimal representation of  $\sigma$  as the product of transpositions  
(I.e. our diagrammatic representation of  $\sigma$  as a braid projection):

$$= \begin{array}{c} \text{X} \\ \text{X} \end{array}$$

$$= \begin{array}{c} \boxed{\hat{\sigma}} \end{array}$$

**Figure 4.67** The braid  $\hat{\sigma}$  corresponding to the permutation (132)


Note that in our previous example the length  $t(\sigma)$  of the permutation  $\sigma$  is equal to 2.

**Definition 4.68** The  $q$ -deformed factorial  $\{n\}!$  (where  $q = A^2$ ) is given by

$$\{n\}! = \sum_{\sigma \in S_n} (A^{-4})^{t(\sigma)} = \prod_{k=1}^n \left[ \frac{1 - A^{-4k}}{1 - A^{-4}} \right] \quad (4.69)$$


(Note: The last equality follows from well-known combinatorial arguments. See [S86].)

Having introduced the *length* of a permutation  $\tau(\sigma)$ , the diagrammatic representation of the group  $S_n$  as braid projections  $\hat{\sigma}$ , and the *q-deformed factorial*  $\{n\}!$  we are now in a position to define the *q-symmetrizer*

**Definition 4.70** The *q-symmetrizer*, , denotes the sum of n-tangles for  $n \in \mathbb{Z}$  defined by:

$$\text{Diagram: square with vertical line, labeled } n \text{ above it} = \frac{1}{\{n\}!} \sum_{\sigma \in S_n} (A^{-3})^{t(\sigma)} \text{Diagram: square with vertical line, labeled } \hat{\sigma} \text{ above it} \quad (4.71)$$

Next we offer a proposition for our sum-of-tangles projector, which is parallel to Proposition 4.62 for abstract projectors.

**Proposition 4.72** If  $g_n \in T_n$  denotes the image of  in the Temperley-Lieb algebra, then

- i)  $g_n^2 = g_n$
- ii)  $g_n U_i = U_i g_n = 0$ , for  $i=1,2,\dots,n-1$ .

Hence by Proposition 4.62 we conclude that  $g_n = f_{n-1} = \text{Diagram: square with vertical line, labeled n above it}$ . Restated,  $f_{n-1}$ , the projector defined abstractly as a linear combination of products of abstract generators of the Temperley-Lieb algebra  $\{1_n, U_1, U_2, \dots, U_{n-1}\}$ , is equal to  $g_n$ , the projector defined diagrammatically as the sum of tangles. Before proving Proposition 4.72 we demonstrate this equality for the case of the Temperley-Lieb (tangle theoretic) algebra on two strands.

**Example 4.73** Show that  $f_1 \in T_2$  is equal to  $g_2 \in T_2$ :

Let us begin with some preliminaries that will be needed for our calculation of  $g_2$ .

$$i) S_2 = \{(1), (12)\} \Rightarrow \{||, \times\} = \left\{ \begin{array}{|c|} \hline \hat{1} \\ \hline \hat{2} \\ \hline \end{array} \right., \quad \begin{array}{|c|} \hline \hat{\sigma_1} \\ \hline \end{array} \right\}$$

$$ii) t(1_2) = \text{number of transpositions in } 1_2 = 0$$

$$iii) t(\sigma_1) = \text{number of transpositions in } (12) = 1$$

$$iv) \{2\}! = \sum_{\sigma \in S_2} (A^{-4})^{t(\sigma)} = 1 + A^{-4}$$

v) Recall the basic fact that any  $n$ -tangle may be extended via the bracket identity:

$$[\times] = [A \asymp + A^{-1}] = \left[ A \overset{\cup}{\cap} + A^{-1} || \right]$$

We are now prepared to prove that  $f_1$  in  $T_2$  is equal to  $g_2$  in  $T_2$ .

Proof:

$$[g_2 \in T_2] = \begin{array}{|c|} \hline \text{ } \\ \hline \end{array} = \frac{1}{\{2\}!} \sum_{\sigma \in S_2} (A^{-3})^{t(\sigma)} \begin{array}{|c|} \hline \hat{\sigma} \\ \hline \end{array}$$

$$= \frac{1}{\{2\}!} [(A^{-3})^{t(12)} || + (A^{-3})^{t(\sigma_1)} \times] \quad \{\text{by } i\}$$

$$= \frac{1}{\{2\}!} [(A^{-3})^0 || + (A^{-3})^1 \times] \quad \{\text{by } ii, iii\}$$

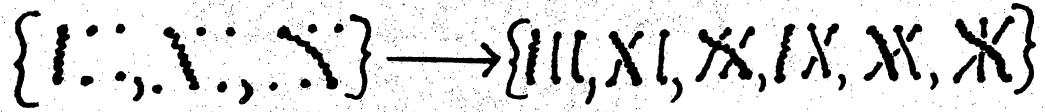
$$= \frac{1}{\{2\}!} [|| + A^{-3} \times]$$

$$\begin{aligned}
&= \frac{1}{(1+A^{-4})} \left[ \parallel + A^{-2} \overset{\cup}{\cap} + A^{-4} \parallel \right] \\
&= \frac{1}{(1+A^{-4})} \left[ (1+A^{-4}) \parallel + (A^{-2}) \overset{\cup}{\cap} \right] \\
&= \parallel + \left( \frac{A^{-2}}{1+A^{-4}} \right) \overset{\cup}{\cap} \\
&= \parallel + \left( \frac{1}{A^2} \right) \left( \frac{1}{1+A^{-4}} \right) \overset{\cup}{\cap} \\
&= \parallel + \left( \frac{1}{A^2 + A^{-2}} \right) \overset{\cup}{\cap} \\
&= \parallel - \frac{1}{d} \overset{\cup}{\cap} \quad \{by \ d = -(A^2 + A^{-2})\} \\
&= f_1 \in T_2 \text{ as detailed in Section 4.72.}
\end{aligned}$$

□

In order to prove Proposition 4.72 we develop a canonical inductive construction for braids  $\hat{\sigma}$  with  $\sigma \in S_n$ . By the convention of lifting to positive

In order to prove Proposition 4.72 we develop a canonical inductive construction for braids  $\hat{\sigma}$  with  $\sigma \in S_n$ . By the convention of lifting to positive braids, the strand from input  $i$  to output 1 will *overcross* all the other strands it meets. So  $\{\hat{\sigma}|\sigma \in S_n\}$  is constructed from the set  $\{\hat{\tau}|\tau \in S_{n-1}\}$  by first placing the strands from input  $i$  to output 1, and then repeating the procedure *beneath* the strands already placed. For example, the construction of  $\{\hat{\sigma}|\sigma \in S_3\}$  from  $\{\hat{\tau}|\tau \in S_2\}$  is illustrated in Figure 4.74.



**Figure 4.74** The canonical inductive construction of the braid set  $\{\hat{\sigma}|\sigma \in S_3\}$

We now prove Proposition 4.72.

Proof:

It can be seen from the canonical inductive construction of the braid set that  $\{\hat{\sigma}|\sigma \in S_n\}$  can be written, for any given  $i \in \{1, 2, \dots, n-1\}$ , as a disjoint union of a set  $W$  of braids not ending in  $\sigma_i$  and a set  $W' = \{w\sigma_i|w \in W\}$ . Hence we may write

$$\{n\}!g_n = \sum_{w \in W} (A^{-3})^{t(w)}w + (A^{-3})^{t(w)+1}w\sigma_i$$

But  $w\sigma_i U_i = (-A^3)wU_i$  in  $T_n$ , hence  $g_n U_i = 0$  for  $i = 1, 2, \dots, n-1$ . This completes the proof of property (ii).

To prove (i) we must show that  $g_n = 1_n + U$  as in the proof of Proposition 4.62 (ii), for then  $g_n^2 = g_n(1 + U) = g_n$  because  $g_n U = 0$ . Consider the sum  $\tilde{g}_n := \sum_{\sigma \in S_n} (A^{-3})^{t(\sigma)}\hat{\sigma}$ . Any particular  $\hat{\sigma}$  in the sum gives, when expanded using the bracket relations, a term of the form  $(A^{-1})^{t(\sigma)}1_n + U$ , because there are precisely  $t(\sigma)$  adjacent transpositions that need smoothing to reach the identity braid. Hence the coefficient of  $1_n$  in the sum for  $\tilde{g}_n$  is  $\sum_{\sigma \in S_n} (A^{-4})^{t(\sigma)} = \{n\}!$ , from which the result follows.  $\square$

**Example 4.75** Show that  $g_n^2 = g_n$  in  $T_2$ :

$$g_2^2 = \left( \parallel - \frac{1}{d} \overset{\cup}{\cap} \right) \left( \parallel - \frac{1}{d} \overset{\cup}{\cap} \right)$$

(This is a result of the previous example.)

$$= \left( \parallel - \frac{1}{d} \overset{\cup}{\cap} - \frac{1}{d} \overset{\cup}{\cap} + \frac{1}{d^2} \overset{\cup}{\cap} \overset{\cup}{\cap} \right)$$

$$= \parallel - \frac{1}{d} \overset{\cup}{\cap} - \frac{1}{d} \overset{\cup}{\cap} + \frac{1}{d^2} d \overset{\cup}{\cap}$$

$$= \parallel - \frac{1}{d} \overset{\cup}{\cap}$$

$$= g$$

□

An important detail when working with the  $q$ -symmetrizer is to address the question of what occurs when we fit a loop (a turnbacked cable) with our projector. We use property (ii) of Proposition 4.72 in  $T_2$  to demonstrate what the results would be in such a case.

But, of course, we must first settle preliminaries. Note the following smoothing of a particular tangle.

$$\begin{aligned}
& \text{Diagram: A vertical line with a loop on the left labeled } A \text{ and a loop on the right labeled } A^{-1}. \\
&= A \text{ (crossing) } + A^{-1} \text{ (crossing) } \\
&= A \circ U + A^{-1}U \\
&= AdU + A^{-1}U \\
&= [A(-A^2 - A^{-2}) + A^{-1}]U \\
&+ (-A^3 - A^{-1} + A^{-1})U \\
&= -A^3U
\end{aligned}$$

Keep the result of the above smoothing in mind for our next example.

**Example 4.76** Proof of  $g_n U_i = 0$  in  $T_2$ :

$$\begin{aligned}
g_2 U_1 &= \text{Diagram: A box with a crossing inside} = \text{Diagram: A box with a crossing inside} \\
&= \frac{1}{\{2\}!} \left[ \text{Diagram: A crossing} + A^{-3} \text{Diagram: A crossing} \right] \\
&= \frac{1}{\{2\}!} \left[ \bigcup + A^{-3} \text{Diagram: A crossing} \right] \\
&= \frac{1}{\{2\}!} \left[ \bigcup + A^{-3} (-A^3 U) \right] \\
&= \frac{1}{\{2\}!} \left[ \bigcup - \bigcup \right]
\end{aligned}$$



$$= 0$$

□

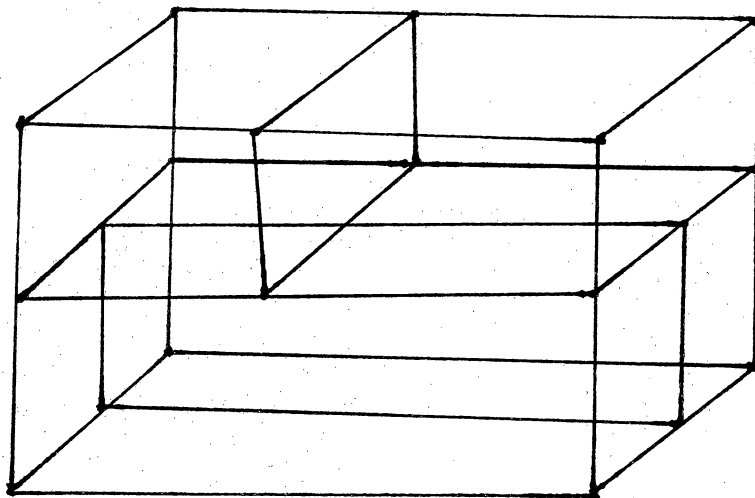
Hence, we see that the T-L projector obliterates the loop.

## 4.7 Partition Function Weights

The Turaev-Viro (TV) invariant of 3-manifolds is similar to the CFS invariant in that it is obtained via state summation. The KL invariant of 3-manifolds is also constructed via state summation and both methods of construction depend upon Mateev moves [Mat88], but the KL invariant is based upon the recoupling theory of q-spin networks [Kau94]. Kauffman-Lins' invariant is founded upon the algebra of tangles, as recoupling theory is actually tangle-theoretic.

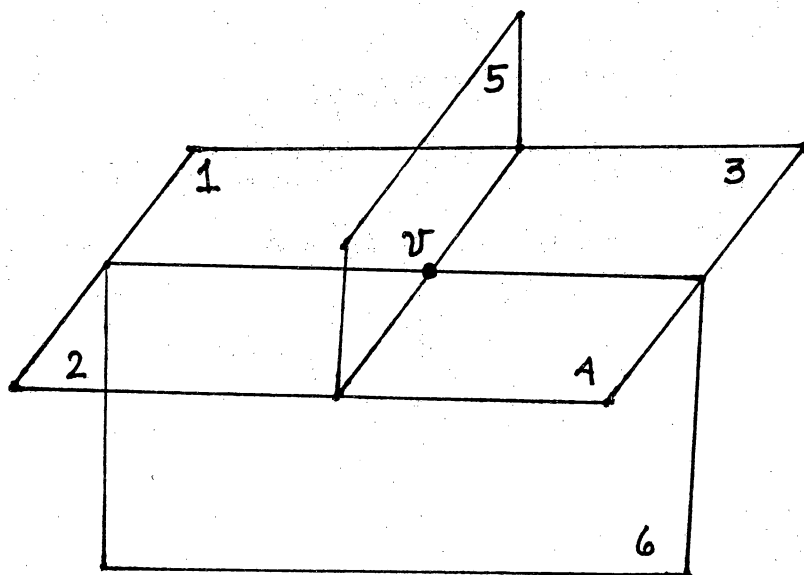
In CFS theory our 3-manifold was triangulated into a structure composed of kite-like 3-cells (the meeting place of at least three triangles at a 3-hinge), so one could imagine space being constructed of a network of these 3-cells. In other three dimensional theories space is decomposed into a network of tetrahedra. In KL theory we consider an alternative triangulation by developing a special spine which is simply the three dimensional dual complex of the tetrahedron. Hence, in KL theory we imagine space being composed of a network of special spines.

In order to understand the construction of the Kauffman-Lins version of the Turaev-Viro invariant we offer the following description of a special spine, the dual to a tetrahedral triangulation of a 3-manifold [TV92]. We begin our development by considering an arrangement of four 3-cells.



**Figure 4.77** *A four 3-cell arrangement of space*

We next remove the 3-cells, leaving only the skeletal remains which consist of six 2-cells (faces) meeting at one vertex  $v$ .



**Figure 4.78** *Skeletal remains of four 3-cells*

Our skeletal structure is dual to the tetrahedron, as each 1-cell (edge) of the tetrahedron pierces a 2-cell (face) of the structure.

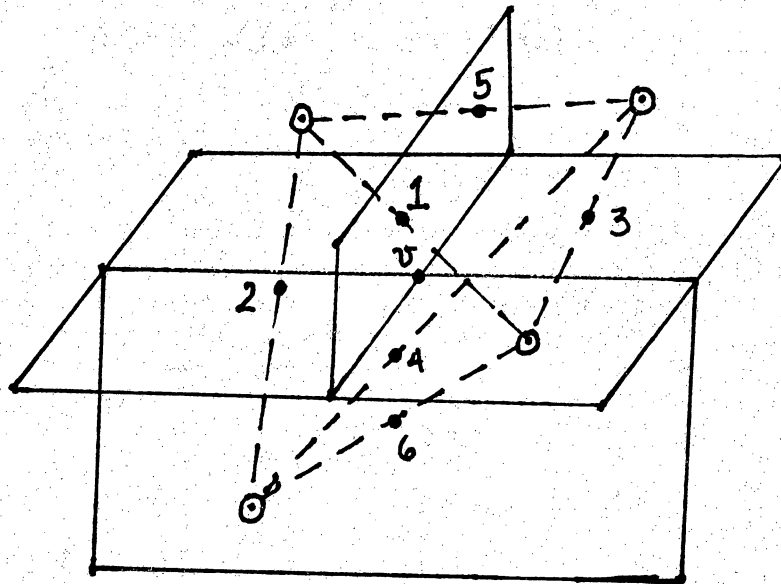


Figure 4.79 *Dual to tetrahedron*

What remains is our special spine in which each of the four edges is a meeting place of three 2-cells.

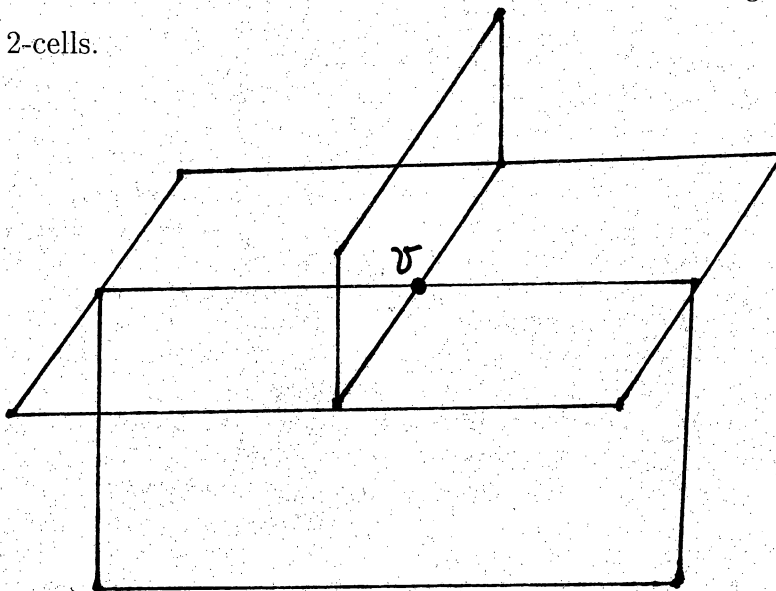


Figure 4.80 *Special spine*

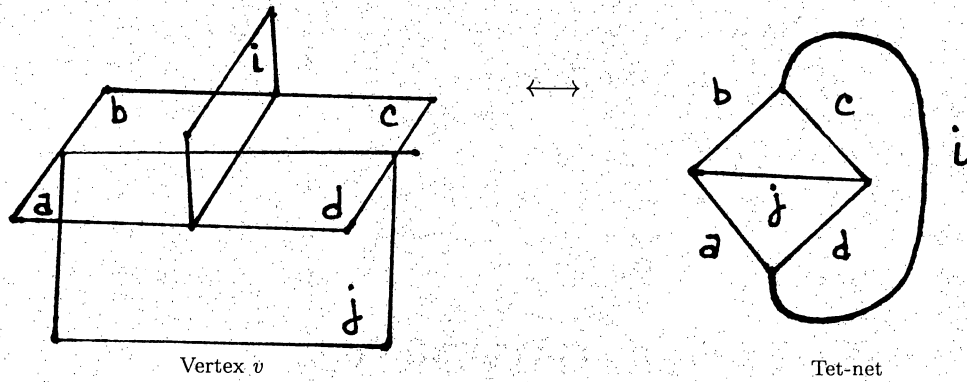
We have interpreted the meeting of six 2-cells as the *dual* to one tetrahedron. This amounts to a local view of our triangulated 3-manifold. As a whole a 3-manifold consists of a honeycomb composition of the Ping-Pong table-like structures approximating the manifold, just as the tetrahedral lattice approximates the manifold in other three dimensional TLFT theories. It is a global dual complex with one or more 3-cells, each homeomorphic to a ball. Such an approximation of the manifold is referred to as a *special spine*. So our Ping-Pong table-like structure can be viewed as one vertebra of a special spine.

Before diving into the theory supporting our tangle-theoretic approach to the Turaev-Viro invariant, we will offer a brief outline of the various constituents which comprise the partition function. We begin with a definition.

**Definition 4.81** A *spin network* is a graph with trivalent vertices and values assigned to each emanating line that satisfy certain admissibility conditions which shall be discussed in Lemma 4.109.

We develop a topological invariant of our manifold via the special spine lattice using Kauffman-Lins' method of associating to each vertex a spin network called a *tetrahedral network*, to each edge a spin network referred to as a *theta network*, and to each face a *Chebyshev polynomial* for each particular coloring of faces of the special spine. Each of these items will be examined in detail in later sections.

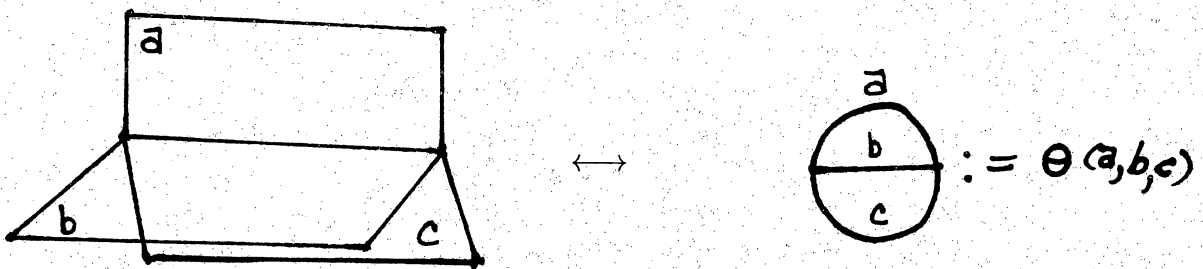
To each vertex  $v$  in our tetrahedral dual we associate a graphical weight called a tet-net (tetrahedral network) as indicated in the following sketch.



**Figure 4.82** *Vertex weight*

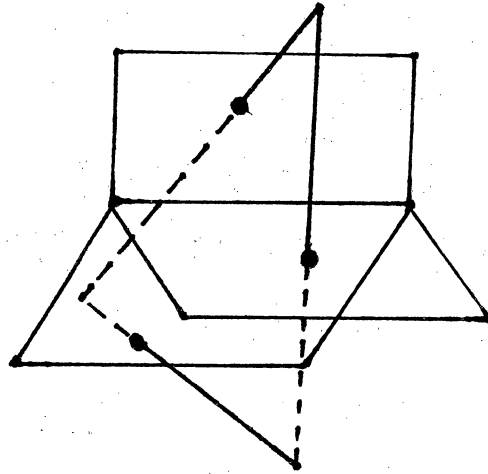
The weight of a vertex  $v$ , denoted  $TET(v|\sigma)$  is the value of the tetrahedral network corresponding to  $v$ , where  $\sigma$  represents the coloring of the edges of the network. So face colorings on the special spine on the left are associated to colorings of edges in the *tet-net* diagram on the right.

To each edge in our tetrahedral dual we associate an edge weight referred to as a theta-net (theta network) as indicated below.



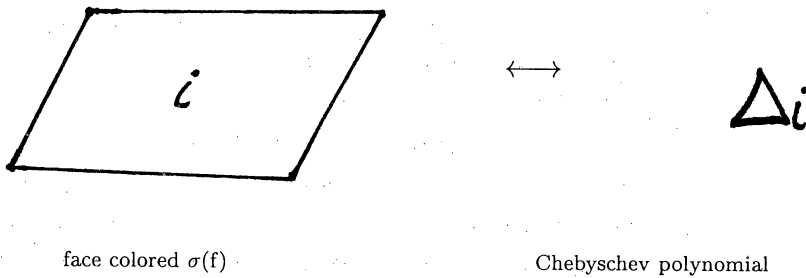
**Figure 4.83** *Edge weight*

The weight of an edge  $e$  colored  $\sigma$ , denoted  $\theta(e|\sigma)$ , is the value of the theta network corresponding to  $e$ . Keep in mind that these *edges* of our special spine are dual to the *faces* of the tetrahedron as depicted below.



**Figure 4.84** *An edge relative to a face of our tetrahedron*

To each face of our dual structure we associate a Chebyshev polynomial [Kau94], and since faces of our dual are representative of edges in our original tetrahedron, one may consider the Chebyshev polynomial assignment as one made to the edge of the tetrahedron.



**Figure 4.85** *Face weight*

In the above assignments we have effectively reduced the spinal approximation of the manifold to a network of graphs with trivalent vertices; spin

networks, to be specific. In chapter two we described restrictions on the CFS weight assignments which insured topological invariance of our partition function. The *admissibility conditions* referred to in definition 4.81 correspond to the CFS restrictions. We will clearly define these conditions in section 4.11.

Having colored the 2-cells of our special spine and having introduced the vertex, edge and face weights, we may now state the Kauffman-Lins version of the partition function for a finite set of colors  $0, 1, 2, \dots, r - 2$  associated to 3-manifold  $\mathcal{M}^3$ :

$$\mathbf{TV}_{\mathcal{M}^3, r} = \sum_{\sigma} \prod_{v, e, f} \frac{TET(v|\sigma) \Delta_{\sigma(f)}^{\chi(f)}}{\theta(e|v)^{\chi(e)}} \quad (4.86)$$

$\chi$  represent the Euler characteristic



## 4.8 Topological Invariance

In the Chung-Fukuma-Shapere theory we demonstrated topological invariance of the partition function using Alexander's theorem. Turaev and Viro [TV92] recast Alexander's theorem in a series of 3-manifold special spine moves developed by Matveev [Mat88] and Piergallini [Pie88]. Special spine partition functions that are invariant under the first two moves depicted below, the *lune move* and the *Y-move*, and that behave under the last two in the manner we will prescribe in Section 4.11, are said to be topologically invariant.

### I. Lune Move

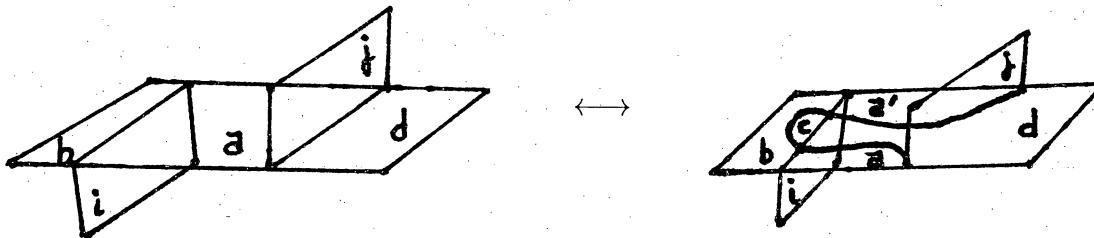


Figure 4.87 The lune move involves the creation/removal of two vertices

### II. Y-Move

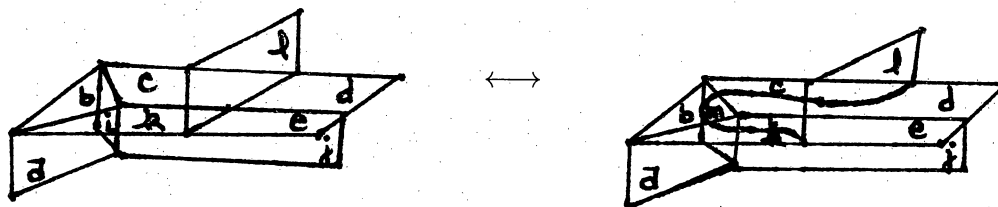
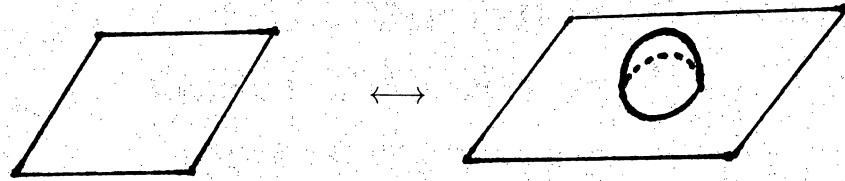


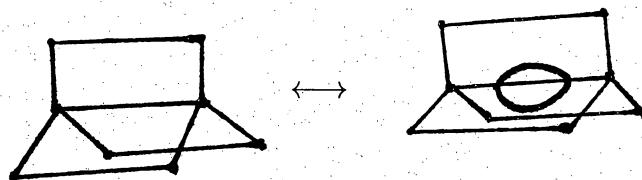
Figure 4.88 The Y-move interpolates between a two and three vertex spine

### III.a) Bubble Move



**Figure 4.89** *The bubble move creates/removes a 3-cell*

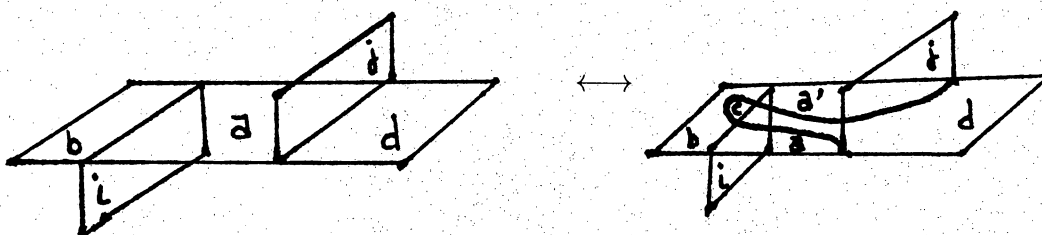
### III.b) Edge Dilation



**Figure 4.90** *The edge dilation move creates/removes a 3-cell on an edge*

You will note that by moves I. and II., moves III.a) and b) are equivalent.

When we have developed an arsenal with which to prove invariance under the four moves we will find it less cumbersome to work with two dimensional sketches. To that end we now modify our diagrams into their corresponding two dimensional shadow world notation.



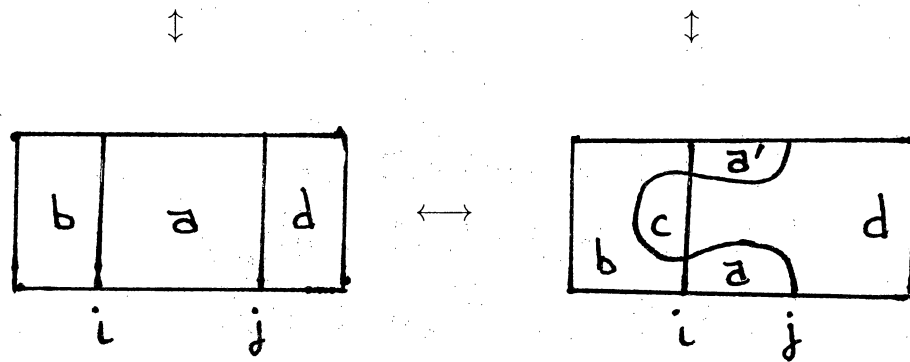


Figure 4.91 *Shadow world lune move*

We have essentially 'steam rolled' the 3-D spine. Comparing upper and lower leftside diagrams we note that in 3-D the faces adjacent to the plane,  $i$  and  $j$ , have in 2-D become an interior curve and line segment.

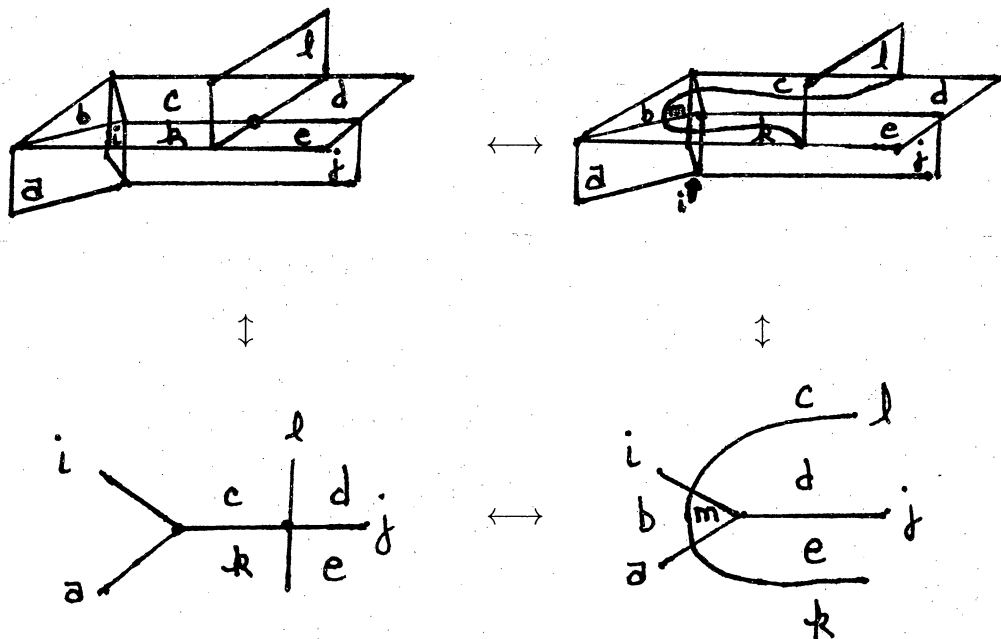
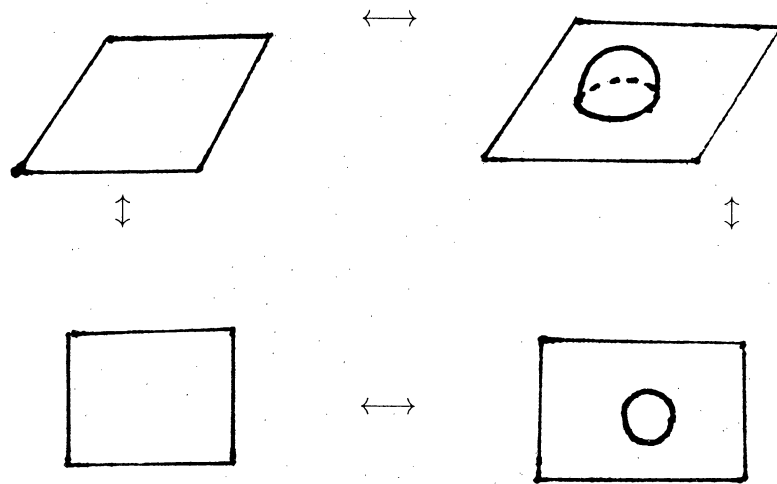
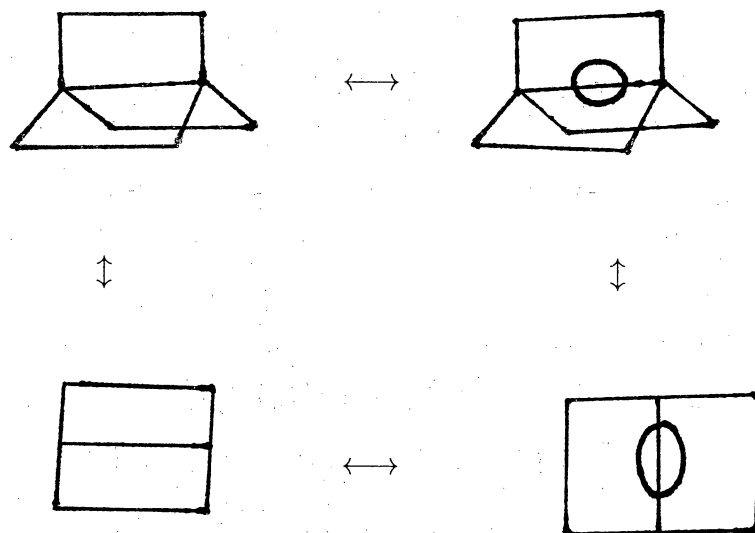


Figure 4.92 *Shadow world Y-move*

Comparing upper and lower leftside diagrams we see that a vertex in the 3-D spine is represented as a vertex in the 2-D diagram where the emanating edges correspond to perpendicular faces in the 3-D spine.



**Figure 4.93** *Shadow world bubble move*

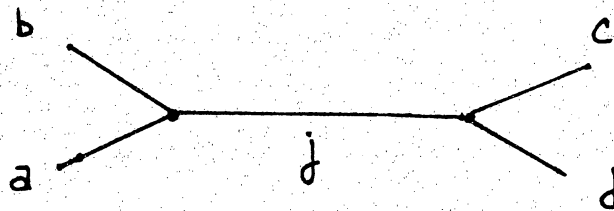


**Figure 4.94** *Shadow world edge dilation*

With our shadow world representation established we are prepared to develop the required foundation for our tangle-theoretic approach to the Turaev-Viro state

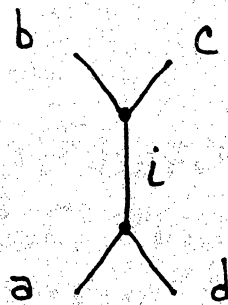
sum invariant. Thus far we have seen that the spinal approximation of a 3-manifold can be reduced to a sum of the products of various trivalent-graphical networks. Each emanating line of a 3-vertex actually represents a bundle of cables, the number of which is designated by the coloring of the special spine and restricted by the  $q$ -admissibility conditions of upcoming lemmas in Section 4.11.

The concept of a recoupling theory is, in some ways, plumber's work. We will redefine the 3-vertex by *refitting* the three emanating cables with  $q$ -symmetrizers. In the grand Recoupling Theorem we *repipe* the network of a horizontal two-vertex trivalent arrangement of emanating cables as depicted below



**Figure 4.95** *Horizontal 2-vertex trivalent graph*

into a sum of vertical arrangements where various cable bundles have been recoupled.

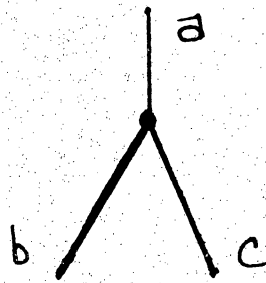


**Figure 4.96** *Vertical 2-vertex trivalent graph*

Kauffman and Lins prove the topological invariance conditions using the Recoupling Theorem and an upcoming lemma which reexpresses a particular network in terms of theta-nets and antisymmetrized cable bundles.

## 4.9 3 Vertex as Sum of Tangles

We have arrived at the point in our presentation of the Temperley-Lieb recoupling theory where all of the background material will be synthesized to issues concerning vertices of the spinal approximation of the 3-manifold. The entire purpose, for instance, of defining the sum-of-tangle projectors (also called  $q$ -symmetrizers) is to use them to refit the three cable bundles emanating from each vertex in the spine. There is a correspondence between a special sum of tangles and the 3-valent graphical vertex which we have seen is so important to the evaluation of Kauffman-Lins version of the Turaev-Viro partition function of a 3-manifold approximation. We begin with a 3-vertex depicted by

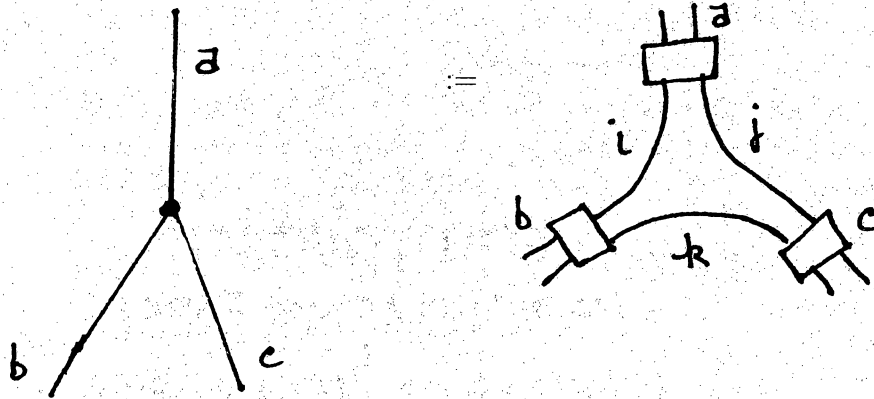


where  $(a + b - c)$ ,  $(a + c - b)$  and  $(b + c - a)$  are positive even integers  
and  $a + b + c \equiv 0 \pmod{2}$

These requirements are referred to as the general admissibility conditions for a 3-vertex.

The following definition of the 3-vertex effectively refits the cable bundles emanating from the vertex with  $q$ -symmetrizers from Section 4.6.

**Definition 4.97** 3-Vertex as Sum of Tangles



where we let

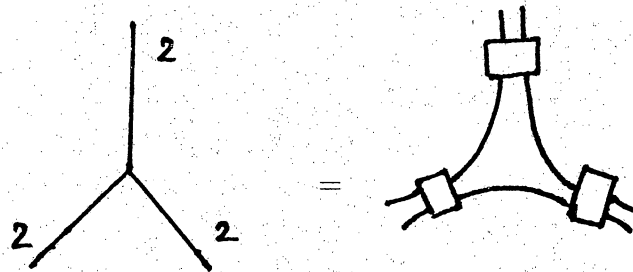
$$i = \frac{a+b-c}{2}$$

$$j = \frac{a+c-b}{2}$$

$$k = \frac{b+c-a}{2}$$

We now demonstrate a full expansion of the entire vertex as a sum of tangles that are free from any under or over crossings for one particular case.

**Example 4.98** Letting  $d = -A^2 - A^{-2}$ , as usual, we will prove that



$$= \text{[Diagram of a Y-junction]} - \frac{1}{d} \left[ \text{[Diagram of two parallel strands with a crossing]} + \text{[Diagram of two parallel strands with a crossing]} + \text{[Diagram of two parallel strands with a crossing]} \right] + \frac{2}{d^2} \left[ \text{[Diagram of two parallel strands with a crossing]} \right]$$

Proof:

Recalling that  $\square^2 = \parallel - \frac{1}{d} \bigcup$  and that by Proposition 4.72(i)  $\begin{array}{c} \square \\ \square \\ \square \end{array} = \begin{array}{c} \square \\ \square \\ \square \end{array}$  :

$$\begin{array}{c} \text{Diagram 1} \end{array} = \begin{array}{c} \text{Diagram 2} \end{array} - \frac{1}{d} \begin{array}{c} \text{Diagram 3} \end{array}$$

$$= \begin{array}{c} \text{Diagram 4} \end{array} - \frac{1}{d} \begin{array}{c} \text{Diagram 5} \end{array} - \frac{1}{d} \begin{array}{c} \text{Diagram 6} \end{array}$$

$$= \begin{array}{c} \text{Diagram 7} \end{array} - \frac{1}{d} \begin{array}{c} \text{Diagram 8} \end{array} - \frac{1}{d} \begin{array}{c} \text{Diagram 9} \end{array}$$



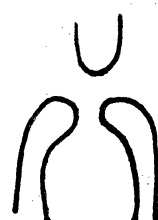
$$+\frac{1}{d^2}$$



$$-\frac{1}{d}$$



$$+\frac{1}{d^2}$$



$$= \text{diagram} - \frac{1}{d} \left[ \text{diagram} + \text{diagram} \right] + \text{diagram} + \frac{2}{d^2} \left[ \text{diagram} \right] \quad \square$$

## 4.10 Topological Invariance Proof Tools

Having accumulated all the necessary material with which to prove topological invariance, our tangle-theoretic plumber's toolbox is sufficiently stocked. Our assignment is to use the appropriate equipment in order to outline three propositions which shall be required in the next section to prove the topological invariance moves of Section 4.8. We only offer a flavor of these propositions. For complete proofs we refer the reader to Kauffman and Lins' work. [Kau94]

One important component of the Turaev-Viro state sum invariant is the quantum 6j symbol [KR89].

$$\left\{ \begin{array}{ccc} a & b & i \\ c & d & j \end{array} \right\}_q$$

Rather than describe precisely how Kauffman-Lins' 6j symbols are defined, we refer the reader to the works of Kirillov and Reshetikhin [KR89], and Piunikhin [Piu92]. Also note that the subscript  $q$  has been omitted on occasion, but it is always understood that our symbols are indeed *quantum* 6j symbols, specifically related to the Universal Enveloping algebra of quantum  $sl(2)$ .

The foundation for all three of the required propositions consists of the following upcoming items: The Recoupling Theorem 4.99, Lemma 4.100 and Lemma 4.101. In order to demonstrate that the necessary constituents supporting these three items have been properly introduced we now outline their proofs.

**Theorem 4.99** *Recoupling Theorem*


$$\begin{array}{c} b \quad c \\ \diagdown \quad \diagup \\ a \quad j \quad d \end{array} = \sum_i \left\{ \begin{array}{ccc} a & b & i \\ c & d & j \end{array} \right\} \begin{array}{c} b \quad c \\ \diagup \quad \diagdown \\ a \quad i \quad d \end{array}$$


The proof for the Recoupling Theorem relies upon, among many other things, the  $q$ -symmetrizers of Section 4.6. □

**Lemma 4.100** *Let  $q = e^{i\pi/r}$ . Let*

$$\Delta_n = (-1)^n (q^{n+1} - q^{-n-1}) / (q - q^{-1}).$$


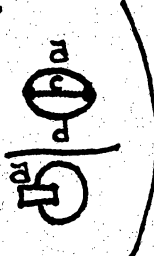

*Then  $\Delta_{r-1} = 0$  while  $\Delta_l \neq 0$  for  $0 \leq l \leq r - 2$ .*

Since this is simply an algebraic statement, its proof is independent of the Temperley-Lieb algebra. But Kauffman and Lins [Kau94] use the tangle theoretic approach to prove it. The proof depends upon the definition of  $f_{n-1}$  as the sum of tangles from Section 4.6,  $f_{n-1} =$  . It also requires the fact that  $tr(f_{n-1}) = \Delta_n$  from Lemma 4.57(iii) in Section 4.5, coupled with a result by Kauffman and Lins [Kau94] that the trace on the representation of a braid is the bracket of the closure of the braid, resulting in

$$tr(f_{n-1}) = \Delta_n =$$


□

**Lemma 4.101** *The network*  *is null if  $a \neq b$ . If  $a=b$  we have*

$$= \left( \begin{array}{c} \text{Diagram 1} \\ \text{Diagram 2} \end{array} \right) \text{Diagram 3}$$




This proof requires Definition 4.97 of a 3-vertex as the sum of tangles from Section 4.9 and the obliteration of the loop of Example 4.76 in Section 4.6.  $\square$

The question now is how do these three items relate to the aforementioned propositions of paragraph one? Let us answer this query by outlining the proofs of the propositions.

We begin with a proposition which we will use in the next section to prove the Lune Move.

**Proposition 4.102** *Orthogonality Identity*

$$\sum_{i=0}^{r-2} \left\{ \begin{array}{ccc} a & b & i \\ c & d & j \end{array} \right\}_q \left\{ \begin{array}{ccc} d & a & k \\ b & c & i \end{array} \right\}_q = \left\{ \begin{array}{ll} 0 & \text{if } k \neq j \\ 1 & \text{if } k = j \end{array} \right.$$

In the proof of this claim the Recoupling Theorem 4.99 is twice applied. Then Lemma 4.101 and the non-vanishing results of Lemma 4.100 are used to demonstrate the equivalence of the *quantum 6j-symbols* in the brackets.  $\square$

Next we outline the proof for a proposition which will be used to prove the Y Move.

**Proposition 4.103** *Biedenharn-Elliot (Pentagon) Identity*

$$\sum_{m=0}^{r-1} \left\{ \begin{array}{ccc} a & i & m \\ d & e & j \end{array} \right\}_q \left\{ \begin{array}{ccc} b & c & l \\ d & m & i \end{array} \right\}_q \left\{ \begin{array}{ccc} b & l & k \\ e & a & m \end{array} \right\}_q = \left\{ \begin{array}{ccc} b & c & k \\ j & a & i \end{array} \right\}_q \left\{ \begin{array}{ccc} k & c & l \\ d & e & j \end{array} \right\}_q$$

For this proof we again use multiple applications of the Recoupling Theorem 4.99 and a double application of Lemma 4.101.  $\square$

Finally, we outline the proof for a proposition which will be used to prove both the Lune and Y Moves.

**Proposition 4.104** *One Expression of the Quantum 6j-Symbol*

$$\left\{ \begin{array}{ccc} a & b & i \\ c & d & j \end{array} \right\}_q = \frac{\text{Diagram 1} \cdot \text{Diagram 2}}{\text{Diagram 3} \cdot \text{Diagram 4}}$$

The diagram shows the quantum 6j-symbol  $\left\{ \begin{array}{ccc} a & b & i \\ c & d & j \end{array} \right\}_q$  expressed as a ratio of two products of diagrams. The numerator consists of two diagrams: a tetrahedron with edges labeled  $a, b, c, d, i, j$  and a cup diagram with a single cup labeled  $i$ . The denominator consists of two diagrams: a cup diagram with a single cup labeled  $c$  and a cup diagram with a single cup labeled  $d$ .

This proof depends upon the Recoupling Theorem 4.99 and Lemma 4.101. □

Satisfied that all of the basic tools required for the proofs of invariance have been properly introduced and demonstrated, we are finally prepared to complete chapter 4 by proving invariance of the Kauffman-Lins version of the Turaev-Viro partition function in the next section.

But before closing this section we reward the diligent reader by offering an elegant demonstration of the simplicity and aesthetic symmetry of the tangle-theoretic approach by proving Proposition 4.104.

*CLAIM:*

$$\left\{ \begin{array}{ccc} a & b & i \\ c & d & j \end{array} \right\}_q = \frac{\text{Diagram 1} \cdot \text{Diagram 2}}{\text{Diagram 3} \cdot \text{Diagram 4}}$$

The diagram is identical to the one in Proposition 4.104, showing the quantum 6j-symbol as a ratio of two products of diagrams. The numerator consists of two diagrams: a tetrahedron with edges labeled  $a, b, c, d, i, j$  and a cup diagram with a single cup labeled  $i$ . The denominator consists of two diagrams: a cup diagram with a single cup labeled  $c$  and a cup diagram with a single cup labeled  $d$ .

*Proof*

The recoupling theorem tells us

$$\begin{array}{c} b \\ \diagdown \\ a \end{array} \begin{array}{c} \text{---} \\ \diagup \\ j \end{array} \begin{array}{c} c \\ \diagdown \\ d \end{array} = \sum_i \left\{ \begin{array}{ccc} a & b & i \\ c & d & j \end{array} \right\}_q \begin{array}{c} b \\ \diagdown \\ a \end{array} \begin{array}{c} c \\ \diagdown \\ d \end{array} \begin{array}{c} i \\ \diagup \\ j \end{array}$$

Closing strands  $b$  and  $c$  and summing we have

$$\begin{array}{c} i \\ | \\ \begin{array}{ccc} b & & c \\ \diagdown \quad \diagup \\ a & j & d \end{array} \end{array} = \left\{ \begin{array}{ccc} a & b & i \\ c & d & j \end{array} \right\} \begin{array}{c} i \\ | \\ \bigcirc \\ \diagdown \quad \diagup \\ a & d \end{array}$$

Applying Lemma 4.101

$$\begin{array}{c} i \\ | \\ \begin{array}{ccc} b & & c \\ \diagdown \quad \diagup \\ a & j & d \end{array} \end{array} = \left\{ \begin{array}{ccc} a & b & i \\ c & d & j \end{array} \right\} \begin{array}{c} b \\ \bigcirc \\ i \end{array} \begin{array}{c} i \\ \square \\ a \end{array} \begin{array}{c} b \\ \diagdown \\ d \end{array}$$

Closing strands  $a$  and  $d$ , then looping strand  $i$  around

$$\begin{array}{c} i \\ \bigcirc \\ \begin{array}{ccc} b & & c \\ \diagdown \quad \diagup \\ a & j & d \end{array} \end{array} = \left\{ \begin{array}{ccc} a & b & i \\ c & d & j \end{array} \right\} \begin{array}{c} b \\ \bigcirc \\ i \end{array} \begin{array}{c} i \\ \square \\ a \end{array} \begin{array}{c} d \\ \bigcirc \\ i \end{array}$$

Applying Lemma 4.101 again

$$\left( \begin{array}{c} b \quad c \\ \diagdown \quad \diagup \\ i \\ \diagup \quad \diagdown \\ a \quad d \end{array} \right)_i = \left\{ \begin{array}{ccc} a & b & i \\ c & d & j \end{array} \right\} \frac{\begin{array}{c} b \\ \bigcirc \\ c \end{array}_i \begin{array}{c} a \\ \bigcirc \\ d \end{array}_i}{\begin{array}{c} \square \\ \bigcirc \\ i \end{array} \begin{array}{c} \square \\ \bigcirc \\ i \end{array}} \left( \begin{array}{c} \square \\ \square \end{array} \right)_i$$

By Proposition 4.72(i) of the Temperley-Lieb projector

$$\left( \begin{array}{c} b \quad c \\ \diagdown \quad \diagup \\ i \\ \diagup \quad \diagdown \\ a \quad d \end{array} \right)_i = \left\{ \begin{array}{ccc} a & b & i \\ c & d & j \end{array} \right\} \frac{\begin{array}{c} b \\ \bigcirc \\ c \end{array}_i \begin{array}{c} a \\ \bigcirc \\ d \end{array}_i}{\begin{array}{c} \square \\ \bigcirc \\ i \end{array} \begin{array}{c} \square \\ \bigcirc \\ i \end{array}} \left( \begin{array}{c} \square \end{array} \right)_i$$

Simplifying

$$\left( \begin{array}{c} b \quad c \\ \diagdown \quad \diagup \\ i \\ \diagup \quad \diagdown \\ a \quad d \end{array} \right)_i = \left\{ \begin{array}{ccc} a & b & i \\ c & d & j \end{array} \right\} \frac{\begin{array}{c} b \\ \bigcirc \\ c \end{array}_i \begin{array}{c} a \\ \bigcirc \\ d \end{array}_i}{\begin{array}{c} \square \\ \bigcirc \\ i \end{array}}$$

Solving for quantum 6j-symbol

$$\left\{ \begin{array}{ccc} a & b & i \\ c & d & j \end{array} \right\} = \frac{\left( \begin{array}{c} b \quad c \\ \diagdown \quad \diagup \\ i \\ \diagup \quad \diagdown \\ a \quad d \end{array} \right)_i \left( \begin{array}{c} \square \end{array} \right)_i}{\begin{array}{c} b \\ \bigcirc \\ c \end{array}_i \begin{array}{c} a \\ \bigcirc \\ d \end{array}_i}$$

□

## 4.11 Invariance Proofs

We have established a spinal approximation of the 3-manifold, reducing everything to a web of three vertices, edges and faces. The partition function for our special spine requires the assignment of tetrahedral networks to each 3-vertex, theta networks to each edge and Chebyshev polynomials to each face for each particular coloring of the faces in our web.

Our partition function from section 4.7 is a sum over all possible colorings  $\sigma$  for a finite set of colors  $\{0, 1, 2, \dots, r-2\}$  associated to the 3-manifold  $\mathcal{M}^3$ :

$$\mathbf{TV}_{\mathcal{M}^3, r} = \sum_{\sigma} \prod_{v, e, f} \frac{TET(v|\sigma) \Delta_{\sigma(f)}^{\chi(f)}}{\theta(e|v)^{\chi(e)}}$$

$\chi$  REPRESENTS THE EULER CHARACTERISTIC

TET REPRESENTS THE VERTEX WEIGHT

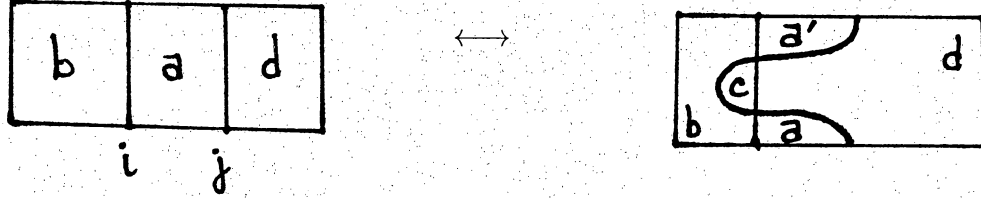
$\Delta$  REPRESENTS THE FACE WEIGHT

$\theta$  REPRESENTS THE EDGE WEIGHT

Special spine partition functions that are invariant under the Lune Move, the Y-Move and that behave in a prescribed fashion under the Bubble Move/Edge Dilation of Section 4.8 are said to be topologically invariant. In this section we will prove that the Kauffman-Lins partition function presented above is indeed a topological invariant of our 3-manifold.



**Theorem 4.105** *Lune Move Invariance*



Proof

Keeping in mind that our sketch depicts only one vertebra on our special spine, let  $R$  represent the partition function  $TV_{\mathcal{M}^3, r}$  for the special spine containing the right hand side vertebra. Let  $R_0$  represent the contribution from the portion of the spine not containing the vertebra. Since  $a, b, d, i$  and  $j$  are the same coloring for both the RHS and the LHS vertebra, it suffices to consider only colorings for  $c$ , hence we will demonstrate that the partition function for the spine containing the RHS and that containing the LHS are the same, summing only over all colors for face  $c$ .

$$R = \left( \begin{array}{c} \text{contribution from} \\ \text{RHS vertebra} \end{array} \right) \left( \begin{array}{c} \text{contribution from} \\ \text{rest of spine} \end{array} \right)$$

$$R = \left[ \frac{(\text{tet} - \text{nets excluding } c)(\text{face weights excluding } c)_{\sigma(f)}^{x(f)}}{(\theta - \text{nets excluding } c)^{x(e)}} \right] \cdot \left[ \sum_c \frac{(\text{tet} - \text{nets including } c)(\text{face weights including } c)_c^{x_c}}{(\theta - \text{nets including } c)^{x(e)}} \right] \cdot R_0$$

FOR THE NEXT STEP NOTE THAT THERE ARE NO TET-NETS FOR THE RHS VERTEBRA; SINCE ALL COLORINGS ARE FIXED (WITH THE EXCEPTION OF C)  $\sigma(f) = f$ ; AND  $\chi(e) = 1$  BY ASSUMPTION.

$$= \left[ \frac{\Delta_{a'}^{\chi_{a'}} \Delta_a^{\chi_a} \Delta_b^{\chi_b} \Delta_d^{\chi_d} \Delta_i^{\chi_i} \Delta_j^{\chi_j}}{\theta_{(a,b,i)} \theta_{(a,d,j)}} \right] \left[ \sum_c \frac{\Delta_c^{\chi_c}}{\theta_{(a',i,b)} \theta_{(a',d,j)}} \right] \bullet R_0$$

FOR THE NEXT STEP WE NOTE THAT EULER CHARACTERISTICS OF FACES  $a'$  AND  $c$  ARE 1; WE MOVE A FACTOR OF  $\Delta_{a'}^{\chi_{a'}}$  INSIDE THE SUMMATION; AND WE CYCLICALLY MANIPULATE TET-NETS.

$$= \left[ \frac{\Delta_{a'}^{\chi_{a'}-1} \Delta_a^{\chi_a} \Delta_b^{\chi_b} \Delta_d^{\chi_d} \Delta_i^{\chi_i} \Delta_j^{\chi_j}}{\theta_{(a,b,i)} \theta_{(a,d,j)}} \right] \left[ \sum_c \frac{\Delta_c^1}{\theta_{(a',i,b)} \theta_{(a',d,j)}} \frac{\Delta_{a'}^1}{\Delta_{a'}^1} \right] \bullet R_0$$

BY PROPOSITION 4.104:

$$= \left[ \frac{\Delta_{a'}^{\chi_{a'}-1} \Delta_a^{\chi_a} \Delta_b^{\chi_b} \Delta_d^{\chi_d} \Delta_i^{\chi_i} \Delta_j^{\chi_j}}{\theta_{(a,b,i)} \theta_{(a,d,j)}} \right] \left[ \sum_c \left\{ \begin{matrix} d & j & c \\ b & i & a \end{matrix} \right\} \left\{ \begin{matrix} i & d & a' \\ j & b & c \end{matrix} \right\} \right] \bullet R_0$$

BY ORTHOGONALITY PROPOSITION 4.102:

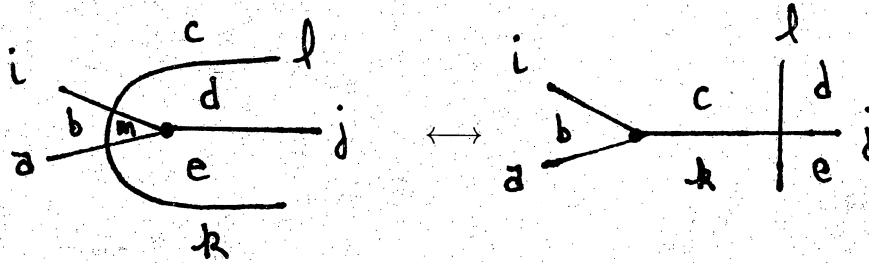
$$= \left[ \frac{\Delta_{a'}^{\chi_{a'}-1} \Delta_a^{\chi_a} \Delta_b^{\chi_b} \Delta_d^{\chi_d} \Delta_i^{\chi_i} \Delta_j^{\chi_j}}{\theta_{(a,b,i)} \theta_{(a,d,j)}} \right] \left[ \begin{matrix} 1, & a' = a \\ 0, & a' \neq a \end{matrix} \right] \bullet R_0$$

Our sketch vacuously implies that when  $a \neq a'$  the right hand side vanishes, which agrees with the result of our calculation  $R=0$ . When  $a = a'$  we note that the Euler characteristic for region  $a$  on the left diagram under the Lune Move is  $\chi_a + \chi_{a'} - 1$ . Hence, for the partition function of the left hand side we have

$$L = \left[ \frac{\Delta_a^{2\chi_a - 1} \Delta_b^{\chi_b} \Delta_d^{\chi_d} \Delta_i^{\chi_i} \Delta_j^{\chi_j}}{\theta_{(a,b,i)} \theta_{(a,d,j)}} \right] \bullet R_0$$

which agrees with our calculation. □

**Theorem 4.106** *Y-Move Invariance*



Proof

We will demonstrate that the partition function for the special spine approximation of a 3-manifold that includes the vertebra on the LHS is equal to the same containing the RHS vertebra.

Let  $L$  be the portion of the partition function corresponding to the LHS vertebra.  $L_0$  is the portion corresponding to the rest of the spine. We will hold colors  $i, b, a, k, e, d, l, j$ , and  $c$  fixed because they are the same for both vertebrae. We will vary color  $m$  on the left hand side.

$$L = \left( \begin{array}{c} \text{contribution from} \\ \text{LHS vertebra} \end{array} \right) \left( \begin{array}{c} \text{contribution from} \\ \text{rest of spine} \end{array} \right)$$

$$L = \left[ \frac{(\text{tet} - \text{nets excluding } m)(\text{face weights excluding } m)^{\chi_{\sigma(f)}^{(f)}}}{(\theta - \text{nets excluding } m)^{\chi(e)}} \right] \\ \bullet \left[ \sum_m \frac{(\text{tet} - \text{nets including } m)(\text{face weights including } m)^{\chi_m^m}}{(\theta - \text{nets including } m)^{\chi(e)}} \right] \bullet L_0$$

NOTE THAT THERE ARE NO TET-NETS THAT EXCLUDE M.

$$= \left[ \frac{\Delta_i^{\chi_i} \Delta_a^{\chi_a} \Delta_j^{\chi_j} \Delta_b^{\chi_b} \Delta_c^{\chi_c} \Delta_d^{\chi_d} \Delta_e^{\chi_e} \Delta_k^{\chi_k} \Delta_l^{\chi_l}}{\theta_{(b,i,c)} \theta_{(b,a,k)} \theta_{(c,l,d)} \theta_{(d,j,e)} \theta_{(e,l,k)}} \right]$$

$$\bullet \left[ \sum_m \left( \frac{\text{diagram 1}}{\theta_{(a,e,m)}} \bullet \frac{\text{diagram 2}}{\theta_{(d,i,m)}} \bullet \frac{\text{diagram 3}}{\theta_{(b,m,l)}} \right) \Delta_m^{\chi_m} \right] \bullet L_0$$

MANIPULATING THINGS A BIT, AND NOTING THAT  $\chi_m = 1$ :

$$= \left[ \frac{\Delta_i^{\chi_i} \Delta_a^{\chi_a} \Delta_j^{\chi_j} \Delta_b^{\chi_b} \Delta_c^{\chi_c} \Delta_d^{\chi_d} \Delta_e^{\chi_e} \Delta_k^{\chi_k-1} \Delta_l^{\chi_l-1}}{\theta_{(b,i,c)} \theta_{(d,j,e)}} \right]$$

$$\bullet \left[ \sum_m \left( \frac{\text{Diagram 1}}{\theta_{(a,e,m)} \theta_{(i,d,m)}} \Delta_m \bullet \frac{\text{Diagram 2}}{\theta_{(b,m,l)} \theta_{(c,d,l)}} \Delta_l \bullet \frac{\text{Diagram 3}}{\theta_{(b,a,k)} \theta_{(l,e,k)}} \Delta_k \right) \right] \bullet L_0$$

BY PROPOSITION 4.104:

$$= \left[ \frac{\Delta_i^{\chi_i} \Delta_a^{\chi_a} \Delta_j^{\chi_j} \Delta_b^{\chi_b} \Delta_c^{\chi_c} \Delta_d^{\chi_d} \Delta_e^{\chi_e} \Delta_k^{\chi_k-1} \Delta_l^{\chi_l-1}}{\theta_{(b,i,c)} \theta_{(d,j,e)}} \right] \bullet \left[ \sum_m \left( \left\{ \begin{matrix} a & i & m \\ d & e & j \end{matrix} \right\} \left\{ \begin{matrix} b & c & l \\ d & m & i \end{matrix} \right\} \left\{ \begin{matrix} b & l & k \\ e & a & m \end{matrix} \right\} \right) \right]$$

BY PROPOSITION 4.103:

$$= \left[ \frac{\Delta_i^{\chi_i} \Delta_a^{\chi_a} \Delta_j^{\chi_j} \Delta_b^{\chi_b} \Delta_c^{\chi_c} \Delta_d^{\chi_d} \Delta_e^{\chi_e} \Delta_k^{\chi_k-1} \Delta_l^{\chi_l-1}}{\theta_{(b,i,c)} \theta_{(d,j,e)}} \right]$$

$$\bullet \left[ \left\{ \begin{matrix} b & c & k \\ j & a & i \end{matrix} \right\} \left\{ \begin{matrix} k & c & l \\ d & e & j \end{matrix} \right\} \right] \bullet L_0$$

$$= \left[ \frac{\Delta_i^{\chi_i} \Delta_a^{\chi_a} \Delta_j^{\chi_j} \Delta_b^{\chi_b} \Delta_c^{\chi_c} \Delta_d^{\chi_d} \Delta_e^{\chi_e} \Delta_k^{\chi_k-1} \Delta_l^{\chi_l-1}}{\theta_{(b,i,c)} \theta_{(d,j,e)}} \right]$$

$$\bullet \left[ \frac{\text{Diagram 1}}{\theta_{(b,a,k)}\theta_{(c,j,k)}} \bullet \frac{\text{Diagram 2}}{\theta_{(k,e,l)}\theta_{(c,d,l)}} \right] \bullet L_0$$

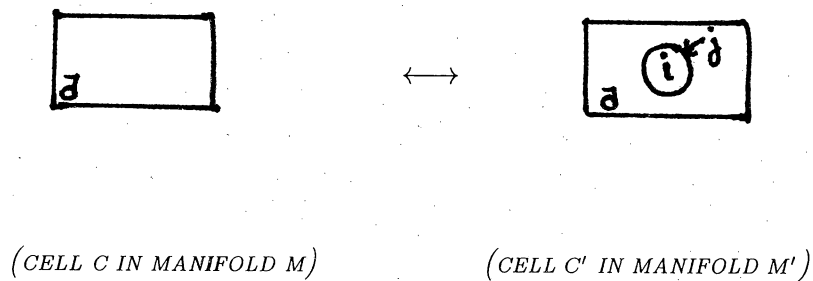
AND SINCE  $L_0 = R_0$ :

$$= R$$

□

We will conclude this chapter with a discussion of the required stipulations our partition function must meet under the Bubble Move. In the following discussion references to manifolds  $M$  and  $M'$  actually refer to *triangulations* of the manifolds.

**Theorem 4.107** *Bubble Move Stipulation*



$$CLAIM : TV_{M'} = (\Delta_a^{-1} \sum_{i,j} \Delta_i \Delta_j) TV_M$$

Proof

Suppose we have a special spinal approximation of manifold  $M$  which contains  $C$ .

We do a Bubble Move on cell  $C$  which results in cell  $C'$  (which is contained in  $M'$ ).

The partition function  $TV_{M'}$  will differ from the partition function  $TV_M$  by only:

i) a change in face  $a$ .

and

ii) additional faces  $i, j$  to be colored.

(There will be no additional vertices or edges.)

Specifically:

i) For  $M$  we have  $\Delta_a^{\chi_a}$ , but for  $M'$  we remove face  $i$  from face  $a$ , noting that  $i$  being homeomorphic to a disk implies that  $\chi_i = 1$ . So for  $M'$  the weight for face  $a$  becomes

$$\Delta_a^{\chi_a-1} = \Delta_a^{\chi_a} \bullet \Delta_a^{-1}.$$

Hence, we need only multiply  $TV_{M'}$  (which contributes one factor of  $\Delta_a^{\chi_a}$ ) by  $\Delta_a^{-1}$ .

ii) We will have an additional factor of the sum over all colorings for the new faces  $i$  and  $j$ .

Therefore, we have the prescribed manner in which the Bubble Move effects the partitions function:

$$TV_{M'} = (\Delta_a^{-1} \sum_{i,j} \Delta_i \Delta_j) TV_M$$

□

In order to agree with the results in the Turaev-Viro paper [TV92] we will use the next two lemmas to make a closing remark.

**Lemma 4.108** *Let  $q = e^{\frac{i\pi}{r}}$ .*

*Let  $a, b \in \{0, 1, 2, \dots, r-2\}$ .*

*Then*

$$\Delta_a^{-1} \sum_{i,j} \Delta_i \Delta_j = \Delta_b^{-1} \sum_{i,j} \Delta_i \Delta_j$$

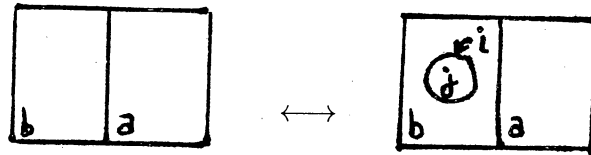
*(Meaning that  $\Delta_a^{-1} \sum_{i,j} \Delta_i \Delta_j$  is independent of  $a$ .)*

*LHS sum is taken over  $q$ -admissible triples  $(a, i, j)$  and RHS  $(b, i, j)$ .*

*( $q$ -admissibility is defined in lemma 4.109)*

Proof

i)



CELL IN  $M$

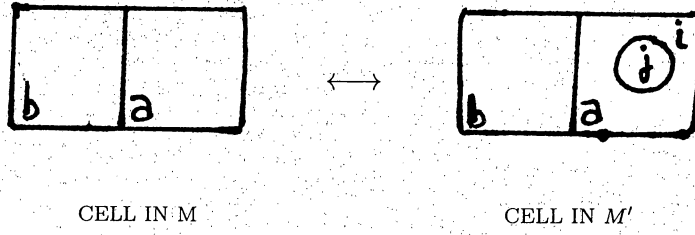
CELL IN  $M'$

$$\Rightarrow TV_{M'} = (\Delta_b^{-1} \sum_{i,j} \Delta_i \Delta_j) TV_M$$

By the Bubble Move.



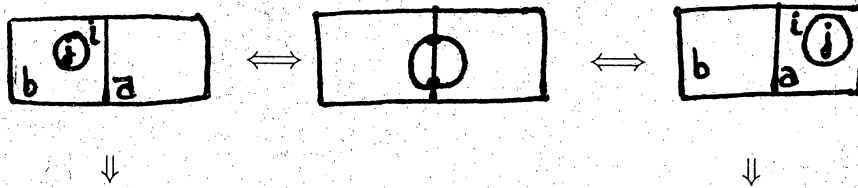
ii)



$$\Rightarrow TV_{M''} = (\Delta_a^{-1} \sum_{i,j} \Delta_i \Delta_j) TV_M$$

By the Bubble Move.

But by the Lune Move we have:



$$(\Delta_b^{-1} \sum_{i,j} \Delta_i \Delta_j) TV_M = (\Delta_a^{-1} \sum_{i,j} \Delta_i \Delta_j) TV_M$$

$$\Rightarrow \Delta_b^{-1} \sum_{i,j} \Delta_i \Delta_j = \Delta_a^{-1} \sum_{i,j} \Delta_i \Delta_j$$

where  $TV_M \neq 0$

□

**Lemma 4.109**  $\forall j \in \{0, 1, 2, \dots, r-2\}$  and  $(a, i, j)$   $q$ -admissible,

$$\tau_q = \Delta_a^{-1} \sum_{i,j} \Delta_i \Delta_j = \frac{-2r}{(q - q^{-1})^2}$$

BY LEMMA 4.108 THIS SUM IS OVER  $q$ -ADMISSIBLE TRIPLE  $(a, i, j)$ .

$$\text{AND } q = e^{\frac{i\pi}{r}}.$$

Note that  $(a, i, j)$   $q$ -admissible means two conditions are met:

$$\left\{ \begin{array}{l} i) \quad (a + i - j), (a + j - i), (i + j - a) \text{ are positive - even.} \\ ii) \quad (a + i + j) \leq 2r - 4 \end{array} \right\}$$

Proof

$$\tau_q = \Delta_a^{-1} \sum_{i,j} \Delta_i \Delta_j,$$

$$\text{for } a \in \{0, 1, \dots, r-2\}$$

Since  $\tau_q$  is independent of  $a$  by Lemma 4.108, let  $a = 0$ .

$$\Rightarrow \tau_q = \Delta_0^{-1} \sum_{i,j} \Delta_i \Delta_j$$

Since  $\Delta_0 = 1$  by definition in Section 4.5:

$$= (1)^{-1} \sum_{i,j} \Delta_i \Delta_j$$

Since we let  $a = 0$  the q-admissible conditions become

$i + j \leq 2r - 4$ , and  $(i - j)$ ,  $(j - i)$   $(i + j)$  all equal zero.

Hence  $i = j = n$ , where  $n \in \{0, 1, \dots, r - 2\}$ .

$$= \sum_{n=0}^{r-2} \Delta_n \Delta_n$$

Let  $x = -q$ .

$$= \sum_{n=0}^{r-2} \left( \frac{x^{n+1} - x^{-n-1}}{x - x^{-1}} \right)^2$$

$$= \frac{1}{(x - x^{-1})^2} \sum_{n=0}^{r-2} (x^{2(n+1)} - 2x^0 + x^{2(-n-1)})$$

$$= \frac{1}{(x - x^{-1})^2} \left[ \sum_{n=0}^{r-2} (x^2)^{n+1} + \sum_{n=0}^{r-2} (x^{-2})^{(n+1)} - \sum_{n=0}^{r-2} 2 \right]$$

Let us digress for a moment to prove a claim.

*CLAIM* :  $\sum_{n=0}^{r-2} y^{n+1} = -1$  if  $y$  is  $r^{th}$  root of unity.

Proof

$$\sum_{n=0}^{r-1} y^n = 0 \text{ because of the root of unity.}$$

$$\text{Let } m = n + 1$$

$$\text{Then } \sum_{n=0}^{r-2} y^{n+1} = \sum_{m=1}^{r-1} y^m = \sum_{m=0}^{r-1} y^m - y^0 = 0 - 1 = -1$$

Back to our proof of Lemma 4.109:

$$= \frac{1}{(x - x^{-1})^2} \left[ \sum_{n=0}^{r-2} (x^2)^{n+1} + \sum_{n=0}^{r-2} (x^{-2})^{(n+1)} - \sum_{n=0}^{r-2} 2 \right]$$

$$= \frac{1}{(x - x^{-1})^2} (-1 - 1 - 2 \sum_{n=0}^{r-2} 1)$$

$$= \frac{1}{(x - x^{-1})^2} [-1 - 1 - 2(r - 2 + 1)]$$

$$= \frac{(-2 - 2r + 2)}{(x - x^{-1})^2}$$



$$= \frac{-2r}{(x - x^{-1})^2}$$

And since  $(x - x^{-1})^2 = [(-x) - (-x)^{-1}]^2$ , we have for  $x = -q$ :

$$\tau_q = \frac{-2r}{(q - q^{-1})^2}$$

□

## CLOSING REMARKS

In summary we have demonstrated that when  $\mathcal{M}^3$  is a manifold approximation containing the cell , and  $\mathcal{M}^{3'}$  is one containing the cell , their TV partition functions are related by Theorem 4.107:

$$TV_{\mathcal{M}}^{3'} = (\Delta_a^{-1} \sum_{i,j} \Delta_i \Delta_j) TV_{\mathcal{M}}^3$$

In Lemma 4.109 we showed that

$$\Delta_a^{-1} \sum_{i,j} \Delta_i \Delta_j = \frac{-2r}{(q - q^{-1})^2} = \tau_q.$$

Hence, when

$\mathcal{M}^3$  includes the edge

or

$\mathcal{M}^{3'}$  includes the edge dialation

we have

$$TV_{\mathcal{M}^{3'}} = \tau_q TV_{\mathcal{M}^3}.$$

Finally, to obtain a topological invariant of the 3-manifold, we define

$$I_{\mathcal{M}^3} = (\tau_q)^{-t+1} TV_{\mathcal{M}^3}$$

where  $t$  is the number of 3-cells in the decomposition of the spinal approximation of the 3-manifold  $\mathcal{M}^3$ .

## Chapter 5

# Category Theory and Topological Quantum Field Theory

Up to this point our TQFTs have been based upon particular types of algebras playing the part of the intermediate element which allows us to construct topologically invariant theories. But it has been proposed by mathematicians that  $n$  dimensional TQFTs may be generalized from the algebraic approach to one utilizing category theory [Cr95], [Fr94]. Baez and Dolan [BD95] carefully investigated the relationship between the two and provided a viable case for recasting popular topological field theories for arbitrary  $n$  dimensions in terms of  $n$ -category theory. Whittling their broad generalization down to our two cases at hand, they describe a three dimensional TQFT as a particular type of representation of the category that has two dimensional manifolds as objects and orientable cobordisms between the manifolds as morphisms. Two dimensional TQFTs are, similarly, a type of representation of the category with one dimensional manifolds as objects and orientable cobordisms as morphisms. Without diving too deeply into the details of such a theory, we will delve into its general aspects. To do so requires that we first investigate the basic foundation of category theory. [D-PC]

## 5.1 Category Theory Foundation

A category consists of a set of abstract objects. Objects can be, for example, a set of points, vector spaces, groups, etc. Our category does not only come equipped with objects, but also with morphisms, entities whose job it is to connect the objects. In typical examples of categories morphisms can be paths, homomorphisms, linear maps, etc.

### Definition 5.1 *Category*

A *category* is composed of a collection of objects and a collection of morphism which satisfy the following stipulations:

Let  $x, y, z$  be objects and  $f, g, h$  morphisms between objects.

1. If  $f : x \rightarrow y$  and  $g : y \rightarrow z$  then there exists a morphism  $fg : x \rightarrow z$  referred to as the *composite* of  $f$  and  $g$ .
2. Composition is associative:  $(fg)h = f(gh)$
3. For any object  $x$  there exists a morphism  $1_x$ , called *identity*, such that:

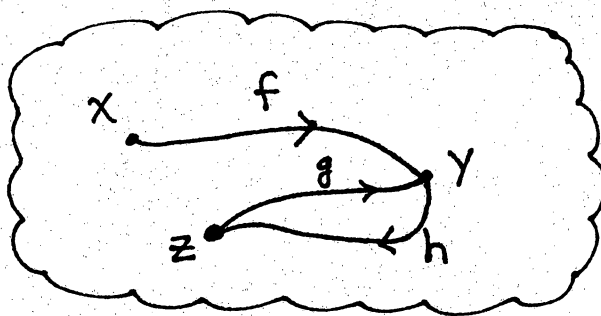
$$1_x : x \rightarrow x$$

and

$$1_x f = f 1_y = f \text{ for any morphism } f : x \rightarrow y$$

It is instructive to view the category, which is intrinsically algebraic, from a geometric perspective as in Fig. 5.2 where we represent objects as dots and morphisms as arrows.





**Figure 5.2** *Geometric representation of a category*

**Example 5.3** *One example of a category is ‘Vect’. This is the category of all vector spaces and the linear maps between them. The vector spaces are the objects and the linear maps are the morphisms of the category. Composition of morphisms is composition of the linear maps and the identity morphism is the identity map.*

Since our category definition provides us with morphisms which relate objects to one another, the question arises: Given two categories  $C$  and  $D$  is there a method with which to associate these two categories? Yes, they are related by something called a functor.

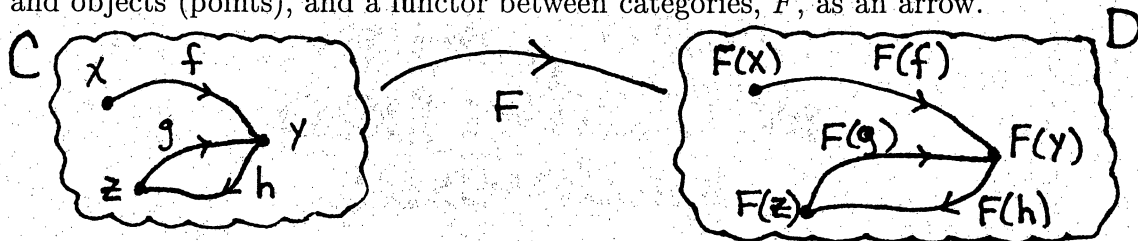
**Definition 5.4** *Functor*

A functor  $F$  from a category  $C$  to a category  $D$  is a map from the set of objects in  $C$  to a set of objects in  $D$ , together with for any objects  $x, y$  in  $C$  maps from  $\text{hom}(x, y)$  to  $\text{hom}(F(x), F(y))$ . More specifically:

Let  $x$  and  $y$  be objects in  $C$  and  $f : x \rightarrow y$  be a morphism in  $C$ . A functor  $F : C \rightarrow D$  assigns to each  $x$  in  $C$  an object of  $D$ , and assigns to each  $f$  in  $C$  a morphism  $F(f)$  in  $D$  such that:

1.  $F(f) : F(x) \longrightarrow F(y)$
2.  $F(f)F(g) = F(fg)$
3.  $F(1_x)$  is the identity morphism of  $F(x)$ , where  $1_x$  is the identity morphism of  $x$ .

Again, it is helpful to view our functor geometrically. One geometric representation (Fig. 5.5) depicts the categories as collections of morphisms (arrows) and objects (points), and a functor between categories,  $F$ , as an arrow.



**Figure 5.5** *Geometric representation of functor  $F$  from category  $C$  to category  $D$ .*

Given any arbitrary category, we can also define its opposite category.

**Definition 5.6** *Opposite Category*

Let  $x$  and  $y$  be objects in the category  $C$ . The category opposite to  $C$  is  $C^{op}$ . It is a category in which the set of objects is equal to the set of objects in  $C$ , but for every morphism  $f : x \rightarrow y$  in  $C$  there exists a corresponding morphism  $f^{op} : y \rightarrow x$  in  $C^{op}$ . Composition of the  $C^{op}$  morphisms is defined by  $f^{op}g^{op} = (gf)^{op}$ . The identity morphism in  $C^{op}$  is  $(1_x)^{op}$ . Composition of identity morphisms on objects are defined via:

$$1_x = 1_x(1_x)^{op} = (1_x)^{op}$$

for  $1_x : x \rightarrow x$  and  $(1_x)^{op} : x \rightarrow x$ .

For an example let us consider the category opposite to  $\mathbf{Vect}$ .

**Example 5.7** *Let  $V$  and  $W$  be vector spaces in the category  $\mathbf{Vect}$ . ' $\mathbf{Vect}^{op}$ ' is a category in which the objects (vector spaces) are the same as those in  $\mathbf{Vect}$ , but for every morphism  $f : V \rightarrow W$  in  $\mathbf{Vect}$  we have a morphism  $f^{op} : W \rightarrow V$  in  $\mathbf{Vect}^{op}$ .*

We now have sufficient foundation to define a twisted sort of creature called a contravariant functor. In reality a contravariant functor from  $C$  to  $D$  is not a

functor at all; it is, however, a functor from  $C$  to  $D^{op}$ . To better understand this abstract concept we offer three versions of the definition of a contravariant functor:

**Definition 5.8** *Contravariant Functor*

1. Let  $C$  and  $D$  be categories. A *contravariant functor*  $F : C \rightarrow D$  is defined to be a functor  $F : C \rightarrow D^{op}$ .
2. A *contravariant functor*  $F$  maps any object  $x$  in  $C$  to some object  $F(x)$  in  $D^{op}$ , and any morphism  $f$  in  $C$  to some morphism  $F(f)$  in  $D^{op}$  such that:
  - (a)  $F(f) : F(y) \rightarrow F(x)$ , for  $f : x \rightarrow y$ .
  - (b)  $F(f)F(g) = F(gf)$ , for composable  $f, g$  in  $C$ .
  - (c)  $F(1_x) = 1_{F(x)}$ , for  $1_x$ , the identity morphism of  $x$ .
3. A *contravariant functor*  $F : Vect \rightarrow Vect$  is a functor  $F : Vect \rightarrow Vect^{op}$ . It maps vector space  $V$  in  $Vect$  to some vector space  $F(V)$  in  $Vect^{op}$ , and linear map  $f : V \rightarrow W$  in  $Vect$  to linear map  $F(f) : F(W) \rightarrow F(V)$  in  $Vect^{op}$ .

A specific example of the contravariant functor  $F : Vect \rightarrow Vect$  described above is the one that takes vector spaces in  $Vect$  to linear functionals on the vector spaces.

**Example 5.9** *Let  $V$  be a vector space in the category  $Vect$ . The contravariant functor  $F : Vect \rightarrow Vect$  is a functor  $F : Vect \rightarrow Vect^{op}$  defined by*  
 $V \longmapsto Hom(V, \mathbb{R})$ .

For a more thorough journey through the concepts of category theory see the work of one of its founding fathers, S. Mac Lane. [ML88]

## 5.2 TQFT Defined

Based upon Atiyah's definition of a topological quantum field theory [At88], Atiyah [At89, At90], Walker [Wal], and Turaev [Tur94] describe an  $n$ -dimensional TQFT as a particular type of "linear representation" of the category  $n\text{Cob}$ .  $n\text{Cob}$  is simply the category containing compact oriented  $(n-1)$ -manifolds as objects, and oriented cobordisms between the manifolds as morphisms.

A cobordism is basically a manifold with boundary that has some components of the boundary labelled as *inputs* and the rest labelled as *outputs*. (see Fig. 5.11) We formally define a cobordism by:

### Definition 5.10 Cobordism

Suppose  $A$  and  $B$  are oriented  $(n-1)$ -dimensional manifolds without boundary. A *cobordism* from  $A$  to  $B$  is defined to be an oriented  $n$ -dimensional manifold with boundary  $M$  whose boundary is the disjoint union of  $(-A)$  and  $B$ , where  $(-A)$  is the orientation reverse of  $A$ .<sup>1</sup>

Let  $x, y, z$  be 1-dimensional manifolds with boundary. An example of the composition of 2-dimensional cobordisms in Fig. 5.11 composes cobordism  $f : x \rightarrow y$  with cobordism  $g : y \rightarrow z$  as depicted.

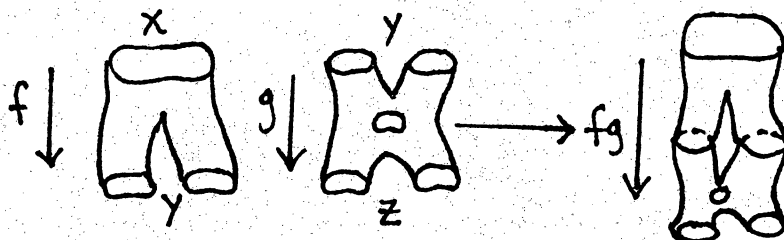


Figure 5.11 Composition of morphisms in  $n\text{Cob}$ .

Atiyah's definition of a TQFT is a special brand of category representation.

We define a linear representation of a category as follows:

<sup>1</sup>See Sawin's paper for a more intricate definition of cobordisms [Sa91]

**Definition 5.12** *Linear Representation of a Category*

A *linear representation* of a category  $C$  is a functor from  $C$  to  $\mathbf{Vect}$ .

Therefore a category representation  $Z$  maps objects in  $n\mathbf{Cob}$  to vector spaces in  $\mathbf{Vect}$ , and morphisms in  $n\mathbf{Cob}$  to linear maps between vector spaces in  $\mathbf{Vect}$ , in such a manner that the original structure of the category  $n\mathbf{Cob}$  is preserved (eg. a morphism  $f$  between two particular objects  $x$  and  $y$  in  $n\mathbf{Cob}$  is mapped as the morphism  $Z(f)$  between objects  $Z(x)$  and  $Z(y)$  in  $\mathbf{Vect}$  in such a manner that  $Z(fg) = Z(f)Z(g)$  and  $Z(1_x) = 1_{Z(x)}$ ).

But, as alluded to earlier, this representation (functor) is of a particular type. Making this vague description precise we see that a TQFT, as defined by Atiyah, is a *rigid symmetric monoidal* functor. We now embark upon an investigation of the details of such conditions on our functor.

In the concept of “category” there is already a juxtaposition of entities of different dimensions: The objects of a category can be thought of as zero-dimensional, and are often drawn that way, merely as dots; and the morphisms can be thought of as one-dimensional, and are often drawn that way as single arrows. In the further development of category theory even more dimensions can be juxtaposed together; this development is sometimes referred to as *higher dimensional category theory* [BD97]. The concept of monoidal category represents one of the first steps in this extension of category theory to include extra dimensions (although, as we will explain, the extra dimension in a monoidal category is hidden in a certain sense).

Roughly, a *monoidal category* is a category equipped with a functorial tensor product operation on objects, as well as a special unit object. The tensor product operation and the unit object together are required to satisfy the same kind of associativity and unit law axioms satisfied by the composition operation (on

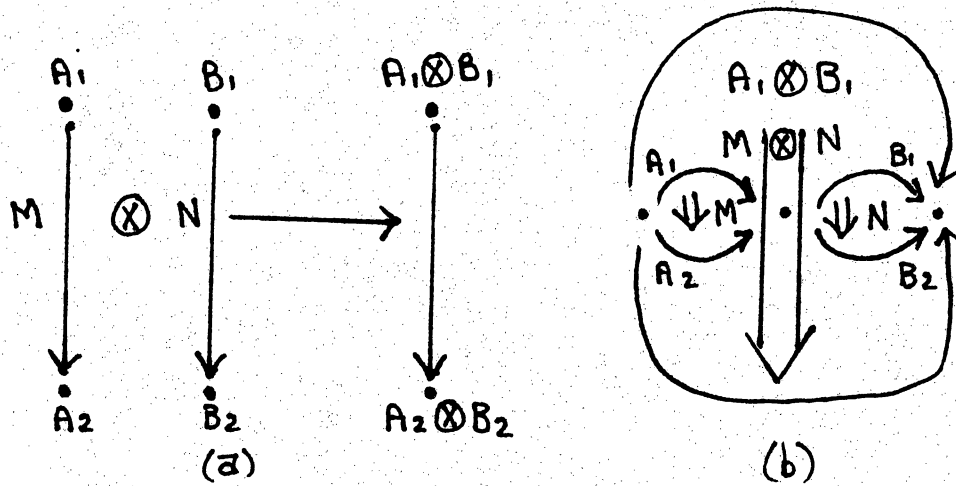
morphisms) and the identity morphisms in a category. (See Fig. 5.14) Thus the objects in a monoidal category are, in a way, analogous to the morphisms in an ordinary category. At the same time, though, the objects in a monoidal category are analogous in a different (but also very obvious) way to the objects in an ordinary category. This is possible because what is really going on here is that a monoidal category involves three consecutive dimensions, and the two consecutive dimensions of an ordinary category can be considered as analogous either to the upper two dimensions of the three in a monoidal category, or to the lower two of the three. (See table 5.13)

**Table 5.13** *The Three Levels of a Monoidal Category*

<i>Shifted Depiction</i>	<i>Level</i>	<i>Entities</i>	<i>Original Depiction</i>
<i>(no depiction)</i>	<i>hidden level</i>	<i>0-dimensional entity</i>	•
•	<i>level of objects</i>	<i>1-dimensional entities</i>	→
→	<i>level of morphisms</i>	<i>2-dimensional entities</i>	⇓

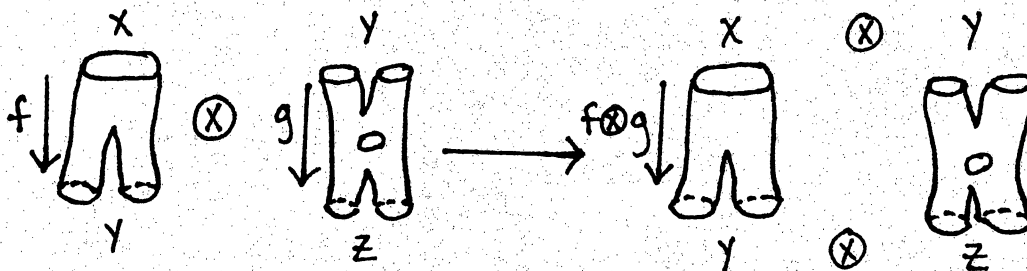
The hidden level serves the purpose of allowing the objects to behave like one dimensional entities; one dimensional entities need to have a zero dimensional entity in contrast to which they can express their one-dimensionality. Because of the uniqueness of the single zero-dimensional entity in a monoidal category, however, there is generally no need to give this entity any special name or label.

Thus, as indicated in Table 5.13, there are two styles which we can use to draw pictures of phenomena in a monoidal category. In Figure 5.14 (a) the functorial tensor product is drawn in the style where objects are depicted as dots, while Figure 5.14 (b) portrays the same data in the style where objects are depicted as arrows.



**Figure 5.14** *Functorial tensor product in monoidal category: shifted depiction (a), and original depiction (b) where all dots are identified.*

The categories  $n\text{Cob}$  and  $\text{Vect}$  each become monoidal categories by the introduction of tensor product operations on them. The tensor product operation on  $n\text{Cob}$  is the disjoint union of  $(n - 1)$ -manifolds; and the functoriality (functor-like qualities) of this operation is sketched in Figure 5.15 in the case  $n = 2$ . The unit object in  $n\text{Cob}$  is the empty set. Our tensor product on the category  $\text{Vect}$  is the usual tensor product of vector spaces, with the one dimensional vector space,  $\mathbb{C}$ , as the unit object. To say that our functor  $Z$  is monoidal is to say that it preserves tensor products and sends the identity object in  $n\text{Cob}$  to the identity object in  $\text{Vect}$ .



**Figure 5.15** *Tensor product of morphisms in  $2\text{Cob}$ ,  $f : y \rightarrow z$ ,  $g : x \rightarrow y$ ,  $f \otimes g : y \otimes x \rightarrow z \otimes y$*

A category is symmetric monoidal if for any pair of objects  $x, y$  in a category, there exists a *braiding*

$$B_{x,y} : x \otimes y \rightarrow y \otimes x$$

which, among other requirements, satisfies the symmetry equation  $B_{y,x}B_{x,y} = 1_{x \otimes y}$ . We call a braiding that satisfies this condition a *symmetry*.  $n\text{Cob}$  and  $\text{Vect}$  are symmetric monoidal, with an example of the symmetry in  $2\text{Cob}$  being the cobordism depicted in Fig. 5.16, and in  $\text{Vect}$  the symmetry is the usual isomorphism of vector spaces  $x \otimes y$  and  $y \otimes x$ .

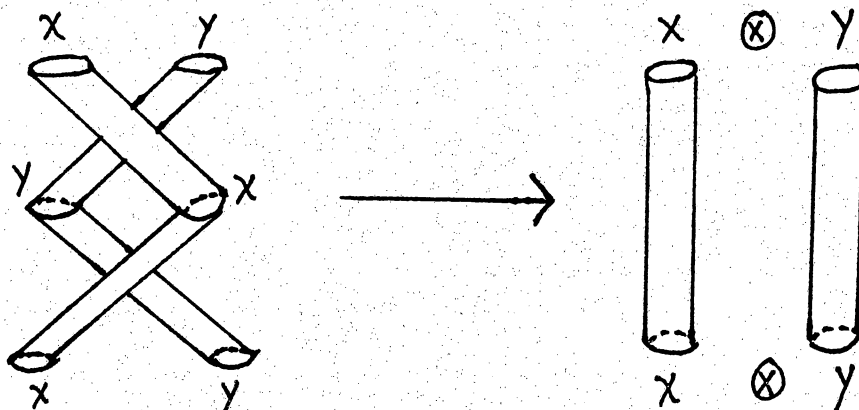


Figure 5.16 *Symmetry in 2Cob.*

Recalling that an object  $x$  in a monoidal category can be thought of as a one dimensional entity or arrow, we now introduce the concept of the *dual object* of an object, which intuitively represents the same arrow except with its orientation reversed.

We define the *star structure* on the objects (oriented 1-cells) in  $2\text{Cob}$  (see Table 5.13) in geometric terms as the reversal of orientation. (See Figure 5.17)

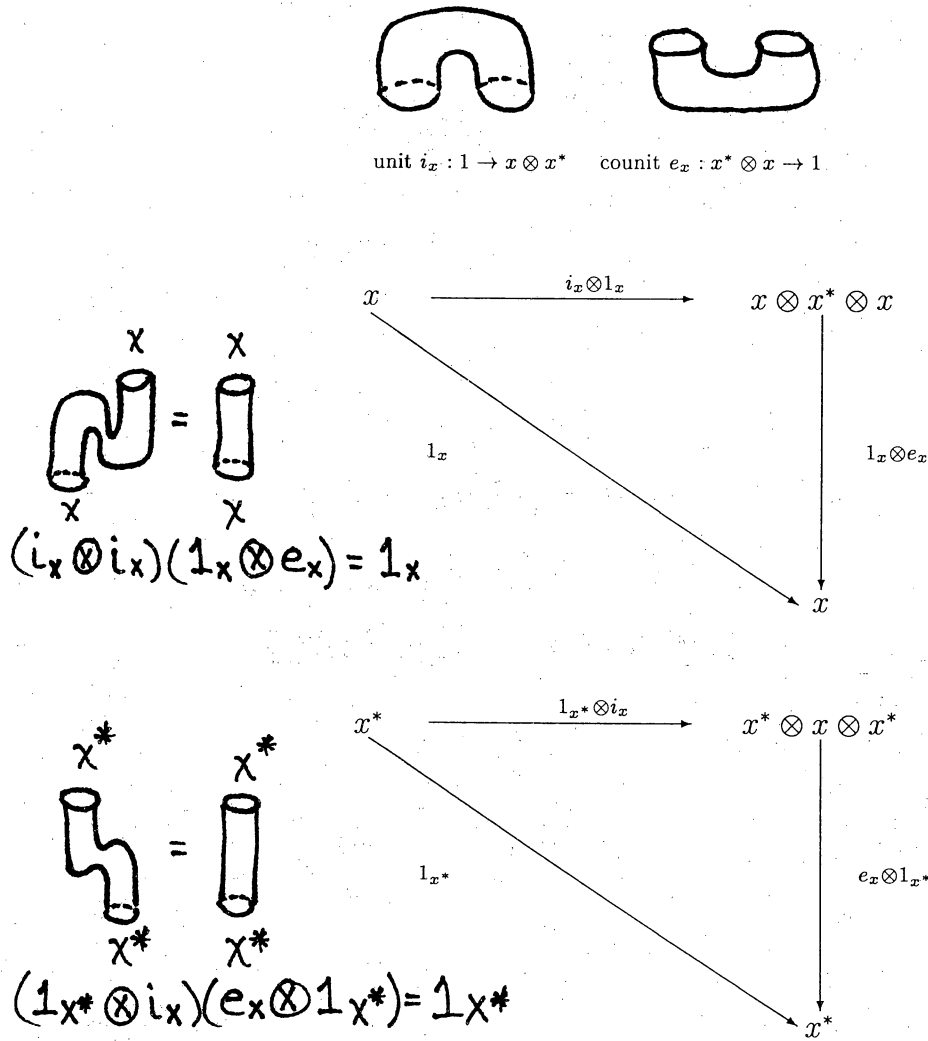


Figure 5.17 *Duality (star) structure on objects in 2Cob*

Technically, the dual (which may or may not exist) of an object  $x$  in a monoidal category is an object  $x^*$  for which there exists a unit map  $i_x : 1 \rightarrow x \otimes x^*$ ,



and a counit map  $e_x : x^* \otimes x \rightarrow 1$  satisfying certain triangular identities. Picturing the unit and counit as cylinders in Fig 5.18, the triangular identities depicted in the commuting diagrams on the right can be alternatively represented by the cylinder sketches to the left.



**Figure 5.18** Unit, counit, and triangular identities

A monoidal category where all objects have duals, as described above, is called a *rigid* monoidal category.

In summary a TQFT is simply a rigid symmetric monoidal functor

$$Z : nCob \rightarrow Vect \quad (5.19)$$

that preserves the rigid symmetric monoidal structure.

A *unitary* topological quantum field theory is a similar functor, but mapping  $nCob$  to  $Hilb$ , the category whose objects are finite dimensional Hilbert spaces and whose morphisms are linear maps. To better conceptualize our new category  $Hilb$  we recall the structure of a Hilbert space: it possesses a zero vector, addition of vectors, subtraction of vectors, scalar multiplication of vectors, and it has a sesquilinear inner product (ie. linear on the second entry, but conjugate linear on the first) defined on it.

In order to define a *unitary* TQFT we must consider a second duality structure. The primary case, the ‘star’  $*$  stucture on objects, was intrinsic to rigid monoidal categories. (See Figure 5.17) The secondary duality structure,  $\dagger : nCob \rightarrow nCob$ , which is vital to our definition of a unitary TQFT, takes an object (a 1-cell in Table 5.13) to itself and morphism (a 2-cell in Table 5.13)  $f : x \rightarrow y$  to its ‘dual’  $f^\dagger : y \rightarrow x$ . (see Figure 5.18) The operation  $\dagger$  is a contravariant functor, so  $(1_x)^\dagger = 1_x$  and  $(fg)^\dagger = g^\dagger f^\dagger$ . We specifically consider  $\dagger$  defined on  $Hilb$ . The contravariant functor  $\dagger : Hilb \rightarrow Hilb$  takes objects to themselves, and each linear map  $f : x \rightarrow y$  to its Hilbert space adjoint  $f^\dagger : y \rightarrow x$ .

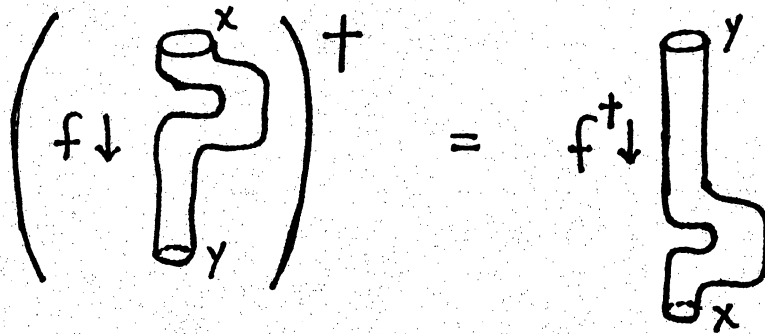


Figure 5.20 Duality structure on morphisms in  $2Cob$

With both duality stuctures,  $*$  for objects and  $\dagger$  for morphisms, properly

introduced we may formally define a unitary TQFT.

**Definition 5.21** A *unitary TQFT* is a rigid symmetric monoidal functor

$Z : n\text{Cob} \rightarrow \text{Hilb}$  satisfying

$$Z(f^\dagger) = Z(f)^\dagger$$

for all morphisms  $f$ .

The authors claim that a two dimensional TLFT is a piecewise-linear version of a unitary TQFT. More precisely, it parallels a rigid symmetric monoidal functor  $Z$  from  $2\text{Cob}$ , the category of compact oriented 1-manifolds as objects and oriented cobordisms as morphisms, to the category  $\text{Hilb}$ , with the required duality compatibility conditions. And a three dimensional TLFT is similar, but maps from  $3\text{Cob}$ , whose objects are compact oriented 2-manifolds.

In general Baez and Dolan describe the duties of an  $n$ -dimensional TQFT as follows: It assigns numbers to closed  $n$ -manifolds and Hilbert spaces to closed  $(n - 1)$ -manifolds<sup>2</sup>. We will carefully consider its first duty in the next section.

---

<sup>2</sup>Baez and Dolan actually propose that the duties of an ‘extended’  $n$ -dimensional TQFT goes further, assigning 2-Hilbert spaces to closed  $(n - 2)$ -manifolds, and so forth until at its lowest level it finally assigns an  $n$ -Hilbert space in  $\text{Hilb}$  to closed 0-manifolds (points) in  $n\text{Cob}$ .

### 5.3 Reinterpreting Two and Three Dimensional TLFT's

With Atiyah's [At88] abstract description of a TQFT construction, the question of how to fit Fukuma/Hosono/Kawai's 2d theory and Chung/Fukuma/Shapere's and Kauffman/Lins' 3d theories into such a description arises. We have only studied these three theories in a cursory manner in which the TLFT gives us a partition function that assigns a numerical constant to each triangulated closed oriented manifold. But taken as a whole a TLFT gives more than this. As indicated by the list of duties in the previous section, a 2-dimensional TLFT assigns numbers to closed 2-manifolds and Hilbert spaces to closed 1-manifolds (see Fig. 5.22), and similarly for the three dimensional case it assigns numbers to closed 3-manifolds and Hilbert spaces to closed 2-manifolds. While we have concentrated on the study of the first duty of a TLFT which is important in the topological classification of manifolds, the second duty has application to quantum field theory. It provides a manner for associating physical operators and states to our manifolds, which may one day be used to describe physical theories such as quantum gravity. We restrict our investigation to the assignment of numerical constants to the manifolds.

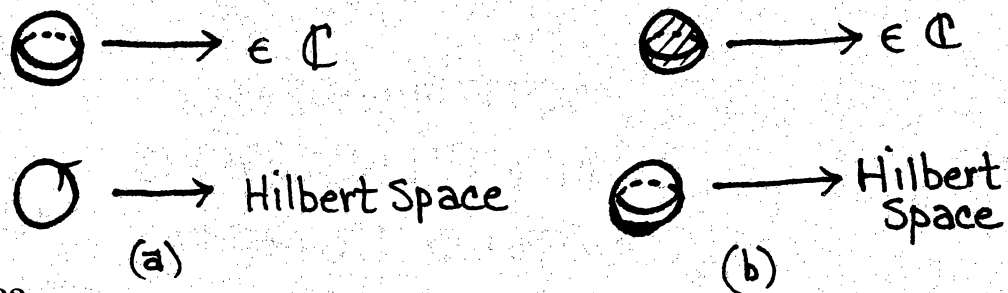
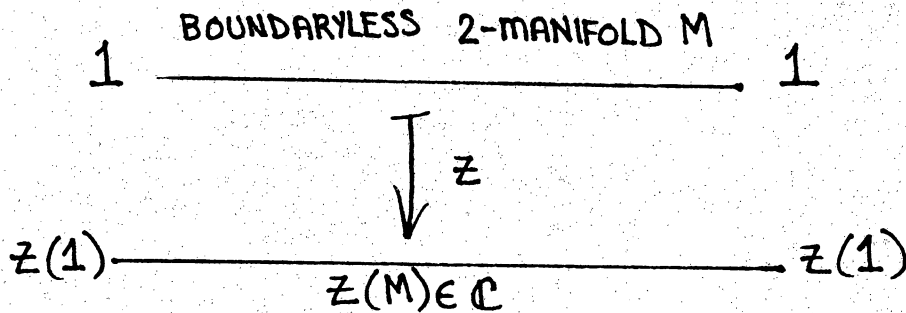


Figure 5.22 Duties of (a) 2d and (b) 3d TLFTs

### 5.3.1 2d Generalization

To analyze exactly how a two dimensional TLFT, as described by Baez and Dolan, accomplishes the first task we must recall the details of its duty. The two dimensional TLFT gives a functor that takes compact oriented 1-manifolds to Hilbert spaces and oriented two dimensional cobordisms to linear maps between Hilbert spaces. A two dimensional cobordism is a manifold whose boundary is the disjoint union of two 1-manifolds.

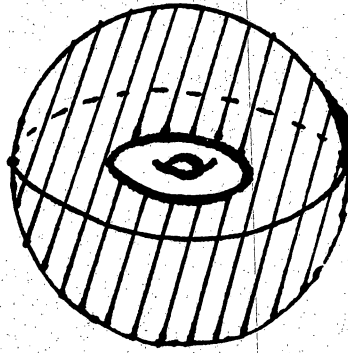
If we consider the trivial case where our cobordism is the 2-manifold whose boundary is the disjoint union of the *unit object* for disjoint unions (the empty 1-manifold, referred to simply as 1) with itself, we get a boundaryless 2-manifold  $M$  for our cobordism. Since our functor  $Z$  is monoidal it preserves the tensor product, so it will map the unit object 1 for disjoint unions in  $2\text{Cob}$  to the unit object  $Z(1)$  for the tensor product in  $\text{Hilb}$ , which is the one dimensional Hilbert space. Because a functor preserves the original structure of the category (see Definition 5.4) it will map the boundaryless 2-manifold  $M$  in  $2\text{Cob}$  to  $Z(M)$ , the linear map from the one dimensional Hilbert space to itself (see Fig. 5.23). Such a linear map may be expressed in matrix form as a  $1 \times 1$  matrix, which is simply a complex number. Hence, for the trivial case where we consider only the cobordisms whose boundaries are disjoint unions of the empty 1-manifold with itself, ie. boundaryless 2-manifolds, our TLFT assigns a numerical constant, just as Fukuma/Hosono/Kawai describe in their theory.



**Figure 5.23** Partition function  $Z$  mapping 2-manifold  $M$  to numerical constant  $Z(M)$  arising from “partition functor”  $Z$ .

### 5.3.2 3d Generalization

Since our three dimensional TQFT has the same range space as the two dimensional TQFT, generalizing to three dimensions is trivial. In a fashion that parallels the two dimensional case, the three dimensional TQFT is simply a functor that takes compact oriented 2-manifolds to Hilbert spaces and oriented three dimensional cobordisms to linear maps between Hilbert spaces. A three dimensional cobordism is a manifold whose boundary is the disjoint union of two 2-manifolds (see Figure 5.24). In the trivial case where our cobordism is the 3-manifold whose boundary is the disjoint union of the *unit object* for disjoint unions (the empty 2-manifold) with itself, we get a boundaryless 3-manifold for our cobordism. Again, since our functor is monoidal it preserves the tensor product, so it will map the unit object for disjoint unions in  $2\text{Cob}$  to the unit object for the tensor product in  $\text{Hilb}$ , which is the one dimensional Hilbert space. So our functor maps the boundaryless 3-manifold in  $3\text{Cob}$  to a linear map from the one dimensional Hilbert space to itself, and expressing the linear map in matrix form results in a complex number.



**Figure 5.24** *Example of 3-manifold  $M$  (shaded) whose boundary is the disjoint union of  $S^2$  and  $T^2$  (nested).*

So Fukuma/Hosono/Kawai topological lattice field theory in two dimensions and both Chung/Fukuma/Shapere and Kauffman/Lins TLFT theories in three dimensions are simply particular examples of Atiyah topological quantum field theories. They are essentially blueprints for constructing TQFTs, emphasizing their number one duty: the assignment of complex numbers to closed orientable 2 or 3-manifolds. The purpose of triangulating the manifold is to allow us to manipulate it in a handy fashion. In its triangulated form it is easy to prove that the theory is indeed invariant under choice of triangulation, validating the algebraic method used to determine the state sum invariant of the manifold.

## 5.4 Conclusion

The bulk of this research paper has essentially been a technical description of the construction of topological quantum field theories via various triangulation methods. In the final chapter we validate these theories by carefully analyzing the two and three dimensional versions of Atiyah's definition of a TQFT. Satisfied that they are indeed valid constructions the question remains how does one construct a two and three dimensional TLFT in a *general* fashion?

In the two dimensional case it has been suggested by Baez and the author [BN-G97] that one may construct a more general theory by labelling the lattice with various components of a category itself, rather than an algebra. Specifically they triangulate the manifold and beginning with a particular type of category they assign its objects to vertices and its morphisms to edges of the lattice. Their theory produces a complex number for each 2-cell in the lattice.

For the CFS three dimensional case it has been suggested by Baez [B-PC] that a similar construction may be developed, simply a categorification of the two dimensional case. CFS triangulate their manifold into a honeycomb of tetrahedra. Baez proposes that beginning with a particular type of 2-category<sup>3</sup> (the extension of a category) one may label vertices with objects, edges with morphisms, and faces with 2-morphisms. The final construction should yield a complex number for each 3-cell in the lattice.

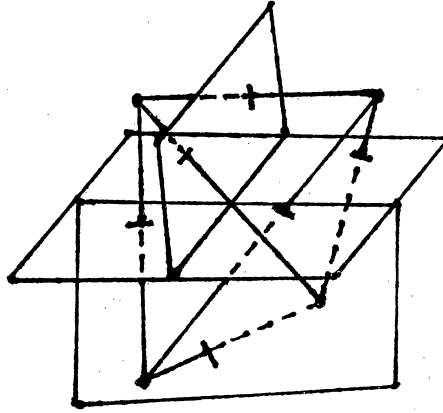
Reconstruction of Kauffman/Lins' version of the Turaev/Viro invariant for 3-manifolds requires a bit of explanation. Their theory is founded upon a *dual* cell decomposition of a manifold (see Figure 5.25 and Table 5.26). Therefore, the suggested reconstruction would require the assignment of objects to three

---

<sup>3</sup>A 2-category [B96] has three components: objects, morphisms and 2-morphisms (morphisms between morphisms).



dimensional spinal complements, morphisms to two dimensional faces, 2-morphisms to one dimensional edges, and a complex number to each zero dimensional vertex since it is dual to the tetrahedron.



**Figure 5.25** *Dual of tetrahedron*

**Table 5.26** *Translation Key for Dual of Tetrahedron*

<i>Tetrahedron</i>	<i>Dual</i>
<i>3d tetrahedron</i>	<i>0d vertex</i>
<i>2d triangle</i>	<i>1d edge</i>
<i>1d edge</i>	<i>2d face</i>
<i>0d vertex</i>	<i>3d spinal complement</i>

While the details of such theories in three dimensions are an open issue, Baez/Dolan have already developed the foundational category structure upon which to construct these theories, not only for three dimensions, but for arbitrary finite dimensions. [BD95] [BD97]

\*

...the Master acts without doing anything  
and teaches without saying anything.  
Things arise and she lets them come;  
things disappear and she lets them go.  
She has but doesn't possess,  
acts but doesn't expect.  
When her work is done, she forgets it.  
That is why it lasts forever.

Verse 2 from the Tao Te Ching [SM88]

# Bibliography

- [A30] J. W. Alexander. *Ann. Math.* **31** (1930), 292.
- [At88] M. Atiyah. *Topological Quantum Field Theories*. Inst. Hautes E'tudes Sci Publ. Math. **68** (1988), 175-186; *The Geometry and Physics of Knots*. (Cambridge University, Cambridge, England, 1990).
- [At89] M. Atiyah. *Topological Quantum Field Theories*. *Publ. Math. IHES*, 68:175-186, 1989.
- [At90] M. Atiyah. *The Geometry and Physics of Knots*. Lezioni Lincee. Cambridge University Press, 1990.
- [B92] D. Boulatov. *Mod. Phys. Lett.* **A7** (1992), 1629.
- [B96] J. Baez. *Higher Dimensional Algebra II: 2-Hilbert Spaces*. To appear in *Adv. Math.*
- [BD95] J. Baez and J. Dolan. *Higher Dimensional Algebra and Topological Quantum Field Theory*. *J. Math. Phys.* **36** (1995), 6073-6105.
- [BD97] J. Baez and J. Dolan. *Higher Dimensional Algebra III: n-Categories and the Algebra of Opetopes*. To appear in *Adv. Math.*
- [BM94] J. Baez and J. Muniain. *Gauge Fields, Knots and Gravity*. World Scientific Pub. (1994)
- [BN-G98] Upcoming paper authored by J. Baez and S. Newman-Gomez.
- [B-PC] J. Baez personal communication.
- [CFS94] S. Chung, M. Fukuma, and A. Shapere. *Structure of Topological Lattice Field Theories in Three Dimensions*. *Int. J. Mod. Phys.* **A 9** (1994) 1305-1360.
- [CFS95] Carter, Flath, Saito. *The Classical and Quantum 6j-Symbols*. Princeton University Press (1995) ed.1, vol.1.
- [Cr95] L. Crane. *Clock and Category: Is Quantum Gravity Algebraic?* *J Math. Phys.* **36** (1995), 6180-6193.
- [D-PC] J. Dolan personal communication.

- [FHK94] M. Fukuma, S. Hosono, and H. Kawai. *Lattice Topological Field Theory in Two Dimensions*. Comm. Math. Phys. **161** (1994) 157-176.
- [Fr94] D. Freed. *Higher Algebraic Structure and Quantization*. Comm. Math. Physics. **159** (1994), 343-398.
- [DMG93] D.M. Goldschmidt. *Group Characters, Symmetric Functions, and the Hecke Algebra*. (American Mathematical Society, Providence. (1993).
- [GV92] M. Gross and S. Varsted. Nucl. Phys. **B378** (1992) 367.
- [J83] V.F.R. Jones *Index of Subfactors* Invent. Math. **72** (1983) 1-25.
- [K95] C. Kassel, *Quantum Groups* Springer, NY. (1995).
- [Kau87] L.H. Kauffman. *State Models and the Jones Polynomial*. Topology **26** (1987) 395-407.
- [Kau91] L.H. Kauffman. *Knots and Physics*. World Scientific Pub. (1991).
- [Kau94] L.H. Kauffman, S.L. Lins. *Temperley-Lieb Recoupling Theory and Invariants of 3-Manifolds*. Princeton University Press. (1994).
- [KR89] A.N. Kirillov, N.Y. Reshetikhin, *Representation of the Algebra  $U_q(sl(2))$ ,  $q$ -Orthogonal Polynomials and Invariants of Links*. Infinite Dimensional Lie Algebras and Groups. (Luminy-Marseille, 1988), Vol. 7 of Adv. Ser. in Math. Phys. ed. by V.G. Kac (World Scientific, Singapore, 1989) (285-389). Reprinted in T. Kohno, *New Developments in the Theory of Knots* (World Scientific, Singapore, 1989).
- [Ku91] G. Kuperberg. *Involutory Hopf Algebra and 3-Manifold Invariants*. Int. J. Math. **2** (1991) 41-66.
- [L91] W.B.R. Lickorish. *Three-Manifolds and the Temperley-Lieb Algebra*. Math. Ann. **290** (1991) 657-670.
- [LR88] *Finite Dimensional Cosemisimple Hopf Algebras in Characteristic 0 are Semisimple*. J. Alg. **117** (1988) 267-289.
- [ML88] S. Mac Lane. *Categories for the Working Mathematician*. Springer, Berlin. (1988).
- [Mat88] S.V. Matveev. *Transformations of Special Spines and the Zeeman Conjecture*. Math. USSR Izvestia. **31** (1988) 423-434.
- [M75] A. Migdal. Sov. Phys. J.E.T.P. **42** (1975) 413.
- [Pen71] R. Penrose. *Applications of Negative Dimensional Tensors*, in D.J.A. Welsh, ed., *Combinatorial Mathematics and Its Applications* (Academic Press, NY, 1971).

- [Pier88] R. Piergallini. *Standard Moves for Standard Polyhedra and Spines III* Convegno Nazionale di Topologia Trieste, 9-12 Guigna 1986, in *Supplemento ai Rendiconti del Circolo Matematico di Palermo* (1988) 391-414.
- [Piu92] S. Piunikhin. *Turaev-Viro and Kauffman-Lins Invariants for 3-Manifolds Coincide*. J. of Knot Theory and Ram. **2** (1992) 105-135.
- [RT91] N. Reshetikhin and V. Turaev. *Invariants of Three-Manifolds Via Link-Polynomials and Quantum Groups*. Invent. Math. **103** (1991) 547-597.
- [Sa96] S. Sawin. *Links, Quantum Groups and TQFTs*. Bull. Amer. Math. Soc. **33** (1996), 413-445.
- [S86] R.P. Stanley. *Enumerative Combinatorics*, Vol. 1, (Wadsworth and Brooks/Cole, Monterey, CA, 1986).
- [S69] M. Sweedler, Hopf Algebras (W.A. Benjamin, Inc., NY, 1969).
- [SM88] S. Mitchell. *Tao Te Ching*. HarperPrennial. (1988).
- [Tur94] V.G. Turaev. *Quantum Invariants of Knots and 3-manifolds*. Walter de Gruyter. (1994)
- [TV92] V.G. Turaev and O.Y. Viro. *State Sum Invariants of 3-Manifolds and Quantum 6j-Symbols*. Topology. **31** (1992) 865-902.
- [Pie88] R. Piergallini. *Standard Moves for Standard Polyhedra and Spines, III* Convegno Nazionale di Topologia Trieste, 9-12 Giugno 1986. In *Supplemento ai Rendiconti del Circolo Matematico di Palermo*. (1988) 391-414.
- [W87] H. Wenzl. *On Sequences of Projections*. C.R. Math. Acad. Sci. Soc. R. Can. **9** (1987) 5-9.
- [W91] E. Witten. Commun. Math. Phys. **141** (1991) 435.
- [Wal] K. Walker. On Witten's 3-manifold Invariants. (preprint)
- [Wt88] E. Witten. *Topological Quantum Field Theory*. Comm. Math. Phys. **117** (1988) 353-386.